UNIVERSITÀ POLITECNICA DELLE MARCHE

FACOLTÀ DI INGEGNERIA

Master's Degree in Biomedical Engineering

Curriculum: eHealth and Clinical Engineering

Role of High Frequency Electroencephalographic Oscillations during sleep in pediatric epileptic patients

Supervisor:

Dott. Ilaria Marcantoni

Candidate:

Sofia Di Ubaldo

Co-supervisor:

Prof. Laura Burattini

Dott. Erica Iammarino

Academic Year 2025/2026

Abstract

Epilepsy is one of the most common neurological disorders in childhood and is characterized by recurrent seizures resulting from abnormal neuronal activity. Electroencephalography (EEG) plays a central role in its diagnosis and monitoring, particularly during sleep, when epileptiform activity can become more evident. Among advanced quantitative EEG measures, high-frequency oscillations (HFOs) have gained increasing attention as potential biomarkers of epileptic activity. However, their relationship with other properties of the EEG signal, such as signal complexity, remains less explored in pediatric patients.

The aim of this thesis was to investigate the role of HFOs during sleep in pediatric patients with epilepsy, with particular attention to their relationship with quantitative changes in EEG complexity. A systematic review was conducted to examine the main quantitative EEG biomarkers investigated during sleep in pediatric epilepsy and to identify current methodological approaches and research gaps. The review highlighted growing interest in HFOs, entropy-based measures, functional connectivity, and other quantitative EEG approaches, together with considerable methodological heterogeneity across studies.

Based on this background, an experimental analysis was performed using an open dataset of overnight EEG recordings from 30 pediatric patients with epilepsy. The analysis focused on N3 sleep, during which HFO occurrence is particularly relevant. The continuous EEG recordings were preprocessed and divided into non-overlapping 4-s windows. Fourteen complexity measures, selected from the literature to characterize different aspects of EEG dynamics, were then computed and analyzed in relation to HFO occurrence. Seven of the fourteen measures showed significant differences between HFO and No-HFO activity using the Wilcoxon signed-rank test with false discovery rate (FDR) correction for multiple comparisons.. Katz Fractal Dimension increased during HFO activity, whereas Petrosian Fractal Dimension, Permutation Entropy, Hjorth Complexity, Shannon Entropy, Tsallis Entropy, and Rényi Entropy decreased. A subsequent temporal analysis examined distant Baseline, Pre-HFO, HFO, and Post-HFO conditions using the Friedman test, followed by post-hoc Wilcoxon signed-rank tests with FDR correction. The most consistent changes were observed during HFO activity itself, while no significant differences were detected between Pre-HFO and distant Baseline or between Post-HFO and distant Baseline. Finally, the fourteen complexity measures were evaluated for subject-independent classification. Three supervised models were tested using leave-one-subject-out (LOSO) validation. Classification of HFO activity versus distant Baseline showed modest performance, with a maximum balanced accuracy of approximately 53.7%. Pre-HFO activity could

not be reliably distinguished from distant Baseline, with a balanced accuracy of approximately 49.3% and an ROC-AUC close to 0.50.

Overall, the results show that HFO occurrence during N3 sleep is associated with measurable changes in specific aspects of EEG complexity. However, these changes were mainly observed during HFO activity and showed limited generalization across subjects. No robust complexity pattern preceding HFO occurrence was identified with the measures and temporal resolution considered in this study. These findings suggest that EEG complexity can provide complementary information for the characterization of HFO-related activity, while its integration with other quantitative EEG features may be necessary to obtain more robust and generalizable markers in pediatric epilepsy.

Contents

1. Introduction 1
1.1 The Brain: Anatomy and Neural Activity 1
1.1.1 Major Brain Regions and Functions 1
1.1.2 Neuronal Organization and Synaptic Communication 3
1.1.3 Oscillatory Activity and Brain Rhythms 6
1.2 Epilepsy: clinical background and pathophysiology 7
1.2.1 Definition, epidemiology and clinical relevance 7
1.2.2 Pathophysiological mechanisms of epilepsy 10
1.2.3 Clinical classification of seizures: focal and generalized 15
1.3 Epilepsy detection with Electroencephalography 17
1.3.1 Electroencephalograghy basics and brain rhythms 17
1.3.2 Electroencephalography acquisition modalities and artifacts 19
1.3.3 Advanced electroencephalographic biomarkers: High Frequency Oscillations 22
1.4 Analysis of signals for seizure detection 25
1.4.1 Time-domain analysis 25
1.4.2 Frequency-domain analysis 27
1.4.3 Feature extraction from electroencephalographic signals 30
1.4.4 Automated detection algorithms 35
1.5 Sleep and Pediatric Epilepsy 38
1.5.1 Importance of Sleep Monitoring in Epilepsy 38
1.5.2 Pediatric Epilepsy: Syndromes and Advanced EEG Biomarkers 40
1.5.3 Quantitative electroencephalography and Advanced Analysis in Pediatric Epilepsy 44
1.5.4 Related works and research gaps 47
Rationale behind the Thesis 49
2. Materials and Methods 51
2.1 Dataset description 51
2.2 Electroencephalography Preprocessing and Artifact Rejection 52
2.3 Electroencephalographic Biomarkers Extraction 53

2.4 High Frequency Oscillation Analysis 59
2.5 Statistical Analysis and Classification 65
3. Results 70
4. Discussion 76
Conclusion I
Bibliography II
APPENDIX I XI
1 Systematic Review XI
1.1 Literature search strategy and design XI
1.2 Study Selection Process XI
1.3 Results of the Literature Search XII
1.4 Discussion of results XIV

1. Introduction

1.1 The Brain: Anatomy and Neural Activity

The nervous system is a complex and highly organized network responsible for the integration and transmission of information throughout the body. In particular, the brain generates coordinated electrical activity through the interaction of large populations of interconnected neurons. These electrical dynamics give rise to rhythmic oscillatory patterns, commonly referred to as brain rhythms, which play a fundamental role in neural communication and information processing.

1.1.1 Major Brain Regions and Functions

The human nervous system is a highly specialized and hierarchically organized network responsible for coordinating physiological processes and enabling the interaction of the organism with both the internal and external environment. Traditionally, it is divided into the central nervous system (CNS) and the peripheral nervous system (PNS) [1]. The CNS consists of the brain and spinal cord, whereas the PNS comprises the cranial and spinal nerves that extend outside the CNS and connect central neural structures with the rest of the body. As shown in Fig. 1, cranial nerves emerge from the brain, while spinal nerves originate from the spinal cord and extend throughout the body. Through these peripheral connections, the PNS transmits sensory inputs to the CNS and conveys motor commands toward peripheral effectors [1].

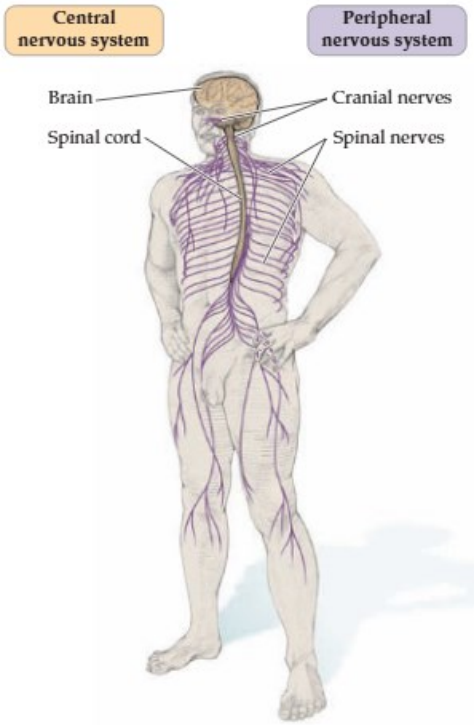


Figure 1. Anatomical organization of the human nervous system into the central nervous system, comprising the brain and spinal cord, and the peripheral nervous system, comprising the cranial and spinal nerves. [1].

Functionally, the PNS can be subdivided into the somatic nervous system, responsible for voluntary motor control and conscious sensory perception, and the autonomic nervous system, which regulates involuntary physiological activities such as cardiac function, respiration, and digestion. The autonomic nervous system is further divided into the sympathetic and parasympathetic branches, whose complementary and often antagonistic actions contribute to the maintenance of physiological homeostasis [2]. From a structural perspective, the human brain contains approximately 86 billion neurons organized into highly interconnected neural networks [3]. The remarkable density and complexity of these neuronal connections support advanced information processing and underlie higher cognitive functions. Moreover, quantitative analyses have demonstrated that the human brain follows the same cellular scaling principles observed in other primates, suggesting that it represents a linearly scaled-up primate brain rather than a structurally unique organ [3].

Within the CNS, the brain represents the principal structure responsible for sensory integration, motor coordination, cognition, and behavior. Its organization reflects a combination of structural specialization and functional integration, in which anatomically distinct regions perform specific tasks while remaining interconnected through complex neural pathways [1]. Anatomically, the brain is commonly divided into three major regions: the cerebrum, the cerebellum, and the brainstem. The cerebellum is located posteriorly and inferiorly to the cerebrum, while the brainstem connects the brain with the spinal cord and is composed of three main structures: the midbrain, pons, and medulla oblongata. The cerebrum is the largest and most developed portion of the brain and includes the cerebral cortex, a highly folded outer layer characterized by gyri and sulci that significantly increase the cortical surface area and consequently enhance processing capacity [1]. The cerebral cortex is organized into two hemispheres connected by the corpus callosum and subdivided into four principal lobes: frontal, parietal, temporal, and occipital (Fig. 2). Each lobe is predominantly associated with specific functional domains. The frontal lobe is mainly involved in voluntary motor control, planning, reasoning, and executive functions. The parietal lobe plays a central role in somatosensory integration and spatial perception, whereas the temporal lobe contributes to auditory processing, language comprehension, and memory-related functions. The occipital lobe is primarily dedicated to visual processing [2]. Below the cortical surface, several subcortical structures contribute to the modulation and coordination of neural activity. Among these, the thalamus functions as the principal relay station for sensory information directed toward the cerebral cortex, while the basal ganglia participate in the initiation and modulation of movement through extensive connections with cortical motor areas [1]. These structures are also involved in cognitive and behavioral processes through the formation of distributed cortico-subcortical circuits.

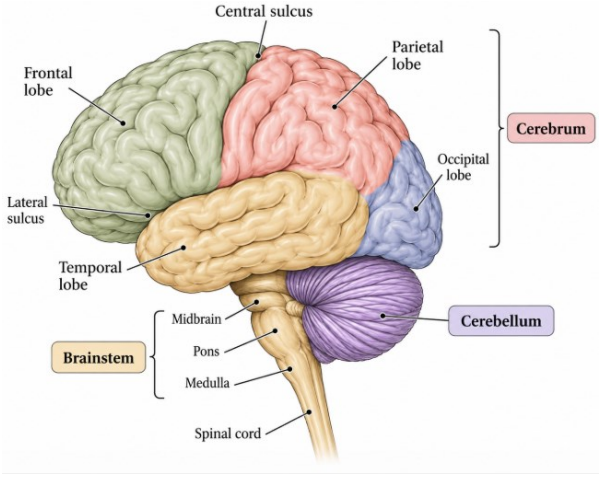


Figure 2. Main anatomical subdivisions of the human brain, showing the cerebral lobes, cerebellum, and the main components of the brainstem [1].

Although anatomical subdivisions are useful for describing brain organization, neural activity cannot be interpreted as the isolated function of single regions. Instead, brain function emerges from the interaction of distributed and functionally interconnected areas. Functional connectivity studies have demonstrated that the cerebral cortex is organized into multiple large-scale networks composed of functionally coupled regions distributed across distinct cortical areas [4]. This network-based organization is particularly important for higher-order cognitive functions, which rely on the integration of information across spatially separated brain regions rather than on strictly localized processing. In addition to the cerebrum, the cerebellum plays a fundamental role in the coordination, timing, and precision of voluntary movements, as well as in motor learning and postural control. The brainstem, composed of the midbrain, pons, and medulla oblongata, regulates essential autonomic functions including respiration, cardiovascular activity, and arousal, while also representing the main communication pathway between the brain and spinal cord [1].

1.1.2 Neuronal Organization and Synaptic Communication

The nervous system is composed of a complex network of specialized cells responsible for processing and transmitting information throughout the body. At the cellular level, it mainly consists of neurons and glial cells, which interact closely to ensure the correct functioning of neural circuits and the maintenance of the neural environment [1]. Neurons represent the fundamental functional units of the nervous system and are specialized for the generation, integration, and transmission of electrical signals. Through highly organized communication networks, they support all nervous system functions, ranging from simple reflex responses to higher cognitive processes [1].

In addition to neurons, the nervous system contains a large population of glial cells distributed throughout both the central and peripheral nervous systems. Traditionally considered supporting elements, glial cells are now recognized as active participants in neural function. They contribute to metabolic and structural support, regulation of the extracellular environment, maintenance of homeostasis, and formation of myelin sheaths that increase the speed of signal conduction along axons [2]. Moreover, glial cells are involved in the modulation of synaptic transmission and neuronal communication, highlighting their essential role in neural activity [2]. Despite the considerable diversity in neuronal morphology, most neurons share a common structural organization consisting of the cell body (soma), dendrites, and axon (Fig.3), [1].

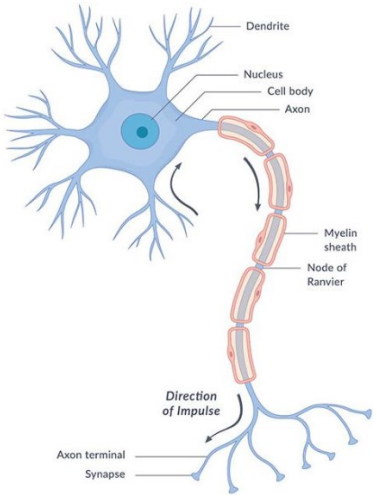


Figure 3. General structure of a neuron showing dendrites, soma, axon, myelin sheath, and synaptic terminals involved in neural signal transmission [5].

The soma contains the nucleus and the cellular machinery necessary for protein synthesis and metabolic activity, while also acting as the principal site for signal integration. Extending from the soma, dendrites form branched structures specialized in receiving synaptic inputs from other neurons. Their extensive arborization increases the receptive surface of the neuron and enables the establishment of numerous synaptic connections within neural networks [1]. The axon is a single elongated projection specialized in transmitting electrical signals over long distances. It originates from the axon hillock, a region where incoming electrical signals are integrated and where action potentials are typically initiated [2]. In many neurons, the axon is surrounded by a myelin sheath produced by glial cells, which electrically insulates the membrane and significantly increases conduction velocity. At its distal end, the axon branches into terminal boutons that establish synaptic contacts with other neurons or target cells. This structural organization gives rise to a functional polarity within the neuron, meaning that different neuronal compartments are specialized for distinct stages of information processing and transmission: dendrites primarily receive synaptic inputs, the soma integrates these signals, the axon conducts electrical impulses away from the cell body, and the

synaptic terminals transmit information to other neurons or target cells [2]. Neuronal communication depends on the electrical properties of the cell membrane, which are determined by ionic gradients and selective membrane permeability. Under resting conditions, neurons maintain a stable electrical potential difference across the membrane, known as the resting membrane potential, mainly generated by the distribution of ions such as sodium, potassium, and chloride and by the activity of ion channels and membrane pumps [1]. When synaptic inputs produce sufficient membrane depolarization to reach a critical threshold, an action potential is generated. The rising phase of the action potential is primarily caused by the opening of voltage-gated sodium channels and the consequent influx of Na^+ ions into the neuron, which produces rapid membrane depolarization. Subsequently, sodium channels become inactivated and voltage-gated potassium channels open, allowing K^+ ions to flow out of the cell and promoting membrane repolarization. A transient hyperpolarization may follow before the membrane potential returns toward its resting level. This rapid and transient electrical signal propagates along the axon without decrement through the coordinated activation and inactivation of voltage-gated ion channels [2]. Information within neural circuits is encoded through patterns of neuronal activity, in which both firing frequency and temporal organization contribute to signal transmission and processing [1]. Communication between neurons occurs primarily at specialized junctions known as synapses, where signals are transmitted from one cell to another. A synapse consists of a presynaptic terminal, belonging to the neuron that transmits the signal, and a postsynaptic membrane, belonging to the receiving cell, separated by a narrow space known as the synaptic cleft [1]. Synapses can be broadly classified into chemical and electrical synapses, although chemical synapses represent the predominant form in the human brain [1]. In chemical synapses, the arrival of an action potential at the presynaptic terminal triggers the opening of voltage-gated calcium channels and the subsequent release of neurotransmitters through vesicle fusion. These neurotransmitters diffuse across the synaptic cleft and bind to receptors located on the postsynaptic membrane, producing excitatory or inhibitory effects depending on the type of receptor involved [1]. These effects generate postsynaptic potentials, which are graded changes in the membrane potential of the postsynaptic cell and can be either excitatory or inhibitory. Unlike action potentials, which are all-or-none electrical signals that propagate along the axon, postsynaptic potentials vary in amplitude and can summate in space and time. Their combined effect determines whether the postsynaptic neuron reaches the threshold required to generate an action potential [1].

Electrical synapses, in contrast, allow the direct passage of ionic currents between adjacent cells through gap junctions, enabling extremely rapid and synchronized communication between neurons [1]. Although neurons represent the basic functional elements of the nervous system, brain function emerges from the coordinated activity of large populations of interconnected neurons organized into

complex networks. Neural circuits involve both local and long-range connections, allowing electrical activity and information to be transmitted and integrated across different regions of the brain [1]. At the network level, neuronal populations exhibit coordinated oscillatory patterns generated by the interaction between excitatory and inhibitory neurons and shaped by synaptic connectivity and intrinsic cellular properties. These oscillations contribute to the coordination of neuronal activity and facilitate communication between spatially distributed brain regions [6]. Therefore, the electrical activity generated at the cellular and synaptic levels can propagate through interconnected neural networks, enabling the exchange and integration of information across different areas of the brain.

1.1.3 Oscillatory Activity and Brain Rhythms

Brain function emerges from the coordinated activity of large populations of interconnected neurons, whose interactions generate characteristic temporal patterns of electrical activity throughout the central nervous system [7]. At the network level, this coordinated activity can give rise to rhythmic fluctuations that contribute to the temporal organization of brain processes and support communication between distributed brain regions. These rhythmic patterns of electrical activity are referred to as brain rhythms or neural oscillations and represent a fundamental characteristic of brain function [7]. Consequently, neural oscillations are not regarded as simple background activity or physiological noise, but rather as a key mechanism involved in the regulation and coordination of information processing in the brain [8]. Neural oscillations are commonly classified into distinct frequency bands, each associated with specific functional and physiological states. Although frequency boundaries may vary slightly across studies, brain rhythms are generally divided into delta, theta, alpha, beta, and gamma bands [7]. Delta oscillations (approximately 0.5–4 Hz) are predominantly associated with deep sleep and reduced levels of consciousness. Theta rhythms (4–8 Hz) are frequently related to cognitive and memory-related processes, whereas alpha oscillations (8–13 Hz) are mainly observed during relaxed wakefulness, particularly with closed eyes. Beta rhythms (13–30 Hz) are commonly linked to active thinking, motor activity, and sensorimotor processing, while gamma oscillations (above 30 Hz) are associated with higher cognitive functions including perception, attention, and information integration [8].

A key aspect of neural oscillations is the synchronization of neuronal populations. By providing a common temporal framework, oscillatory activity enables groups of neurons to coordinate their firing, thereby facilitating effective communication between distributed neural circuits. This synchronization is considered essential for selective transmission and integration of information across functionally specialized brain regions [10].

According to the "communication through coherence" framework, the efficacy of neuronal interactions depends on the phase relationship between oscillations in interconnected brain areas. When oscillatory phases are aligned, synaptic inputs arrive during periods of increased neuronal excitability, enhancing the probability of successful signal transmission. Conversely, phase misalignment may reduce the effectiveness of incoming signals, thereby dynamically regulating communication between neural populations [10]. The generation of neural oscillations results from the interaction between intrinsic neuronal properties and the organization of neural circuits [7]. At the network level, rhythmic activity emerges from the coordinated interplay between excitatory and inhibitory neuronal populations. Inhibitory interneurons play a central role in synchronizing the activity of excitatory pyramidal neurons and in shaping coherent oscillatory patterns, especially within the gamma-frequency range. The frequency and temporal characteristics of these rhythms are further influenced by membrane conductances, ion channel kinetics, and synaptic time constants [11]. Beyond local cortical networks, large-scale brain rhythms are strongly influenced by thalamo-cortical interactions. Through its reciprocal connections with the cerebral cortex, the thalamus contributes to the generation and modulation of neural oscillations and promotes the synchronization of activity across widespread brain regions [7].

1.2 Epilepsy: clinical background and pathophysiology

Epilepsy is a chronic neurological disorder characterized by a predisposition to generate recurrent seizures and associated with a wide range of clinical manifestations. Beyond its neurological nature, epilepsy represents a complex condition with significant implications for patients' quality of life and overall health. Understanding its definition, epidemiological distribution, and clinical impact is essential to contextualize its relevance as a major public health issue and to motivate the need for effective diagnostic and monitoring strategies.

1.2.1 Definition, epidemiology and clinical relevance

The International League Against Epilepsy (ILAE) defines epilepsy as a disease of the brain characterized by an enduring predisposition to generate epileptic seizures together with the associated neurobiological, cognitive, psychological, and social consequences [12]. According to the operational clinical definition proposed by the ILAE, epilepsy can be diagnosed under any of the following conditions: the occurrence of at least two unprovoked seizures more than 24 hours apart; one unprovoked seizure associated with a recurrence risk that is considered sufficiently high comparable to that observed after two unprovoked seizures; or the diagnosis of a recognized epilepsy syndrome

(Fig.5), [12]. This definition reflects the concept of epilepsy as a condition characterized by a persistent predisposition to recurrent seizures rather than an isolated seizure event. A fundamental aspect of epilepsy diagnosis concerns the distinction between provoked and unprovoked seizures. Provoked seizures, also referred to as acute symptomatic seizures, occur in association with transient conditions affecting brain excitability, such as fever, metabolic disturbances, alcohol withdrawal, or acute brain injury, and do not necessarily indicate epilepsy [12]. In contrast, unprovoked seizures are not associated with an immediate reversible cause and may reflect an underlying epileptogenic abnormality that predisposes the brain to recurrent seizure activity [12]. The ILAE definition also highlights the importance of recurrence risk in clinical evaluation. Following a first unprovoked seizure, the probability of recurrence may vary according to factors such as structural brain lesions, epileptiform EEG abnormalities, and specific clinical syndromes [12]. Furthermore, the diagnosis of a recognized epilepsy syndrome is itself considered sufficient for the diagnosis of epilepsy, an aspect particularly relevant in pediatric neurology, where several age-dependent syndromes present characteristic clinical and electroencephalographic features that support early identification and classification [12].

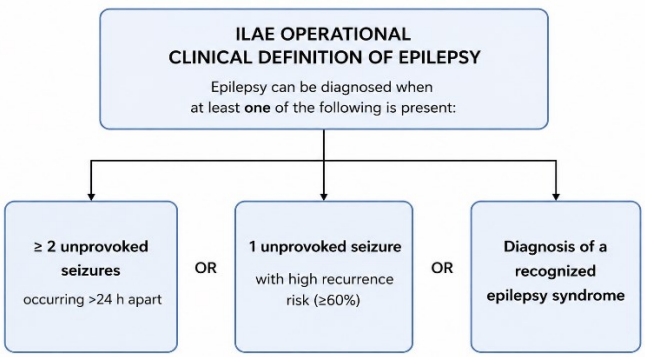


Figure 4. Operational clinical definition of epilepsy according to the International League Against Epilepsy (ILAE), adapted from Fisher et al. [12].

Epidemiological studies have demonstrated considerable variability in the prevalence and incidence of epilepsy across different geographic regions and populations. A large systematic review and meta-analysis estimated the pooled point prevalence of active epilepsy at 6.38 cases per 1,000 individuals and the pooled incidence rate at 61.44 cases per 100,000 person-years [13]. Higher prevalence and incidence rates have frequently been reported in low- and middle-income countries, where factors such as central nervous system infections, perinatal complications, limited healthcare access, and treatment gaps may contribute to the increased burden of the disease [13]. Epidemiological analyses have also shown an age-dependent distribution of epilepsy, with incidence rates generally higher during early childhood and older adulthood [13].

The epidemiology of epilepsy is characterized by substantial heterogeneity between studies, partly resulting from differences in diagnostic criteria, case definitions, study methodologies, and population characteristics [13]. For this reason, standardized epidemiological frameworks and consistent definitions are considered essential for improving the comparability and reliability of epilepsy research across different clinical settings and populations [14]. Standardized measures such as point prevalence and incidence rate are particularly important for accurately estimating disease burden, evaluating healthcare needs, and supporting etiological investigations [14].

Beyond its epidemiological impact, epilepsy represents one of the most common serious neurological disorders worldwide and constitutes a major public health concern because of its long-term clinical, psychosocial, and socioeconomic consequences [15]. The burden of epilepsy extends beyond the occurrence of seizures and affects multiple aspects of an individual's life, including physical health, cognitive function, mental health, education, employment, and social participation. As a consequence, many patients experience substantial limitations in daily activities and reduced quality of life [15]. Psychiatric and cognitive comorbidities are highly prevalent in epilepsy and contribute significantly to disease burden. Depression and anxiety are among the most common psychiatric disorders associated with epilepsy, while cognitive impairment may affect memory, attention, and executive function. In addition, social stigma and discrimination continue to represent important challenges for many patients, further worsening psychosocial well-being and social integration [15]. The clinical relevance of epilepsy is further increased by the risk of severe complications and premature mortality. Patients with epilepsy present significantly higher mortality rates compared with the general population, particularly in cases characterized by uncontrolled seizures, convulsive seizures, or structural and metabolic etiologies [16]. Among epilepsy-related causes of death, sudden unexpected death in epilepsy (SUDEP) represents one of the most serious complications and is strongly associated with persistent or poorly controlled seizures. Additional causes of epilepsy-related mortality include status epilepticus, seizure-related injuries, and suicide [16]. Epidemiological studies have also shown increased mortality associated with drowning, falls, burns, and transport-related accidents, reflecting the substantial impact of seizures on patient safety and daily functioning [16]. A substantial proportion of patients develop drug-resistant epilepsy, defined as the persistence of seizures despite appropriate antiseizure treatment. Drug-resistant epilepsy is associated with increased morbidity, repeated hospitalizations and poorer long-term clinical outcomes, highlighting the importance of continuous clinical follow-up and optimized therapeutic strategies [15]. Several epilepsy-related causes of mortality are considered potentially preventable, emphasizing the importance of early diagnosis, effective seizure control, and access to specialized healthcare services. Long-term monitoring and appropriate management strategies may therefore contribute to reducing

epilepsy-related morbidity and premature mortality while improving long-term patient outcomes [16].

From a global health perspective, epilepsy represents a major cause of disability and premature mortality worldwide [17]. According to the Global Burden of Disease (GBD) study, epilepsy contributes substantially to disability-adjusted life years (DALYs), which combine years of life lost due to premature mortality and years lived with disability. The burden of epilepsy is disproportionately higher in low- and middle-income countries, where limited access to diagnosis, antiseizure treatment, and specialized neurological care contributes to large treatment gaps and poorer clinical outcomes [17]. In these regions, preventable causes such as central nervous system infections, traumatic brain injuries, and perinatal complications remain important contributors to epilepsy incidence and disease burden. Considerable regional disparities in epilepsy burden have also been associated with differences in socioeconomic conditions, healthcare infrastructure, and availability of medical resources [17]. In pediatric populations, epilepsy is particularly critical because recurrent seizures and abnormal neuronal activity may interfere with brain maturation and neurodevelopmental processes. Consequently, epilepsy during childhood can negatively affect cognition, learning abilities, behavior, and long-term neurological outcomes [15], [17]. These factors emphasize the need for early diagnosis and appropriate long-term management in pediatric epilepsy in order to reduce seizure burden and limit the impact of the disease on cognitive and developmental functions.

1.2.2 Pathophysiological mechanisms of epilepsy

Epilepsy is a complex neurological disorder characterized by abnormal neuronal activity arising from alterations at multiple levels of brain organization. At the cellular level, changes in neuronal excitability contribute to the generation of abnormal electrical discharges. At the network level, the interaction between neuronal populations supports the synchronization and propagation of epileptic activity. In addition, both genetic and structural factors play a significant role in the development of epilepsy, reflecting its heterogeneous nature. Therefore, understanding epilepsy requires considering the interaction between cellular, network, genetic, and structural mechanisms.

Neuronal hyperexcitability represents one of the fundamental pathophysiological mechanisms underlying epileptic activity and refers to an increased tendency of neurons and neural circuits to generate abnormal electrical discharges [18]. Epileptic seizures arise from excessive and atypical neuronal firing caused by alterations in the mechanisms that normally regulate excitability and maintain stable patterns of brain activity. Under physiological conditions, neuronal activity is tightly regulated through the interaction between intrinsic membrane properties and synaptic mechanisms.

These processes control action potential generation and preserve the balance between excitation and inhibition within neural circuits. In epileptic conditions, however, this regulation becomes disrupted, causing neurons to respond excessively to synaptic or intrinsic stimuli and facilitating sustained neuronal firing [18]. At the cellular level, neuronal excitability is strongly influenced by membrane conductances and by the activity of voltage-gated ion channels regulating ionic fluxes across the neuronal membrane [18], [19]. Alterations involving sodium, potassium, and calcium channels can therefore significantly modify neuronal excitability by affecting action potential generation and propagation as well as synaptic transmission [19]. In particular, increased inward depolarizing currents or reduced potassium-mediated repolarization may facilitate prolonged depolarization and repetitive neuronal discharge activity, thereby lowering the threshold for seizure generation. In addition, abnormalities in ion channel function may disrupt the normal regulation of neuronal firing and further contribute to hyperexcitability [19]. Changes in the extracellular ionic environment, including alterations in potassium and calcium concentrations, may also promote membrane depolarization and synchronized neuronal activity. Moreover, genetic alterations affecting ion channel function, commonly referred to as channelopathies, can directly predispose neuronal networks to epileptic activity by modifying intrinsic membrane excitability [19]. A characteristic feature of epileptiform activity is the presence of paroxysmal depolarization shifts (PDSs), consisting of prolonged membrane depolarizations associated with bursts of action potentials followed by hyperpolarization phases [18]. These abnormal depolarizing events are considered one of the principal cellular hallmarks of epileptiform discharges [18]. In addition to intrinsic membrane abnormalities, synaptic mechanisms play a central role in the modulation of neuronal excitability (Fig.6). Enhanced excitatory neurotransmission, primarily mediated by glutamatergic synapses through AMPA[1] and NMDA[2] receptors, can increase depolarizing input within neural circuits, whereas impaired inhibitory signaling associated with dysfunctional GABAergic[3] transmission may

[1] AMPA receptors are ionotropic glutamate receptors responsible for fast excitatory synaptic transmission in the central nervous system [18].

[2] NMDA receptors are glutamate-gated ion channels involved in excitatory neurotransmission and synaptic plasticity, characterized by voltage-dependent activation and calcium permeability [18].

[3] GABAergic transmission refers to inhibitory synaptic signaling mediated by gamma-aminobutyric acid (GABA), the principal inhibitory neurotransmitter of the central nervous system [18].

reduce the ability of neuronal networks to suppress excessive excitation. Dysfunction of inhibitory interneurons and alterations in inhibitory synaptic activity may therefore facilitate seizure onset and spread by weakening physiological inhibitory control mechanisms [18], [19].

Repeated epileptic activity may also induce long-term alterations in synaptic organization and connectivity, promoting recurrent excitation and increasing susceptibility to seizure recurrence over time [19]. While neuronal hyperexcitability provides a substrate for abnormal electrical activity, epileptic seizures emerge from the dynamic interaction of distributed neuronal networks rather than isolated neuronal dysfunction alone [20], [21]. In particular, thalamocortical circuits play a central role in the generation and maintenance of rhythmic epileptiform activity. Reciprocal connections between cortical and thalamic structures form recurrent activation loops capable of sustaining the oscillatory patterns observed in several seizure types, including spike-wave discharges [20]. Epilepsy is therefore increasingly considered a disorder of large-scale brain network organization. Functional connectivity studies have shown that seizure activity involves continuously evolving interactions between interconnected cortical regions, reflecting the dynamic nature of epileptic networks [21]. Although seizures were traditionally interpreted as purely hypersynchronous events, experimental evidence indicates that neuronal activity during seizures is highly heterogeneous and changes throughout seizure evolution [22]. Early seizure phases may involve irregular or partially decoupled neuronal activity, whereas more coordinated patterns frequently emerge during later stages and may contribute to seizure termination. The spread of epileptic activity depends on the progressive recruitment of interconnected neuronal populations across cortical and subcortical regions [22]. Electrophysiological techniques such as EEG and intracranial recordings have provided important insights into these network dynamics, allowing the characterization of seizure onset, evolution, and termination through the analysis of neuronal rhythms and functional connectivity [21].

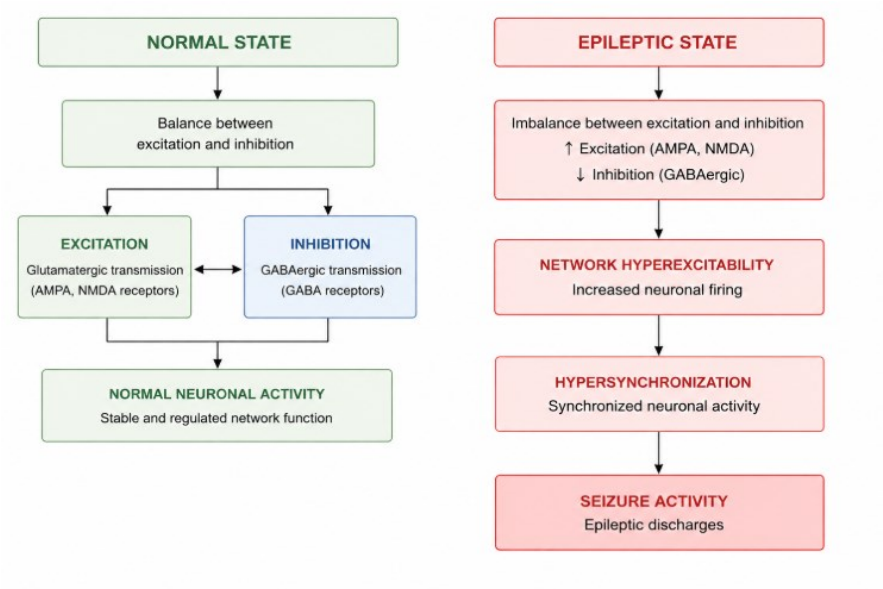


Figure 5. Schematic representation of the imbalance between excitatory and inhibitory mechanisms underlying neuronal hyperexcitability and epileptic activity, adapted from Blumenfeld et al [19].

In addition to cellular and network mechanisms, the development of epilepsy can also be influenced by genetic and structural factors. Genetic factors play a central role in the development of epilepsy and have contributed to the recognition of epilepsies as a heterogeneous group of disorders characterized by different underlying mechanisms [23]. Advances in genetic technologies have enabled the identification of an increasing number of epilepsy-associated genes, improving the understanding of epilepsy pathophysiology and supporting more accurate diagnostic approaches [23]. The genetic basis of epilepsy includes multiple types of genomic alterations, such as chromosomal abnormalities, copy number variations, genomic rearrangements, and single-nucleotide mutations that may alter gene function and contribute to epileptogenesis. These abnormalities may be inherited or may arise de novo during gamete formation or early embryonic development. In particular, somatic mutations affecting cells involved in brain development may disrupt neuronal network organization and facilitate the emergence of epileptic activity [23]. Among the different pathogenic mechanisms, channelopathies represent one of the best characterized causes of epilepsy. These disorders result from mutations affecting genes encoding ion channels involved in the regulation of neuronal excitability and synaptic activity. Mutations in sodium channel genes, particularly *SCN1A*, are frequently associated with a broad spectrum of epileptic syndromes, whereas alterations involving potassium channel genes such as *KCNQ2* and *KCNQ3* have also been linked to different epilepsy phenotypes [23]. In addition to ion channel dysfunction, epilepsy-related genetic alterations may involve mechanisms regulating synaptic transmission, transcription pathways, vesicle trafficking,

cellular signaling, and metabolic processes, all of which may influence neuronal communication and network stability.

The relationship between genotype and clinical phenotype is often complex. Similar clinical manifestations may arise from distinct genetic mechanisms, whereas mutations affecting the same gene can produce different epilepsy syndromes [23]. Moreover, genetic alterations involving pathways responsible for brain development may contribute to structural abnormalities associated with epilepsy, including malformations of cortical development. These abnormalities can disrupt normal neuronal organization and facilitate the formation of epileptic networks. Overall, advances in epilepsy genetics have progressively shifted the understanding of epilepsy from a purely symptomatic disorder toward a heterogeneous group of conditions involving complex interactions between genetic, developmental, and network mechanisms [23]. Structural factors also represent an important cause of epilepsy and refer to the presence of identifiable abnormalities in brain structure associated with an increased risk of seizure generation [24]. According to the ILAE classification, a structural etiology is defined when a structural abnormality is identified and electroclinical evaluation, together with neuroimaging findings, supports the inference that the lesion is responsible for the patient's seizures. Structural abnormalities may arise from acquired conditions such as stroke, traumatic brain injury, infections, and hypoxic–ischemic encephalopathy, or from developmental abnormalities involving cortical organization [24]. In both cases, alterations of normal brain architecture may interfere with neuronal connectivity and favor the development of epileptic activity. Importantly, structural and genetic etiologies are not mutually exclusive, and a patient's epilepsy may be classified into more than one etiological category simultaneously. Certain developmental brain abnormalities may have an underlying genetic basis while also presenting as structural lesions detectable on neuroimaging [24].

For this reason, the integration of clinical assessment with neuroimaging findings is essential for accurate etiological classification. Magnetic resonance imaging, particularly when performed using dedicated epilepsy protocols, plays a central role in identifying structural abnormalities and supporting diagnostic evaluation. The recognition of structural etiologies is especially important in drug-resistant epilepsy, as it may guide therapeutic planning and support the evaluation of potential surgical treatment [24].

1.2.3 Clinical classification of seizures: focal and generalized

The classification of epileptic seizures represents a fundamental component of epilepsy diagnosis and clinical management, providing a structured framework for communication, diagnostic evaluation, and treatment planning [25]. According to the International League Against Epilepsy (ILAE), epileptic seizures are transient events resulting from abnormal excessive and synchronous neuronal activity in the brain and may manifest through a broad spectrum of motor, sensory, autonomic, cognitive, emotional, or behavioral symptoms [25], [15]. The current ILAE framework adopts an operational clinical approach to seizure classification, integrating observable clinical manifestations with electroencephalographic and neuroimaging findings when available [24], [25]. This approach reflects the current understanding that, despite advances in neurophysiology and neuroimaging, a fully mechanistic classification of seizures and epilepsies is not yet achievable [24]. A central aspect of the current classification concerns the identification of seizure onset, as this provides important information regarding the underlying epileptic networks and may guide diagnostic evaluation and therapeutic decisions [25]. Based on seizure onset, epileptic seizures are categorized into focal onset, generalized onset, and unknown onset seizures (Fig. 7) [25]. Focal seizures originate within neuronal networks limited to one hemisphere, although epileptic activity may subsequently propagate to involve additional cortical and subcortical regions. In contrast, generalized seizures arise within and rapidly engage bilaterally distributed networks involving both hemispheres from seizure onset [25], [15]. When seizure onset cannot be clearly determined because of insufficient clinical or electroencephalographic information, seizures are classified as having unknown onset [25]. The current ILAE framework also distinguishes between seizure type, epilepsy type, and epilepsy syndrome, which represent different levels of diagnostic classification [24]. Seizure type refers to the clinical manifestation of the individual seizure event, whereas epilepsy type describes the broader pattern of epileptic activity and includes focal epilepsy, generalized epilepsy, combined generalized and focal epilepsy, and unknown epilepsy. In some patients, a specific epilepsy syndrome may also be identified on the basis of characteristic clinical, electroencephalographic, imaging, and age-related features [24]. Focal seizures are further characterized according to the level of awareness during the event, which represents an important clinical feature in the current ILAE classification [25]. Awareness refers to the patient's knowledge of self and environment during the seizure and may be either preserved or impaired. In addition, focal seizures are classified according to their initial manifestations into motor and non-motor onset seizures [25]. Motor onset seizures may include automatisms, tonic activity, clonic movements, myoclonic jerks, or atonic manifestations, whereas non-motor onset seizures may instead present with sensory, cognitive, emotional, autonomic, or behavioral symptoms [25]. The earliest prominent clinical manifestation is particularly important

because it may reflect the anatomical region involved at seizure onset [25], [15]. An additional category includes focal seizures evolving to bilateral tonic–clonic seizures, in which epileptic activity initially arises within a localized network and subsequently spreads to involve both hemispheres [25]. This pattern reflects the dynamic nature of seizure propagation and the ability of epileptic activity to recruit distributed neuronal networks during seizure evolution [25], [15].

Generalized seizures are characterized by rapid bilateral involvement from seizure onset and typically produce widespread clinical manifestations [25]. Common generalized seizure types include absence seizures, characterized by brief episodes of impaired awareness; tonic–clonic seizures, involving sustained muscle contraction followed by rhythmic jerking movements; and myoclonic seizures, consisting of sudden brief muscle jerks. Depending on the seizure type, generalized seizures may present with motor or non-motor manifestations and are commonly associated with impaired awareness during the event [25]. The updated ILAE framework also recognizes the category of combined generalized and focal epilepsy, acknowledging that some patients may present with both generalized and focal seizure types [24]. Electroencephalographic recordings provide important information regarding seizure onset, propagation, and network involvement, supporting the clinical classification of seizure types and contributing to the identification of epileptic activity patterns [15]. Furthermore, epilepsy classification may evolve over time as additional clinical, electroencephalographic, or neuroimaging information becomes available, reflecting the dynamic nature of epilepsy diagnosis and management [25], [24].

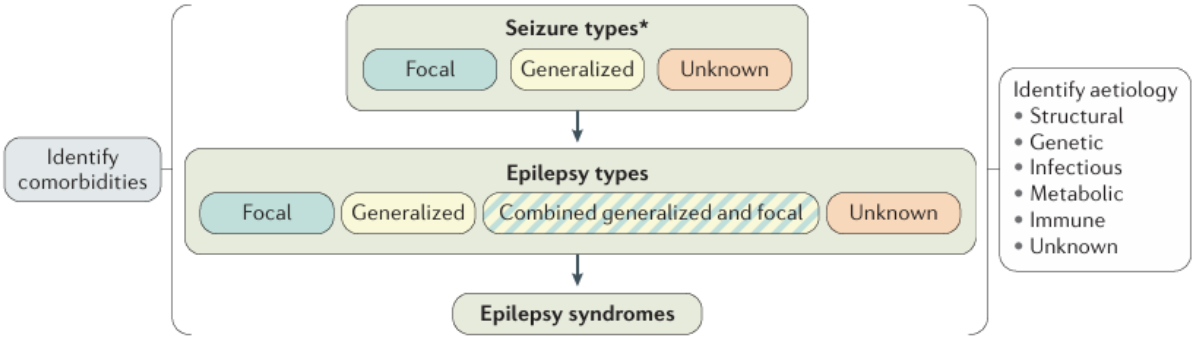


Figure 6. Framework of the ILAE classification of epileptic seizures and epilepsies, including seizure types, epilepsy types, epilepsy syndromes, etiological categories, and associated comorbidities [15].

1.3 Epilepsy detection with Electroencephalography

Electroencephalography (EEG) is one of the main diagnostic tools used in the evaluation of epilepsy, providing non-invasive recordings of brain electrical activity with high temporal resolution. EEG plays a central role in seizure detection, epilepsy classification, and patient monitoring through the identification of abnormal electrophysiological patterns associated with epileptic activity. This chapter introduces the basic principles of EEG, the main acquisition techniques and artifacts affecting recordings, the characteristics of interictal epileptiform discharges, and recent advances in EEG biomarkers for epilepsy detection and monitoring.

1.3.1 Electroencephalograghy basics and brain rhythms

EEG is a technique used to record the electrical activity of the brain. In clinical practice, EEG activity is most commonly recorded non-invasively through electrodes positioned on the scalp, a technique generally referred to as scalp EEG [1], [26]. Scalp EEG provides an indirect measure of neuronal activity by detecting the summed electrical potentials generated by large populations of neurons over time. These signals primarily reflect synchronized postsynaptic potentials rather than action potentials from individual neurons. Experimental evidence indicates that the main contributors to scalp EEG activity are cortical pyramidal neurons, particularly those located within the deeper cortical layers. Because these neurons are arranged in parallel and oriented perpendicular to the cortical surface, the electrical fields generated by excitatory and inhibitory synaptic activity can summate effectively and become detectable at the scalp level [1], [27]. The electrical activity generated within cortical networks propagates through brain tissues, cerebrospinal fluid, skull, and scalp before reaching the recording electrodes, a phenomenon referred to as volume conduction [27]. Consequently, scalp EEG provides excellent temporal resolution but limited spatial resolution, since the recorded signals represent the averaged activity of relatively large cortical regions rather than the activity of individual neurons [1], [27]. EEG oscillations emerge from the interaction between excitatory and inhibitory neuronal populations within cortical and thalamocortical circuits, contributing to the generation of rhythmic brain activity under different physiological conditions [1]. Scalp recordings are obtained using conductive electrodes connected to amplifiers capable of detecting electrical signals with amplitudes typically ranging from microvolts to low millivolts [27]. Proper electrode impedance is essential for reliable signal acquisition, as excessive impedance may increase noise artifacts and compromise recording quality. During acquisition, EEG signals undergo amplification, analogue-to-digital conversion, and filtering procedures that allow the visualization and analysis of clinically relevant frequency components while attenuating electrical interference and physiological artifacts [26].

Standardized electrode positioning is essential to ensure reproducible and comparable recordings across patients and clinical centers. The most widely adopted configuration is the International 10–20 system, in which electrode positions are determined according to proportional distances between anatomical landmarks of the skull, including the nasion, inion, and preauricular points (Fig.8) [26], [27]. Electrode nomenclature follows a standardized convention in which letters indicate the underlying cortical region, whereas odd and even numbers identify the left and right hemispheres, respectively [26]. Standard scalp EEG recordings provide spatial sampling of cortical electrical activity through multiple recording sites distributed over the head surface. However, conventional electrode arrays may provide limited coverage of some brain regions, particularly the inferior and basal temporal areas frequently involved in epileptogenic activity [26].

For this reason, extensions of the traditional 10–20 system, including the 10–10 system and high-density EEG arrays, have been developed to improve spatial sampling and source localization accuracy. High-density scalp EEG systems, typically employing 64 to 256 electrodes, allow for a more detailed characterization of cortical activity and may improve the detection and localization of epileptiform discharges [26]. In pediatric EEG recordings, adequate spatial sampling is particularly important because thinner skull structures may increase the risk of spatial under-sampling and localization errors when a reduced number of electrodes is used. Consequently, current recommendations suggest that pediatric EEG recordings should employ at least the same number of electrodes commonly used in adults [26].

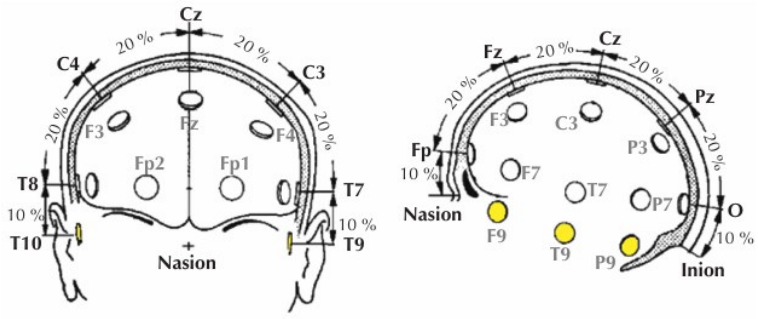


Figure 7. International 10–20 electrode placement system used in clinical scalp EEG recordings [27].

EEG activity is represented by waveforms corresponding to fluctuations in the electrical potential difference recorded between pairs of electrodes [28]. The morphology of an EEG waveform is commonly described in terms of amplitude, frequency, and polarity. EEG amplitude reflects the voltage variation of the recorded signal and is generally measured in microvolts (μV), with normal adult brain activity typically ranging between 10 and 100 μV. Variations in EEG amplitude may occur

under physiological conditions, such as eye opening, or in association with pathological states affecting cerebral function [28]. EEG waveforms are traditionally classified according to their frequency content. In clinical EEG practice, the conventional bandwidth ranges approximately from 0.5 to 30 Hz and includes the main physiological rhythms: delta (0.5–4 Hz), theta (4–8 Hz), alpha (8–12 Hz), and beta activity (13–30 Hz) (Fig. 9). Delta rhythms are typically observed during deep sleep, whereas theta activity is commonly associated with drowsiness and early sleep stages [28]. Alpha activity represents the dominant posterior rhythm during relaxed wakefulness with closed eyes and is attenuated by eye opening or mental effort, while beta activity is generally associated with alertness and active cognitive processing. In addition to conventional EEG frequency bands, higher-frequency oscillations such as gamma activity and high-frequency oscillations (HFOs) have gained increasing clinical interest owing to advances in digital EEG technology and signal processing methods. Gamma activity, typically above 30 Hz, has been associated with cognitive processes including perception and information integration, whereas HFOs are increasingly investigated as potential biomarkers of epileptic activity [28].

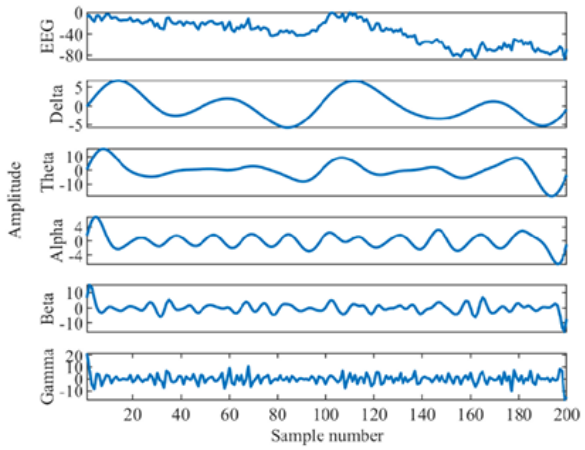


Figure 8. Example of EEG signal decomposition into the main physiological frequency bands [28].

1.3.2 Electroencephalography acquisition modalities and artifacts

Routine EEG represents the standard electroencephalographic examination used in clinical practice for the evaluation of patients with suspected epilepsy and other neurological disorders [29]. According to the ILAE recommendations, routine EEG remains an essential non-invasive method for the assessment of electrophysiological brain activity and plays an important role not only in epilepsy diagnosis, but also in syndrome classification and clinical follow-up. The principal indication for EEG recording is the clinical suspicion of seizures or epilepsy, although EEG may also contribute to the evaluation of paroxysmal neurological events and differential diagnoses [29]. Standard routine

EEG recordings are generally short-term examinations lasting approximately 20–30 minutes and are commonly performed without simultaneous video monitoring. Despite the relatively limited recording duration, routine EEG remains widely used because it is accessible, inexpensive, and often sufficient in many clinical situations [30]. To improve the detection of epileptiform abnormalities, routine EEG recordings are frequently combined with activation procedures, including hyperventilation, intermittent photic stimulation, eye opening and closure, and sleep recording [29], [30]. Among these procedures, sleep is considered particularly valuable because epileptiform discharges are influenced by vigilance state and occur more frequently during non-rapid eye movement (NREM) sleep than during wakefulness [29]. Several studies reviewed in the ILAE guideline demonstrated that sleep EEG may provide additional diagnostic information in patients with suspected epilepsy and initially normal wake EEG recordings. The diagnostic sensitivity of EEG further increases with repeated examinations and may be enhanced by sleep deprivation protocols [29]. In pediatric patients, sleep recordings are especially useful because movement and muscle artifacts during wakefulness may significantly reduce recording interpretability. The guideline also recommends scheduling EEG examinations in infants and young children during periods that facilitate spontaneous sleep onset, such as the postprandial period [29].

In addition to routine EEG, several prolonged acquisition modalities are currently used in epilepsy evaluation [30]. Long-term EEG recordings provide extended sampling of brain activity and increase the probability of detecting interictal abnormalities or capturing clinical events. Ambulatory EEG represents an outpatient prolonged recording modality that may last from one to several days and can be performed with or without synchronized video acquisition.

This approach allows monitoring in the patient's habitual environment while reducing the need for hospitalization [30]. Video-EEG monitoring combines prolonged EEG recording with simultaneous video documentation of patient behavior and is considered the gold standard for the evaluation of difficult or unclear seizure disorders. Simultaneous correlation between electroencephalographic abnormalities and clinical manifestations allows clinicians to determine whether recorded events are epileptic or non-epileptic, classify seizure type, and, in focal epilepsies, identify the probable seizure onset zone [30]. Although video-EEG monitoring has traditionally been performed in specialized inpatient epilepsy monitoring units, advances in digital recording technology have progressively expanded its use in ambulatory and home settings in selected patients. One of the main objectives of EEG recordings in epilepsy is the identification of interictal epileptiform discharges (IEDs), which are abnormal transient EEG waveforms occurring between epileptic seizures [31]. In contrast to ictal activity, which reflects electrical activity occurring during a seizure, interictal activity refers to

epileptiform abnormalities detected between seizure events. The most common IED patterns include spikes, sharp waves, and spike-and-slow-wave complexes [32]. Their identification is clinically relevant because the presence of IEDs supports the diagnosis and classification of epilepsy; however, a normal EEG does not exclude epilepsy, since epileptiform abnormalities may not occur during the recording or may not be detectable using routine scalp EEG [33].

Since EEG signals are characterized by low amplitudes, they require amplification and digitization before further analysis. During EEG acquisition, differential amplifiers measure the potential difference between electrode pairs while reducing external interference and common-mode noise. After analogue-to-digital conversion, EEG recordings can undergo computational processing and signal analysis. Acquisition parameters such as sampling rate, filtering settings, and reference configuration influence signal quality and must be carefully considered during EEG interpretation and automated analysis. EEG recordings are frequently affected by artifacts, defined as electrical potentials that do not originate from the signal of interest but are nevertheless detected during EEG acquisition [34]. Artifacts may arise from physiologic or nonphysiologic sources and can obscure the EEG tracing or mimic epileptiform abnormalities, potentially leading to misinterpretation. Nonphysiologic artifacts are commonly related to the recording equipment, electrode connections, or environmental electrical interference. Poor electrode contact, excessive electrode impedance, cable movements, and alternating current interference at 50–60 Hz may generate waveforms that resemble pathological EEG activity. Electrode artifacts are particularly suspected when abnormal activity is limited to a single channel or lacks a physiologically plausible electrical field [34]. Physiologic artifacts originate from biological processes other than cerebral electrical activity and are frequently encountered during routine EEG recordings. Common physiologic artifacts include ocular activity, muscle activity, cardiac signals, and movement-related artifacts. Eye movement artifacts are generated by the corneoretinal electrical dipole and are especially evident during blinking, drowsiness, and rapid eye movement sleep (Fig.9) [34]. Myogenic artifacts produced by muscles such as the frontalis and temporalis may generate high-frequency activity that can resemble epileptiform discharges [34]. Similarly, electrocardiographic artifacts may periodically appear within EEG channels and occasionally imitate epileptiform abnormalities, although their regular synchronization with cardiac rhythm usually facilitates recognition. Additional artifacts related to swallowing, chewing, sweating, respiratory movements, or cable motion may further interfere with EEG interpretation, particularly during prolonged recordings or pediatric examinations [34]. Accurate recognition of artifacts therefore represents an essential component of EEG interpretation and clinical analysis.

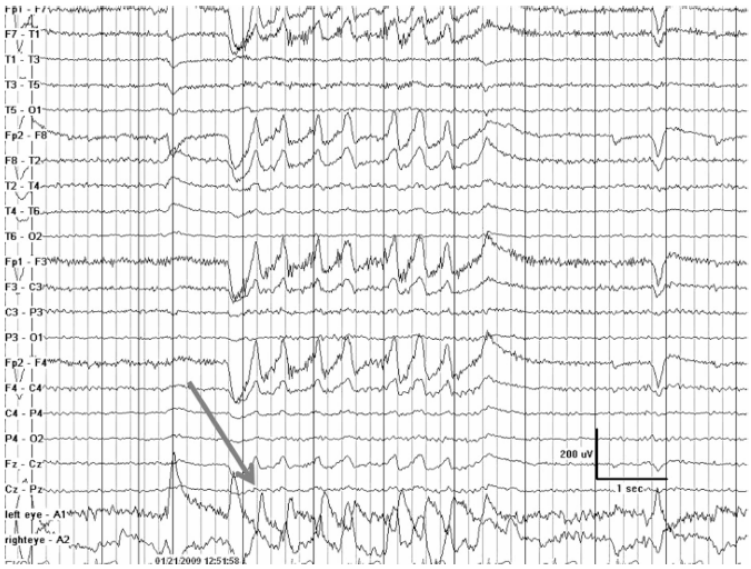


Figure 9. Example of ocular artifacts recorded during scalp EEG. Eye movements generate characteristic slow deflections due to the corneoretinal electrical dipole and may interfere with EEG interpretation [34].

1.3.3 Advanced electroencephalographic biomarkers: High Frequency Oscillations

Although interictal epileptiform discharges remain the most established EEG markers of epilepsy, increasing attention has recently been directed toward the identification of advanced EEG biomarkers capable of improving the characterization and monitoring of epileptic processes [35]. In general, a biomarker can be defined as a measurable characteristic associated with a physiological or pathological process, while biomarkers of epileptogenesis specifically refer to indicators linked to the transformation of normal brain tissue into tissue capable of generating spontaneous recurrent seizures [35], [36]. Because electroencephalography is non-invasive, widely available, and characterized by high temporal resolution, EEG-based biomarkers represent particularly promising tools for epilepsy research and clinical evaluation [35]. In addition to conventional epileptiform abnormalities, several EEG-derived features have been investigated as potential biomarkers, including high-frequency oscillations (HFOs), connectivity measures, and EEG microstates [37]. Among these candidates, HFOs have received particular attention because of their potential association with epileptogenic brain activity [37], [38].

High-frequency oscillations are brief and transient oscillatory events occurring at frequencies above the conventional EEG frequency bands. In epilepsy research, HFOs are generally investigated within the 80–500 Hz frequency range and are commonly divided into ripples (80–250 Hz) and fast ripples (250–500 Hz) [38]. An example of an HFO is shown in Fig. 10. The event is displayed in the raw EEG signal (Fig. 10A), after signal processing that enhances the high-frequency component (Fig. 10B), and in the corresponding time-frequency representation (Fig. 10C) [38].

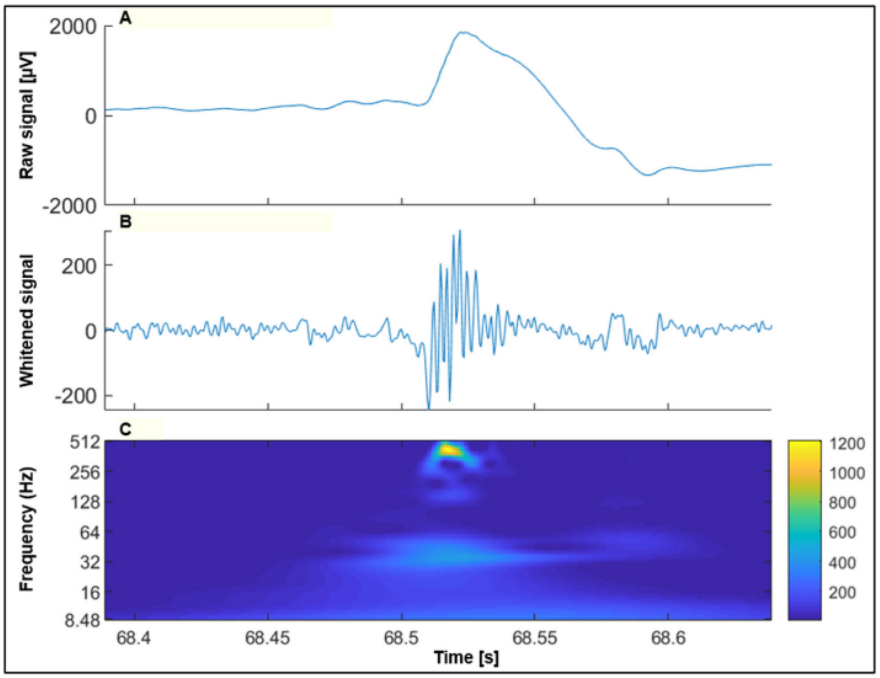


Figure 10. Example of an HFO and its time-frequency characteristics [38].

Importantly, HFOs are not exclusively pathological phenomena. Physiological high-frequency activity can occur during normal brain functions, including sleep and memory-related processes, whereas pathological HFOs have been associated with epileptogenic brain tissue [37]. Therefore, the presence of an HFO alone does not necessarily indicate epileptic activity, and distinguishing physiological from pathological HFOs represents an important challenge for their use as clinical biomarkers [38].

Experimental and clinical studies have investigated HFOs as potential markers of epileptogenic brain regions. In particular, HFOs have been studied in relation to the seizure onset zone and to the delineation of epileptogenic tissue [38]. Fast ripples have been particularly associated with pathological activity, although the relationship between frequency and pathological significance is not absolute [37], [38]. In animal models of epileptogenesis, the occurrence of HFOs within hippocampal structures has also been correlated with the later development of spontaneous seizures, suggesting that these oscillations may reflect pathological network reorganization during epileptogenesis [35].

Initially, HFOs were mainly studied using invasive intracranial recordings; however, advances in EEG acquisition and signal-processing techniques have progressively enabled their detection through non-invasive scalp EEG [35], [36]. This development is particularly relevant for extending HFO analysis beyond patients undergoing invasive presurgical monitoring. In pediatric populations, scalp-

recorded ripples observed after a first unprovoked seizure have also been associated with an increased risk of subsequent epilepsy development [35]. Nevertheless, scalp HFO detection remains technically challenging. Because HFOs are brief, high-frequency events, their reliable identification requires appropriate acquisition parameters, including sufficiently high sampling rates, as well as careful differentiation from physiological high-frequency activity and artifacts [37], [38]. In particular, muscle and movement artifacts may contain high-frequency components that can interfere with HFO identification. These challenges have motivated the development of both visual and automated approaches for HFO detection and analysis [37].

Despite their promising clinical potential, HFOs have not yet reached routine implementation as established EEG biomarkers. Methodological variability in recording and detection procedures, together with the difficulty of distinguishing physiological from pathological HFOs, continues to limit their standardization and clinical interpretation [38]. More generally, no EEG biomarker other than conventional interictal epileptiform discharges has yet achieved sufficient sensitivity, specificity, and reproducibility for routine clinical application [36], [37]. Current evidence therefore suggests that future clinical approaches may benefit from combinations of complementary biomarkers rather than relying on a single isolated parameter [36].

1.4 Analysis of signals for seizure detection

The analysis of EEG signals for seizure detection requires the application of signal processing techniques capable of extracting meaningful information from complex brain activity. EEG signals are inherently time-varying, non-stationary, and often non-linear, making their interpretation particularly challenging. As a result, advanced analytical methods are necessary to characterize the underlying neuronal dynamics and identify pathological patterns associated with epilepsy [39].

In general, EEG signal analysis follows a structured workflow that includes signal acquisition, preprocessing, feature extraction, and classification (Fig 11). After acquisition, EEG recordings are processed to reduce noise and artifacts, allowing the extraction of representative features from the raw signal. These features can be derived from different domains, including the time and frequency domains, and provide a compact representation of the signal suitable for subsequent analysis. Finally, classification algorithms, including machine learning approaches, can be applied to identify patterns associated with epileptic activity and support seizure detection and diagnosis [39].

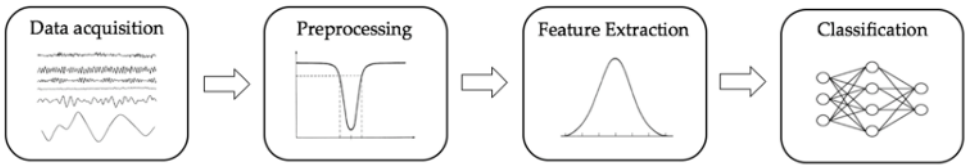


Figure 10. Signal analysis divided in signal acquisition, preprocessing, feature extraction and classification [39].

1.4.1 Time-domain analysis

Time-domain analysis represents one of the most direct and widely used approaches for EEG signal characterization. In this framework, the EEG signal is analyzed in its original form as a function of time, without applying transformations into alternative domains. By examining the temporal evolution of the signal, it is possible to observe variations in waveform morphology and amplitude, allowing the identification of characteristic patterns associated with different physiological and pathological brain states [39],[40]. Because epileptic seizures arise from transient disturbances of neuronal activity, EEG signals can be used to distinguish between normal brain activity, interictal activity, and seizure-related activity (Fig 12). In clinical practice, EEG interpretation relies heavily on the recognition of characteristic waveform patterns and their temporal evolution, making time-domain analysis a fundamental step in the assessment of epileptic EEG recordings [41]. Temporal analysis allows the identification of both normal and abnormal waveform patterns and is particularly useful for determining the presence or absence of characteristic brain rhythms. Since EEG signals are often correlated in time, current samples can be estimated from previous observations, a property that forms the basis of several temporal modeling techniques [39].

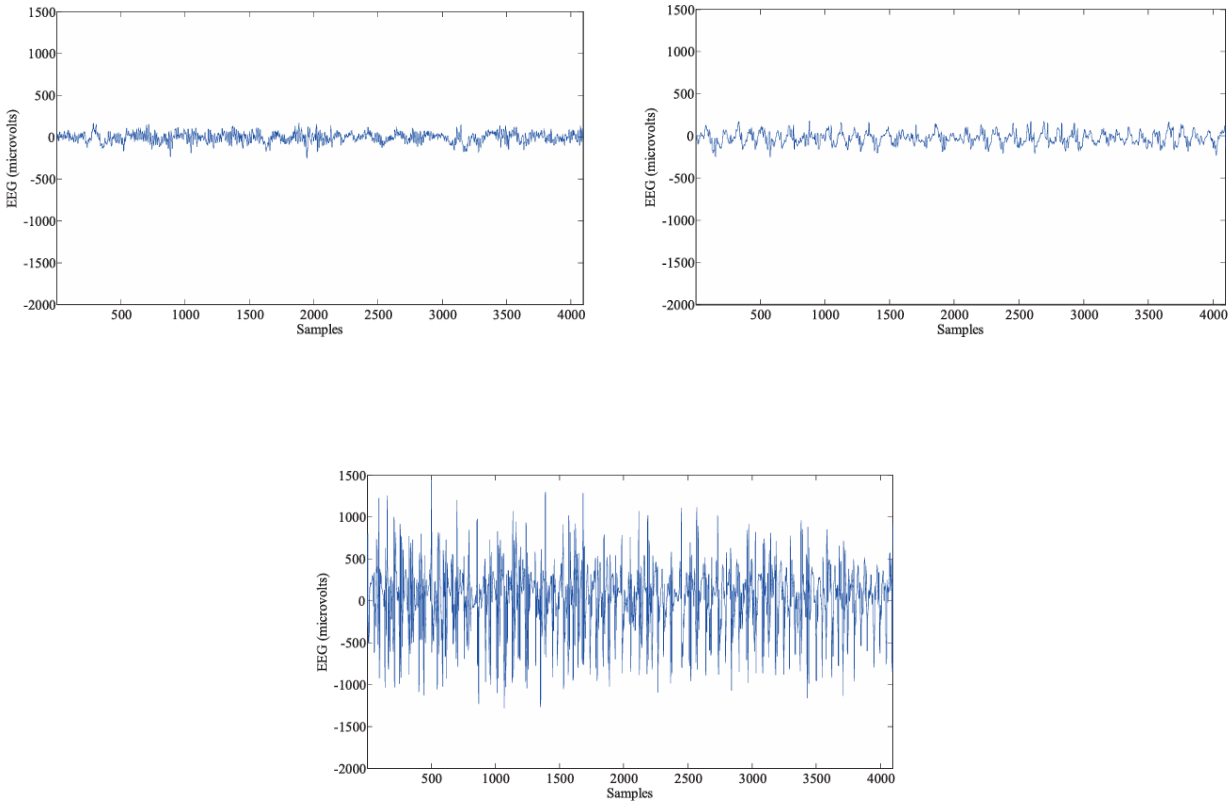


Figure 12. Typical EEG signals (a) normal, interictal and ictal activity [41].

Some of the principal methods employed in time-domain EEG analysis include linear prediction and component analysis techniques such as Principal Component Analysis (PCA), Independent Component Analysis (ICA), and Linear Discriminant Analysis (LDA) [40]. Linear prediction models estimate the current signal sample as a linear combination of previous input and output samples and have been applied to waveform generation, storage, transmission, and seizure detection.

In particular, linear prediction error energy methods have been successfully used for the identification of epileptic seizures from EEG recordings [40]. Component analysis techniques are also widely employed in EEG processing. PCA reduces data dimensionality by transforming high-dimensional observations into a smaller set of orthogonal components that capture most of the signal variance. ICA decomposes EEG recordings into statistically independent components and can be used both for artifact removal and for the extraction of seizure-related activity. Similarly, LDA identifies linear combinations of features that maximize class separation and has been used to improve discrimination between normal and epileptic EEG patterns [40]. Beyond these analytical techniques, several quantitative descriptors can be extracted directly from the EEG waveform in the time domain. Commonly used temporal features include statistical measures such as the mean value, standard deviation, first-order difference, second-order difference, and entropy, which provide information

about signal amplitude, variability, and complexity [39]. Additional descriptors include Hjorth parameters, which characterize the signal in terms of activity, mobility, and complexity, as well as fractal dimension and high-order crossings, all of which have been employed to capture different aspects of EEG dynamics and support the discrimination of physiological and pathological brain states [39].

One of the major advantages of time-domain analysis is its simplicity and intuitive interpretation. The direct observation of waveform morphology allows clinicians to identify relevant EEG abnormalities without requiring complex mathematical transformations. Indeed, conventional EEG interpretation is still largely based on visual inspection, where neurologists evaluate waveform morphology, amplitude, frequency, regularity, spatial distribution, and temporal persistence of abnormalities in order to identify epileptic activity [42].

Despite these advantages, conventional time-domain analysis presents important limitations when dealing with epileptic EEG signals. Epileptic activity is often characterized by transient and non-stationary phenomena that may not be fully captured through visual inspection or simple temporal descriptors. Seizure events may appear similar when examining raw EEG recordings while exhibiting different underlying signal structures that are not readily discernible through conventional analysis alone [42]. Furthermore, EEG signals arise from highly complex neuronal interactions and exhibit nonlinear behavior, limiting the ability of purely time-domain approaches to fully characterize epileptic dynamics [40]. For these reasons, more advanced signal processing techniques have been developed to complement temporal analysis. In particular, frequency-domain and time–frequency approaches provide additional information regarding the spectral content and transient characteristics of EEG signals.

1.4.2 Frequency-domain analysis

Frequency-domain analysis investigates EEG signals by examining how signal energy is distributed across different frequency components rather than focusing exclusively on the temporal evolution of waveform amplitudes. This approach is particularly useful when oscillatory activity represents a key characteristic of the signal and temporal analysis alone does not provide sufficient information. Neuronal oscillations can be represented through sinusoidal functions using the Fourier Transform (FT), allowing the identification of the dominant frequency components present in EEG recordings [39]. By transforming the signal from the time domain into the frequency domain, spectral analysis provides complementary information that facilitates the characterization of rhythmic brain activity

and the extraction of quantitative features related to signal frequency content. Several methods can be employed for frequency-domain analysis, including the Fast Fourier Transform (FFT), Short-Time Fourier Transform (STFT), spectrogram-based approaches, autoregressive methods, and eigenvector-based techniques [39]. Among these, the FFT is one of the most widely used techniques due to its computational efficiency and its ability to preserve the spectral information contained in the original signal [43]. The mathematical basis of this approach is the Fourier Transform, which converts a signal from its time-domain representation into a frequency-domain representation (1):

$$X(f) = F\{x(t)\} = \int_{\{-\infty\}}^{\{+\infty\}} x(t)e^{\{-j2\pi ft\}}dt \quad (1)$$

where $x(t)$represents the EEG signal in the time domain, $X(f)$its frequency-domain representation, $f$the frequency, and $j = \sqrt{-1}$ the imaginary unit. Through this transformation, EEG signals are decomposed into their constituent frequency components, enabling the identification of dominant oscillations and the quantitative analysis of spectral activity within specific frequency ranges [43].

A fundamental concept in frequency-domain analysis is the Power Spectral Density (PSD), which describes how the power of a signal is distributed across the frequency spectrum. PSD estimation allows the selective representation of EEG samples and the identification of the principal frequency components contributing to the recorded signal [43]. The PSD is generally estimated from the Fourier Transform of the signal autocorrelation sequence, and among the available non-parametric approaches, Welch's method is one of the most commonly employed techniques. This method divides the signal into overlapping segments, computes the periodogram of each segment, and averages the resulting spectra to obtain a more stable estimate of the power spectrum [43].

The information provided by PSD analysis is closely related to the physiological organization of EEG activity into distinct frequency bands. As discussed in Section 1.4.1, EEG rhythms can be classified into specific frequency ranges associated with different functional states of the brain. Spectral analysis enables the quantification of signal power within these bands, providing a compact and informative representation of neuronal activity. Consequently, band-power features have become widely used descriptors in EEG characterization and feature extraction, supporting the identification of both physiological rhythms and pathological patterns [43]. In the context of epilepsy, spectral analysis provides valuable information regarding the transition between normal, interictal, and ictal brain states. EEG recordings obtained during epileptic seizures exhibit patterns that differ significantly from normal and interictal EEG activity, reflecting alterations in the electrophysiological behavior of neuronal networks (Fig 13) [40]. During the pre-ictal and ictal phases, abnormal synchronization of

neuronal populations produces changes in frequency distribution and signal complexity that can be detected through spectral analysis techniques.

As a result, frequency-domain methods such as PSD estimation, Fourier-based analysis, and related spectral techniques have been extensively employed to identify features associated with epileptic activity and to support automated seizure detection and classification systems [40].

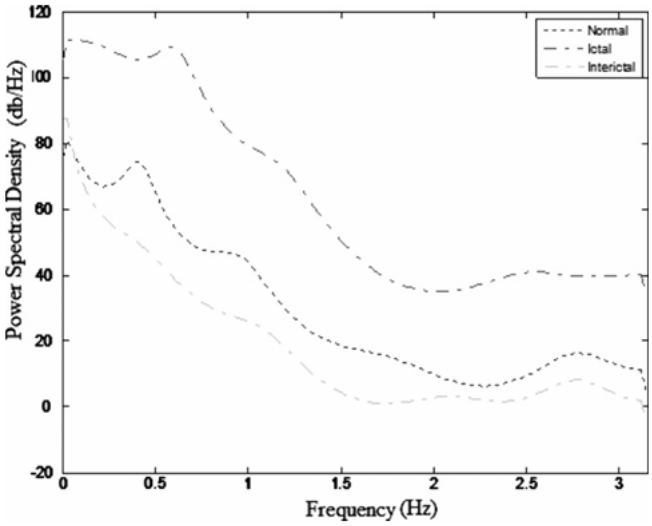


Figure 13. Power Spectral Density (PSD) estimated from normal, interictal, and ictal EEG recordings. The figure illustrates how the distribution of spectral power varies across different brain states, highlighting the changes in frequency content associated with epileptic activity [40].

Despite their widespread use, Fourier-based methods present important limitations when applied to EEG signals. As already said, epileptic recordings are inherently non-stationary and often contain transient events whose characteristics vary over time. Conventional FFT-based analysis decomposes signals into sinusoidal components and represents them exclusively in terms of frequency content. However, the infinite basis functions employed by the Fourier Transform are primarily suitable for periodic and non-transient signals, making it difficult to adequately characterize short-duration events commonly observed in EEG recordings [42]. Furthermore, Fourier analysis does not preserve temporal localization: while the resulting spectrum identifies which frequencies are present in the signal, it does not indicate when those frequencies occur. Since the Fourier coefficients are determined using the entire signal duration, local variations and transient abnormalities cannot be readily identified [42]. To overcome these limitations, time–frequency analysis techniques have been increasingly adopted for EEG processing. Among these methods, the Wavelet Transform (WT) has emerged as one of the most effective tools for the analysis of epileptic EEG signals.

It captures subtle variations in EEG recordings that are often difficult to identify through visual inspection and provides simultaneous information in both the time and frequency domains [44].

1.4.3 Feature extraction from electroencephalographic signals

EEG recordings generate large amounts of data that are often complex, non-stationary, and highly variable due to the intrinsic characteristics of neural activity. As a consequence, the direct analysis of raw EEG signals is generally difficult and computationally demanding. To overcome this limitation, feature extraction is commonly performed after signal preprocessing in order to obtain a more compact and informative representation of the recorded data [39]. Feature extraction consists of deriving a set of descriptors from the original EEG recordings that preserve the most relevant information while reducing redundancy. Its primary objective is to reduce the amount of data by generating non-redundant features that retain the essential characteristics of the signal and facilitate subsequent classification tasks. Rather than processing the entire set of EEG samples, the analysis can therefore be conducted on a reduced representation that captures the most informative aspects of brain activity [39]. This process is closely related to dimensionality reduction. EEG recordings are typically represented in a high-dimensional space, where data may be sparse, partially redundant, and computationally expensive to process. Feature extraction transforms the original dataset into a lower-dimensional representation while preserving its most significant properties, thereby improving computational efficiency and facilitating pattern recognition [39]. The resulting features provide a quantitative description of EEG activity and can subsequently be analyzed using signal processing and machine learning techniques. Depending on the information of interest, features may be extracted from the temporal, spectral, time–frequency, or nonlinear characteristics of the signal (Fig.14). These descriptors constitute the basis for the identification of physiological and pathological brain states and play a fundamental role in automated seizure detection systems [39].

Domain of Analysis	Feature Extraction Method	Feature
Time	• Statistical analysis • Nonlinear analysis	• Mean • Variance • Standard deviation • Skewness • Kurtosis • Approximate Entropy (ApEn) • Sample Entropy (SampEn) • Fractal Dimension (FD) • Lyapunov Exponents (LE) • Hurst Exponent (HE)
Frequency	• Power Spectral Density (PSD) estimation • Spectral analysis	• Band power (delta, theta, alpha, beta, gamma) • Relative band power • Spectral entropy (SE) • Peak (dominant) frequency
Time-Frequency	• Discrete Wavelet Transform (DWT) • Wavelet Packet Transform (WPT)	• Energy (average power) of wavelet sub-bands • Mean absolute value of coefficients • Standard deviation of coefficients • Ratios between adjacent sub-bands • Wavelet Packet Entropy (WPE)

Figure 14. Classification of EEG features commonly employed in automated seizure detection systems, including time-domain, frequency-domain, and time–frequency descriptors. Adapted from Lujàn et al. [39].

Among the available approaches, time-domain features are extracted directly from raw or preprocessed EEG recordings without requiring transformation into another domain. These descriptors are widely used because they are computationally simple, easy to implement, and capable of effectively characterizing EEG activity in low-noise conditions [45]. Common statistical measures include the mean (2), variance (3), and standard deviation (4), which describe the central tendency and variability of signal amplitudes:

$$\mu = \frac{1}{N}\sum_{i=1}^{N} x_i \quad (2) \qquad \sigma^2 = \frac{1}{N}\sum_{i=1}^{N}(x_i - \mu)^2 \quad (3) \quad \sigma = \sqrt{\left\{\frac{1}{N}\sum_{i=1}^{N}(x_i - \mu)^2\right\}} \quad (4)$$

where x_i represents the i-th EEG sample, N is the total number of samples, μ is the mean value of the signal, and σ is the standard deviation.The mean represents the average value of the EEG samples, whereas variance and standard deviation quantify the dispersion of the data around the mean. High standard deviation values indicate greater variability of the signal, while lower values reflect a more concentrated distribution of amplitudes [45]. Additional information can be obtained through higher-order statistical descriptors such as skewness and kurtosis. Skewness measures the asymmetry of the amplitude distribution, distinguishing between positively and negatively skewed signals, whereas kurtosis describes the shape of the distribution and its tendency to exhibit pronounced peaks and heavy tails. Together, these parameters provide a concise description of EEG waveform morphology and may contribute to the identification of differences between physiological and pathological conditions [45].

Although statistical features offer a useful summary of signal amplitude distributions, they may not fully describe the complex dynamics underlying cerebral activity. EEG signals arise from the interaction of large neuronal populations and exhibit nonlinear and non-stationary behavior. Consequently, conventional linear approaches may be insufficient to capture subtle changes associated with epileptic processes. Nonlinear signal analysis has become an important tool for EEG characterization because it can reveal dynamical properties that are not adequately represented by traditional time- and frequency-domain measures [40]. To address these limitations, numerous nonlinear features have been proposed for automated epilepsy detection. These descriptors are designed to quantify properties such as complexity, irregularity, predictability, and self-similarity, thereby providing additional information about the underlying neuronal dynamics. Commonly used nonlinear measures include entropy-based features, fractal dimension techniques, higher-order

statistics and Lyapunov exponents, all of which have demonstrated potential for distinguishing pathological EEG recordings [40]. Among these approaches, entropy measures are particularly relevant because they quantify the degree of regularity and complexity of a time series. Approximate Entropy (ApEn) and Sample Entropy (SampEn) are widely employed to evaluate the predictability and irregularity of EEG signals. Lower entropy values indicate a more regular and predictable structure, whereas higher values are associated with increased complexity. Entropy-based features have proven effective in differentiating normal, interictal, and seizure EEG segments, making them valuable biomarkers for automated seizure detection and classification [40]. Additional nonlinear descriptors include the Fractal Dimension (FD), Lyapunov Exponents (LE), and the Hurst Exponent (HE).

Fractal dimension quantifies the geometric complexity and self-similar properties of EEG waveforms, whereas Lyapunov exponents measure the sensitivity of a dynamical system to small variations in its initial conditions and therefore provide insight into the chaotic behavior of brain activity. The Hurst exponent characterizes the long-term dependence and persistence of a time series [40].

Frequency-domain analysis complements time-domain methods by describing how signal power is distributed across different frequencies. These features are typically extracted from the Power Spectral Density (PSD), which provides a quantitative representation of the spectral content of EEG signals [46]. Among the most commonly used spectral descriptors is band power, obtained by integrating the spectral energy within specific EEG frequency ranges, namely delta, theta, alpha, beta, and gamma bands. The distribution of power across these frequency bands reflects the rhythmic organization of neuronal activity and can reveal alterations associated with epileptic processes. Spectral energy derived from the PSD therefore represents one of the principal features used to characterize EEG rhythmicity [46]. To account for inter-subject variability and emphasize the contribution of individual rhythms to the overall EEG activity, band power can be normalized with respect to the total spectral power, yielding the relative band power (5):

$$RBP_i = \frac{BP_i}{\sum_{k=1}^{N} BP_k} \quad (5)$$

where $BP_i$is the power of the i-th frequency band and $\sum_{k=1}^{N} B\,P_k$is the total spectral power. This feature expresses the proportional contribution of each frequency band and facilitates comparisons

between different recordings. Another widely used spectral descriptor is spectral entropy (SE) (6), which quantifies the complexity and irregularity of the frequency distribution:

$$SE = -\sum_{i=1}^{N} p_i \log_2(p_i) \quad (6)$$

where $p_i$represents the normalized power spectral density, it measures how uniformly signal power is distributed across frequencies. Lower values indicate that spectral energy is concentrated within a limited frequency range, whereas higher values reflect a more homogeneous distribution of power throughout the spectrum [46]. Peak frequency, also referred to as dominant frequency, corresponds to the frequency at which the PSD reaches its maximum value. Because normal and epileptic EEG recordings often exhibit different dominant oscillatory patterns, peak frequency can provide useful discriminatory information for automated seizure detection systems [46]. Together, these spectral features provide a concise representation of EEG oscillatory activity and are widely employed to identify frequency alterations associated with neurological disorders and epileptic events.

Although frequency-domain analysis provides valuable information regarding the spectral composition of EEG signals, epileptic activity is inherently non-stationary and often characterized by transient phenomena whose frequency content changes over time.

For this reason, time–frequency analysis techniques have become increasingly important in EEG processing. Among these approaches, the Discrete Wavelet Transform (DWT) is one of the most widely adopted methods for seizure detection and EEG characterization [41]. Wavelet analysis represents a signal as a linear combination of functions generated through the translation and dilation of a prototype function known as the mother wavelet. This decomposition produces a set of wavelet coefficients that provide a compact representation of the signal and can subsequently be used for feature extraction and classification tasks [41]. A major advantage of wavelet analysis is its ability to simultaneously preserve temporal and spectral information: wavelets possess strong time–frequency localization properties, allowing the identification of both the frequency content of a signal and the time at which specific events occur. Compared with conventional Fourier-based approaches, wavelet techniques are therefore particularly effective for analyzing transient EEG phenomena and abrupt signal variations commonly observed during epileptic activity [41]. The DWT performs a multiresolution decomposition of the EEG signal through successive low-pass and high-pass filtering operations. This process separates the signal into approximation coefficients, which contain low-

frequency information, and detail coefficients, which represent higher-frequency components. By iteratively decomposing the approximation coefficients, EEG activity can be analyzed at multiple frequency scales, enabling a more detailed characterization of brain dynamics (Fig.15) [41].

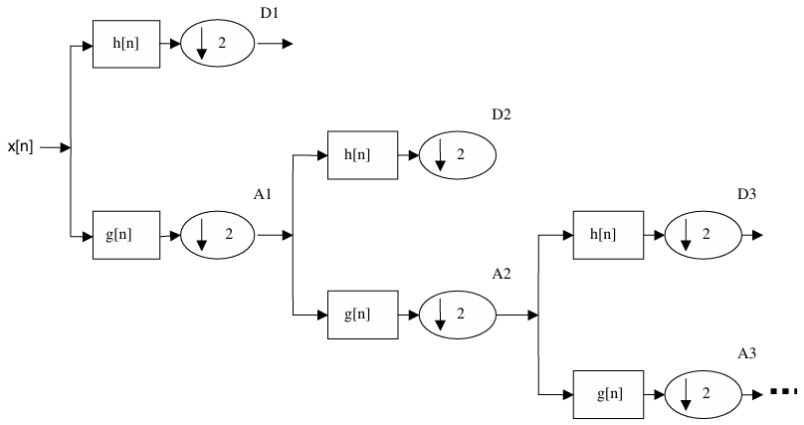


Figure 15. Multiresolution decomposition of an EEG signal using the Discrete Wavelet Transform (DWT). The signal is iteratively decomposed through low-pass g[n] and high-pass h[n] filters, producing approximation coefficients (A) and detail coefficients (D) at succesive levels of resolutions [41].

Following wavelet decomposition, quantitative features can be extracted from the resulting coefficients. One of the most commonly employed descriptors is the energy, or average power, associated with each wavelet sub-band. Because wavelet coefficients reflect the distribution of signal energy in both the time and frequency domains, they provide an effective representation of the non-stationary nature of EEG recordings [41]. The energy contained within each sub-band quantifies the contribution of a specific frequency range to the overall signal and can therefore reveal characteristic alterations associated with epileptic activity. Several statistical measures can be derived from wavelet coefficients, including average power, mean absolute value, standard deviation, and ratios between adjacent sub-bands. Features based on average power and mean values primarily describe the frequency distribution of the signal, whereas standard deviation and coefficient ratios provide additional information regarding changes in spectral energy across neighboring frequency ranges [41].

Since epileptic EEG recordings often exhibit characteristic modifications in signal energy within specific frequency bands, sub-band energy measures have become widely used features for seizure detection and EEG classification. In addition to energy-based descriptors, entropy measures can be extracted from the wavelet decomposition to quantify signal complexity. Among these approaches, Wavelet Packet Entropy (WPE) has attracted considerable attention because it combines the multiresolution capabilities of the Wavelet Packet Transform (WPT) with a quantitative assessment of signal irregularity and information content. The WPT is particularly suitable for EEG analysis

because it decomposes both approximation and detail components, thereby providing a more detailed time–frequency representation of non-stationary signals than conventional wavelet approaches [47].

To identify the most informative wavelet decomposition, Wang et al. employed an entropy-based best-basis selection procedure. The authors describe Shannon entropy as a measure of uncertainty and complexity, where larger entropy values correspond to greater complexity of the underlying dynamical process [47]. For a signal represented by wavelet packet coefficients s_i, Shannon entropy (7) is defined as:

$$E(s) = \sum_i s_i^2 \, log(s_i^2) \quad (7)$$

where s_i denotes the coefficients of the signal in an orthonormal wavelet basis [47].

Wavelet entropy provides information about the dynamical behavior of EEG signals and can therefore be used as a criterion for selecting the most informative wavelet packet decomposition [47]. From a signal-processing perspective, it reflects how signal energy is distributed across the different wavelet sub-bands. A more uniform distribution of energy generally corresponds to higher entropy values and greater signal complexity, whereas concentration of energy within a limited number of sub-bands results in lower entropy values. Consequently, wavelet entropy represents a compact measure of EEG complexity and has been successfully employed to distinguish normal and epileptic brain activity [47].

1.4.4 Automated detection algorithms

Automated EEG analysis systems generally follow a sequential processing pipeline consisting of signal acquisition, preprocessing, feature extraction, and classification. This framework enables the transformation of raw EEG recordings into clinically meaningful information through a series of progressively specialized processing stages [39]. Following feature extraction, the resulting feature vectors are provided as inputs to classification algorithms. Rather than operating directly on the raw EEG signal, these methods rely on a reduced set of descriptors that summarize the most informative characteristics of brain activity. This strategy not only reduces computational complexity but also facilitates the identification of patterns associated with specific physiological or pathological conditions [39]. Classification therefore represents one of the fundamental stages of EEG signal analysis, allowing the recognition of signal classes that may not be readily identifiable through visual inspection and supporting automated decision-making processes. Among supervised machine learning techniques, Support Vector Machines (SVM), k-Nearest Neighbors (k-NN), Decision Trees,

Random Forests, and Artificial Neural Networks (ANNs) are among the most widely used algorithms for EEG analysis. These methods classify EEG recordings according to extracted signal features and have been applied to a broad range of applications, including the identification of cognitive states, emotional responses, neurological disorders, and brain–computer interface commands [39][48]. Support Vector Machines classify data by identifying an optimal decision boundary, known as a hyperplane, that maximizes the separation between classes. Due to their effectiveness in high-dimensional feature spaces and their strong generalization capabilities, SVMs have been extensively employed in EEG-based classification tasks, including epilepsy detection [39][48]. The k-Nearest Neighbors algorithm assigns an unknown sample to the class most frequently represented among its closest neighbors in the feature space. Similarity is typically assessed using distance measures such as Euclidean, cosine, or Chebyshev distance, making k-NN a simple yet effective approach for EEG classification [39]. Decision Trees perform classification through a sequence of hierarchical decisions based on feature values, progressively partitioning the dataset into increasingly homogeneous subsets. Their main advantage lies in their interpretability, since the decision process can be easily visualized and understood. Random Forests extend this concept by combining multiple decision trees through an ensemble voting strategy, thereby improving robustness, reducing overfitting, and enhancing classification performance in complex EEG datasets [39][48]. In recent years, deep learning approaches have gained considerable attention due to their ability to automatically learn hierarchical feature representations directly from data. Unlike traditional machine learning techniques, which generally require handcrafted features, deep learning models progressively extract increasingly complex representations through multiple processing layers (Fig. 16). These architectures emulate certain aspects of biological neural networks and learn from large amounts of data through interconnected input, hidden, and output layers. During training, the network iteratively adjusts its internal parameters to optimize classification performance [39].

	Machine Learning	Deep Learning
Data format	Works with structured data	Works with raw or minimally processed data
Database size	Performs well on smaller datasets	Benefits from large datasets
Training	Requires handcrafted features and human expertise	Learns hierarchical features automatically from data
Algorithm	Traditional algorithms (e.g., SVM, k-NN, Random Forest)	Neural network-based models (e.g., CNN, RNN, LSTM)
Computational requirements	Lower computational cost	Higher computational cost
Model interpretability	Greater interpretability	Lower interpretability ("black-box" models)
Application	Suitable for simple or well-defined tasks and limited data	Suitable for complex tasks with high variability

Figure 16. Main differences between traditional machine learning algorithms and deep learning architectures used for EEG classification. Adapted from Luján et al. [39].

Among the most widely adopted deep learning architectures for EEG analysis are Artificial Neural Networks (ANNs), Convolutional Neural Networks (CNNs), and Recurrent Neural Networks (RNNs), particularly Long Short-Term Memory (LSTM) networks. ANNs consist of interconnected processing units organized into multiple layers and are capable of learning complex nonlinear relationships between EEG features and target classes. Their flexibility has led to successful applications in areas such as motor imagery classification, emotion recognition, and neurological disorder detection [48].

Convolutional Neural Networks have emerged as one of the most effective approaches for EEG analysis because they can automatically extract discriminative spatial and temporal features directly from the signal. Through convolutional operations performed by filters, CNNs progressively learn increasingly complex representations, from simple local patterns in the early layers to higher-level features in deeper layers [39]. Recurrent Neural Networks, in contrast, are specifically designed to process sequential data by incorporating recurrent connections that allow information from previous time steps to influence subsequent computations. This property makes them particularly suitable for EEG recordings, which exhibit strong temporal dependencies. Long Short-Term Memory networks represent a specialized form of RNN capable of overcoming the limitations of conventional recurrent architectures when modeling long-range temporal relationships [39]. Overall, deep learning methods, particularly CNN- and LSTM-based architectures, have demonstrated significant advantages when dealing with large-scale and highly complex EEG datasets. While traditional machine learning algorithms remain effective in situations involving limited data and carefully engineered features, deep learning models often achieve superior performance by automatically learning informative representations directly from EEG recordings [48].

In epilepsy research, automated detection algorithms are primarily employed to distinguish between normal, interictal, and ictal EEG activity. Following feature extraction, the resulting descriptors are provided as inputs to machine learning or deep learning models that learn characteristic patterns associated with seizure activity. Traditional machine learning approaches generally rely on manually extracted temporal, spectral, or nonlinear features, whereas deep learning methods are capable of automatically learning discriminative representations directly from EEG signals. Algorithms such as SVMs, Random Forests, ANNs, and CNNs have been widely applied for seizure detection and classification, demonstrating promising performance in identifying epileptic activity. By reducing the time required for manual EEG interpretation and supporting continuous long-term monitoring, these systems have the potential to become valuable tools for clinical decision support in epilepsy management [49].

The performance of automated seizure detection systems must be carefully evaluated to assess their reliability in distinguishing epileptic activity from non-seizure EEG patterns. In seizure detection studies, performance is commonly quantified using measures such as sensitivity, specificity, and latency [50]. Sensitivity represents the percentage of seizures correctly identified by the detector, whereas specificity reflects its ability to avoid false detections during non-seizure recordings. High specificity is particularly important in long-term EEG monitoring, where excessive false alarms may substantially reduce the clinical usefulness of an automated system. Latency, on the other hand, corresponds to the delay between the seizure onset identified by an expert and the moment at which the algorithm declares seizure activity. Low latency is desirable because it enables earlier recognition of seizure onset and may facilitate timely clinical intervention. The design of seizure detection algorithms often involves a trade-off between these performance measures. Increasing sensitivity may improve seizure detection rates but can also increase the number of false alarms, whereas stricter detection criteria may reduce false detections at the expense of longer delays or missed seizure events [50].

1.5 Sleep and Pediatric Epilepsy

1.5.1 Importance of Sleep Monitoring in Epilepsy

Sleep plays a fundamental role in the regulation of brain activity and exhibits a well-established bidirectional relationship with epilepsy. Indeed, seizures frequently occur during sleep, while sleep disturbances are common among patients with epilepsy and may further compromise seizure control [51]. This interaction is largely mediated by physiological changes in neuronal synchronization that occur across different sleep stages. In particular, non-rapid eye movement (NREM) sleep is characterized by enhanced synchronization within thalamocortical networks, giving rise to typical EEG patterns such as slow waves and sleep spindles [51][52]. Because epileptic activity is increasingly recognized as a network phenomenon rather than a purely focal process, sleep-related changes in functional connectivity play a major role in modulating the occurrence and propagation of epileptiform discharges [53]. Sleep is conventionally divided into rapid eye movement (REM) sleep and non-REM (NREM) sleep, the latter comprising stages N1, N2, and N3. As sleep deepens, neuronal synchronization progressively increases, reaching its maximum during slow-wave sleep (N3). Under these conditions, focal interictal discharges occur more frequently, creating a favorable environment for the emergence and propagation of pathological EEG activity. In contrast, REM sleep is characterized by a desynchronized EEG pattern and is generally associated with a reduction in epileptiform discharges throughout cortical networks [52][53]. Consequently, the occurrence of

epileptic activity varies considerably across vigilance states, being most prominent during NREM sleep, intermediate during wakefulness, and least frequent during REM sleep (Fig. 17). This highlights the clinical importance of including sleep in EEG recordings, as some epileptic abnormalities may only become evident during specific sleep stages.

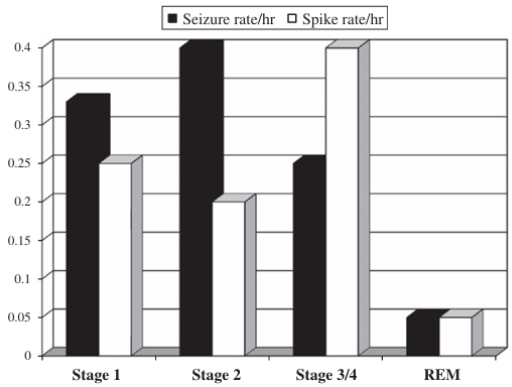


Figure 17. Seizure & spike rate/hour in different stages of sleep [54].

The relationship between sleep and epilepsy is particularly relevant in pediatric populations, where sleep disturbances are common yet frequently under-recognized. Children with epilepsy often exhibit alterations in sleep architecture, including changes in total sleep time, prolonged sleep latency, and increased sleep fragmentation. Furthermore, the influence of sleep on epileptic activity is amplified in the developing brain, where neuronal networks are still undergoing maturation [54]. Ongoing changes in connectivity and increased neuronal plasticity may enhance the expression of epileptiform activity during sleep, making sleep EEG recordings especially valuable for diagnostic purposes in pediatric patients.

In this context, several studies have demonstrated that sleep EEG provides a more sensitive window for the identification of clinically relevant biomarkers. As previously discussed, HFOs represent a promising EEG biomarker of epileptogenic activity. Their occurrence is strongly influenced by sleep, with marked variations across different sleep stages and cycles. HFO rates are highest during NREM sleep, particularly during stage N3, and progressively decrease throughout the night. Moreover, the inclusion of N3 sleep significantly improves the sensitivity of HFO detection, likely reflecting the greater neuronal synchrony characteristic of this stage [55]. A clear example of the diagnostic relevance of sleep monitoring in pediatric epilepsy is electrical status epilepticus during sleep (ESES), an EEG pattern characterized by nearly continuous spike–wave discharges throughout NREM sleep that typically disappear upon awakening [56]. ESES represents a hallmark feature of continuous

spike-and-wave during sleep (CSWS), a childhood epileptic encephalopathy associated with seizures as well as cognitive and behavioral deterioration. For this reason, EEG recordings obtained during sleep are essential for identifying this pattern and evaluating disease severity. Nevertheless, conventional measures such as the spike-wave index (SWI), although widely used to quantify sleep-related epileptic activity, do not always correlate with seizure burden or neurocognitive outcome, highlighting the need for more informative EEG biomarkers [56]. Recent investigations have further clarified the relationship between sleep and epileptogenicity through the analysis of EEG signal complexity. Studies based on multifrequency entropy have shown that brain signal complexity decreases during NREM sleep compared with wakefulness [57]. This reduction is even more pronounced in pediatric patients with epilepsy and is particularly evident within epileptic brain regions, which consistently exhibit lower entropy values than non-epileptic areas. Since reduced entropy has been associated with an increased propensity for seizure generation, these findings suggest that sleep may create physiological conditions that facilitate epileptogenic processes [57].

Consequently, the analysis of sleep EEG provides important insights into the mechanisms underlying epilepsy and further supports the clinical value of sleep monitoring in pediatric populations. Sleep-related EEG activity has also been linked to cognitive function in children with epilepsy. Sleep spindles, a characteristic feature of N2 sleep consisting of oscillatory activity in the 11–16 Hz frequency range, are generated within thalamocortical circuits and are known to contribute to memory consolidation and cognitive processing. In childhood absence epilepsy, significant alterations in spindle activity have been reported, including reductions in spindle density and duration compared with healthy controls. Importantly, spindle density is significantly lower in patients with cognitive impairment and shows a positive association with cognitive performance. These observations suggest that abnormalities in sleep spindle activity may reflect dysfunction within thalamocortical networks and could represent a valuable biomarker of neurocognitive impairment in pediatric epilepsy [58].

1.5.2 Pediatric Epilepsy: Syndromes and Advanced EEG Biomarkers

Pediatric epilepsy encompasses a heterogeneous group of disorders characterized by diverse clinical manifestations, etiologies, and EEG patterns. According to the International League Against Epilepsy (ILAE), epilepsy classification represents a fundamental clinical tool for diagnosis, prognosis, and therapeutic management [59]. The current ILAE framework integrates information derived from seizure semiology, EEG findings, neuroimaging, etiology, and associated comorbidities, and defines epilepsy syndromes as clusters of electroclinical features that tend to occur together, often including characteristic ages of onset, seizure types, prognosis, and neurodevelopmental manifestations.

In pediatric populations, epilepsy syndromes are strongly influenced by brain maturation, and many disorders show characteristic periods of onset and remission reflecting the developmental organization of neuronal networks. In addition to seizures, pediatric epilepsies are frequently associated with cognitive, behavioral, and neurodevelopmental impairments, highlighting the importance of early recognition and accurate EEG-based evaluation [59]. Among pediatric epilepsies, self-limited epilepsy with centrotemporal spikes (SeLECTS), formerly known as benign epilepsy with centrotemporal spikes (BECTS), represents one of the most common age-dependent focal epilepsy syndromes of childhood. It is characterized by centrotemporal epileptiform discharges that are typically activated during drowsiness and non-rapid eye movement (NREM) sleep, reflecting the close interaction between sleep-related neuronal synchronization and epileptic activity [60]. Although traditionally considered a benign condition, neurocognitive and behavioral comorbidities, including attention-deficit/hyperactivity disorder (ADHD), have also been reported. Quantitative EEG approaches have therefore been investigated in SeLECTS, including HFO- and entropy-based measures [61].

Severe pediatric epileptic encephalopathies are also frequently characterized by marked sleep-related EEG abnormalities and neurodevelopmental impairment. Infantile spasms are typically associated with hypsarrhythmia, a highly disorganized EEG pattern that remains an important diagnostic feature, although its interpretation may show limited inter-rater reliability [62]. Similarly, continuous spike-and-wave during sleep (CSWS) and electrical status epilepticus during sleep (ESES) are characterized by extensive spike-wave activity during NREM sleep and are commonly associated with seizures, cognitive deterioration, and behavioral impairment [56]. Quantitative EEG studies suggest that electrophysiological alterations related to ESES may precede clinical diagnosis: children who later developed ESES showed higher spike frequency and increased delta power during sleep EEG recordings [63]. Childhood absence epilepsy (CAE), characterized by generalized 3-Hz spike-and-wave discharges and abnormalities in thalamo-cortical network activity, and Lennox–Gastaut syndrome (LGS), a severe developmental and epileptic encephalopathy characterized by multiple seizure types and heterogeneous EEG abnormalities, also show relevant alterations in sleep-related EEG activity [58], [64]. In LGS, automated time-frequency analysis during NREM sleep identified generalized paroxysmal fast activity (GPFA), additional beta- and gamma-band oscillatory patterns, and alterations in sleep spindle activity [64].

Beyond these conventional electroclinical features, recent EEG research has increasingly focused on quantitative biomarkers capable of characterizing aspects of epileptic activity and network dysfunction that may not be fully captured by visual EEG interpretation. Investigated approaches

include HFOs, functional connectivity, EEG microstates, entropy-based measures, and other computational analyses [38].

As previously discussed, HFOs represent one of the most extensively investigated advanced EEG biomarkers in epilepsy. In pediatric populations, their occurrence is strongly influenced by sleep, with higher scalp HFO rates reported during N3 sleep than during N2 and REM sleep, particularly during the first sleep cycle. HFO rates also decrease with time spent asleep, supporting a relationship between HFO occurrence and sleep dynamics [55]. Their potential clinical relevance has been investigated across different pediatric epilepsy syndromes. In infantile spasms, increased scalp HFO rates and stronger coupling between HFOs and slow-wave activity were associated with active epileptic spasms, while HFO-based models showed higher diagnostic performance than hypsarrhythmia alone [62]. In children with CSWS, persistent scalp HFOs after steroid therapy were associated with seizure relapse and lower intelligence quotient (IQ) scores, whereas HFO resolution correlated with improved seizure control and cognitive outcome [56]. Conventional measures such as ESES and spike-wave index (SWI) did not show the same association with treatment response or cognitive outcome [56].

Alterations in large-scale brain connectivity have also been investigated as potential biomarkers of epileptogenesis in pediatric epilepsy. In infants with tuberous sclerosis complex (TSC), abnormal connectivity patterns were identified before the clinical onset of epileptic spasms [65]. Infants who later developed epileptic spasms showed increased functional connectivity during sleep, together with enhanced local and long-range neural synchronization (Fig. 18), suggesting that alterations in network organization may precede overt seizure manifestations [65].

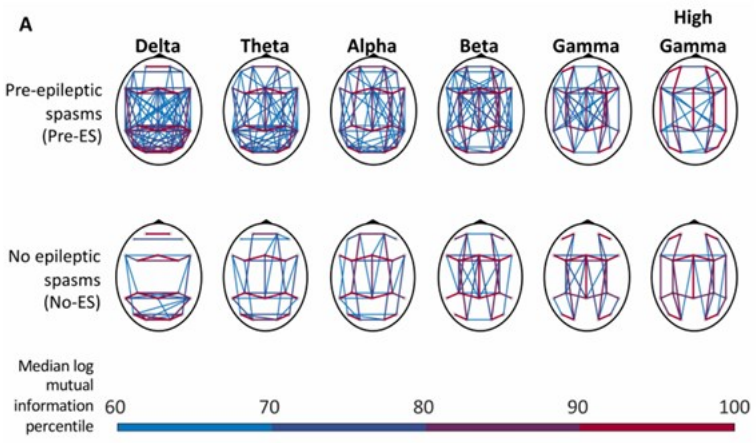


Figure 18. Functional EEG connectivity during sleep in infants with tuberous sclerosis complex (TSC). Increased long-range and interhemispheric connectivity was observed in infants who later developed epileptic spasms [65].

Entropy-based EEG measures provide a complementary approach for characterizing the complexity and irregularity of brain activity. Multifrequency entropy was found to decrease during sleep, particularly during NREM stage N2, both in healthy children and in patients with BECTS [57]. Importantly, entropy values were consistently lower in patients with epilepsy, particularly within epileptic brain regions, suggesting an association between reduced EEG complexity and increased epileptogenicity [57].

Sleep spindle analysis has also been investigated as a marker of network dysfunction and cognitive impairment in pediatric epilepsy. In drug-naïve children with CAE, significant reductions in sleep spindle density and duration during N2 sleep were observed compared with healthy controls (Fig. 19) [58]. Lower spindle density was also associated with cognitive impairment, supporting a relationship between abnormalities in sleep-related thalamo-cortical activity and cognitive function [58].

The main pediatric epilepsy syndromes discussed above, together with their characteristic EEG features, sleep-related abnormalities, and investigated advanced EEG biomarkers, are summarized in Table 1.

Table 1. Summary of the pediatric epilepsy syndromes discussed, including their characteristic EEG features, sleep-related abnormalities, and investigated advanced EEG biomarkers.

Syndrome	Main EEG features	Sleep-related findings	Advanced biomarkers
SeLECTS	Centrotemporal spikes activated during NREM sleep [61]	Increased epileptiform activity during sleep [61]	High-frequency oscillations (HFOs), entropy-based microstate analysis [61]
Infantile spasms	Hypsarrhythmia [62]	HFO coupling with slow-wave activity during sleep [62]	Scalp EEG HFOs [62]
ESES / CSWS	Continuous spike–wave activity during NREM sleep [56]	Increased spike frequency and delta power during sleep [63]	HFO persistence associated with poor outcome [56]
Childhood absence epilepsy (CAE)	Generalized 3-Hz spike-and-wave discharges [58]	Reduced sleep spindle density and duration during N2 sleep [58]	Sleep spindle analysis [58]
Lennox–Gastaut syndrome (LGS)	GPFA and heterogeneous interictal EEG abnormalities [64]	Altered sleep spindle activity during NREM sleep [64]	Automated time–frequency EEG biomarkers [64]

Taken together, these findings highlight the heterogeneity of EEG abnormalities across pediatric epilepsy syndromes and demonstrate how quantitative EEG biomarkers can complement conventional electroclinical assessment. HFOs, connectivity measures, entropy-based analyses, and sleep-related features provide different but potentially complementary information on epileptic activity, network organization, and disease evolution, supporting their continued investigation as diagnostic and prognostic biomarkers in pediatric epilepsy.

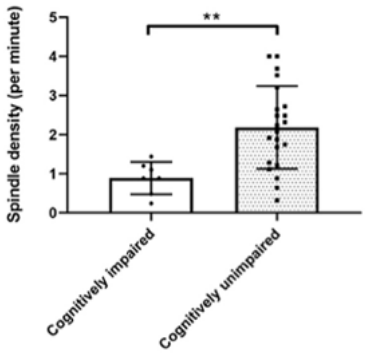


Figure 19. Sleep spindle density during N2 sleep in children with childhood absence epilepsy (CAE). Reduced spindle density was observed in cognitively impaired patients compared with cognitively unimpaired patients [58].

1.5.3 Quantitative electroencephalography and Advanced Analysis in Pediatric Epilepsy

Quantitative electroencephalography (qEEG) refers to the application of computational and mathematical methods for the quantitative analysis of EEG signals. Unlike conventional EEG interpretation, which mainly relies on the visual assessment of waveform morphology, qEEG enables the extraction of measurable features from electrophysiological recordings, allowing a more objective characterization of brain activity. Recent advances in signal processing have introduced both linear and non-linear approaches for EEG analysis. Traditional methods mainly evaluate signal characteristics such as amplitude, frequency, and power spectral density (PSD), whereas non-linear parameters, including entropy, Lyapunov exponents, and Hurst index, are able to characterize the complex and irregular dynamics of neuronal activity [40]. Because EEG signals are intrinsically dynamic and non-stationary, nonlinear dynamical analysis has progressively emerged as an important tool for investigating neurological disorders such as epilepsy. Nonlinear EEG analysis aims to describe neuronal behavior through mathematical measures capable of quantifying complexity, synchronization, and coupling between brain regions [66]. Several studies demonstrated that these measures are sensitive to physiological and pathological alterations in brain dynamics, including changes associated with epileptic activity.

In particular, approaches derived from chaos theory and nonlinear dynamics, such as correlation dimension, entropy-based measures, Lyapunov exponents, and synchronization analysis, provide additional information beyond conventional spectral analysis and may improve the characterization of abnormal electrophysiological patterns [66]. In pediatric epilepsy, these quantitative methods have increasingly been investigated for seizure prediction, identification of epileptogenic patterns, and outcome evaluation through automated EEG analysis and machine learning techniques [40]. Recent studies have increasingly explored the integration of quantitative EEG analysis, automated signal processing, and machine learning techniques in pediatric epilepsy. Mercier et al. combined quantitative EEG analysis with artificial neural network (ANN) models in pediatric patients undergoing epilepsy surgery, analyzing both wakefulness and sleep EEG recordings [67]. Multiple linear and non-linear EEG features were extracted, including PSD, Hjorth parameters, entropy measures, Lyapunov exponents, and Hurst index. Among these biomarkers, Hurst exponent, alpha-band PSD, and mobility index during sleep were significantly associated with post-surgical seizure freedom, while machine learning models based on selected EEG features achieved better predictive performance than models using broader non-selected feature sets [67]. Automated EEG quantification has also been investigated for the early identification of children at risk of developing electrical status epilepticus during sleep (ESES). Azeem et al. demonstrated that children who later developed ESES showed significantly higher spike frequency and increased delta power during sleep EEG recordings several years before clinical diagnosis [63]. The study combined automated spike detection and PSD analysis, and automated spike quantification showed high agreement with human EEG reviewers, supporting the reliability of computational EEG analysis methods [63]. Similarly, automated time–frequency analysis and unsupervised pattern detection techniques have been applied to pediatric epileptic encephalopathies to identify recurring EEG patterns in a more systematic and quantitative manner [64]. In Lennox–Gastaut syndrome (LGS), these approaches identified both established EEG features, such as interictal epileptiform discharges and generalized paroxysmal fast activity (GPFA), and additional oscillatory patterns in the beta- and gamma-frequency ranges during non-rapid eye movement (NREM) sleep (Fig. 20) [64].

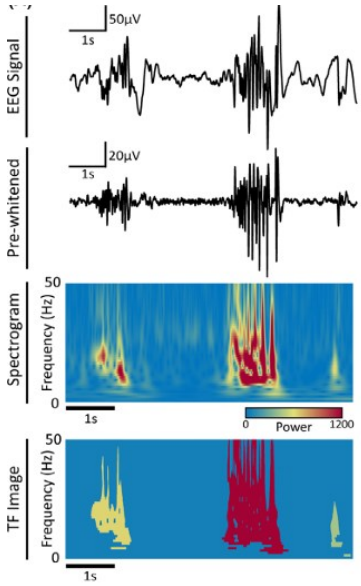


Figure 20. Example of time–frequency EEG decomposition and quantitative feature extraction used for automated identification of electrophysiological patterns in Lennox–Gastaut syndrome [64].

In addition to automated detection and machine learning approaches, nonlinear EEG analysis has increasingly been used to investigate large-scale brain dynamics and signal complexity in pediatric epilepsy. Entropy-based measures and EEG microstate analysis allow the evaluation of both transient brain network organization and the irregularity of neuronal activity. EEG microstates represent quasi-stable scalp topographies associated with large-scale neural networks, whereas entropy measures quantify the complexity and temporal dynamics of EEG signals [68]. Using these approaches, recent studies in children with self-limited epilepsy with centrotemporal spikes (SeLECTS) demonstrated reduced entropy values in patients with ADHD comorbidity, particularly during sleep, indicating lower global EEG complexity and less flexible brain dynamics (Fig. 21) [68]. Similarly, multifrequency entropy analysis in children with benign epilepsy with centrotemporal spikes (BECTS) demonstrated lower entropy values compared with healthy controls during both wakefulness and sleep, with the lowest entropy observed during non-rapid eye movement (NREM) sleep stage 2. In addition, centrotemporal epileptic regions exhibited lower entropy than non-centrotemporal regions, suggesting localized alterations in neuronal dynamics associated with epileptogenicity [57]. Hence, advanced quantitative EEG analysis may provide important information about abnormal synchronization, network dysfunction, and neurocognitive impairment in pediatric epilepsy, particularly during sleep.

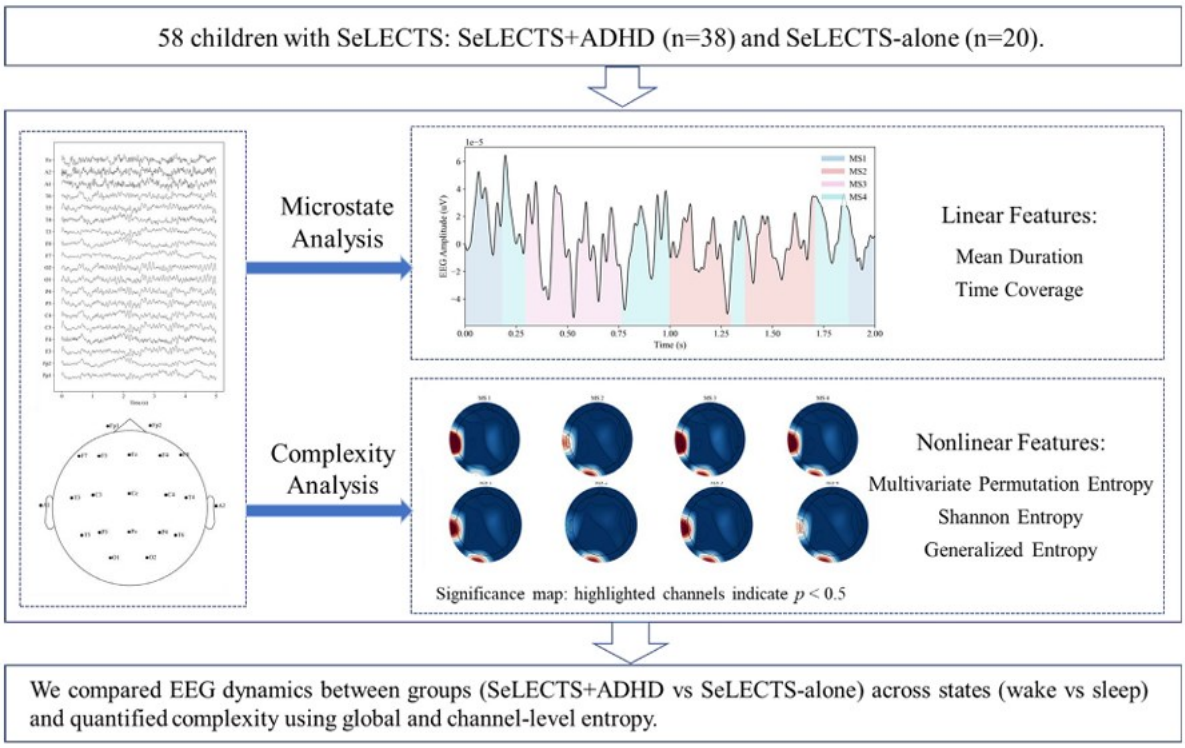


Figure 21. Schematic representation of the computational EEG analysis pipeline, including microstate analysis and entropy-based nonlinear feature extraction used to characterize brain dynamics in children with SeLECTS [68].

1.5.4 Related works and research gaps

A systematic literature review was conducted to identify relevant studies investigating sleep EEG monitoring, advanced EEG biomarkers, and quantitative EEG analysis in pediatric epilepsy. The detailed search strategy, inclusion and exclusion criteria, and study selection process are described in Appendix I.

The selected studies highlight the growing importance of sleep EEG analysis and advanced computational approaches in the characterization of pediatric epilepsy. In particular, sleep was consistently shown to modulate epileptiform activity and brain network dynamics, especially during non-rapid eye movement (NREM) sleep, facilitating the detection of electrophysiological abnormalities that may not be evident during wakefulness alone. In addition, advanced EEG biomarkers may provide clinically relevant information beyond conventional visual EEG interpretation. Several studies investigated sleep-related and network-based biomarkers, including high-frequency oscillations (HFOs), sleep spindle abnormalities, entropy-based measures, functional connectivity alterations, and EEG microstate dynamics, demonstrating their potential role in the identification of epileptogenic activity, cognitive impairment, treatment response, and abnormal brain synchronization. In particular, HFOs and sleep spindle alterations were consistently associated with

pathological brain activity during NREM sleep, whereas connectivity and nonlinear analyses highlighted abnormalities in large-scale brain network organization and synchronization. In parallel, quantitative EEG approaches based on automated signal processing, time–frequency analysis, machine learning techniques, and automated spike detection provided increasingly objective and reproducible methods for the analysis of pediatric EEG recordings and the identification of clinically relevant electrophysiological patterns.

Despite the growing interest in advanced EEG biomarkers, several limitations still affect their application in pediatric epilepsy research. One of the main issues concerns the lack of methodological standardization across studies. Different preprocessing pipelines, recording durations, sleep-stage selections, and feature extraction methods were adopted for the analysis of HFOs, entropy measures, connectivity, and other quantitative EEG parameters, making direct comparison between studies difficult. Another important limitation is the relatively small size and heterogeneity of pediatric cohorts. Most studies were conducted on single-center populations and focused on specific epilepsy syndromes, including infantile spasms, Lennox–Gastaut syndrome (LGS), childhood absence epilepsy (CAE), tuberous sclerosis complex (TSC), and self-limited epilepsy with centrotemporal spikes (SeLECTS). Consequently, many proposed biomarkers still require validation in larger and more heterogeneous pediatric populations. The reviewed literature also shows that most studies investigated individual biomarkers separately, such as HFOs, entropy measures, or connectivity alterations, whereas integrated multimodal approaches remain limited. In addition, although sleep was consistently identified as an important factor influencing epileptiform activity and biomarker detection, overnight EEG recordings and sleep-stage standardization were not uniformly addressed across studies. Recent studies further highlighted the limitations of conventional visual EEG interpretation and the need for more objective computational approaches. Hu et al. investigated the interrater reliability of EEG waveform classification in Lennox–Gastaut syndrome and reported substantial variability among expert reviewers, particularly for complex EEG patterns such as generalized paroxysmal fast activity (GPFA) [69]. Many disagreements occurred when one reviewer classified an EEG event as abnormal while another considered it insignificant, suggesting the use of different visual thresholds during EEG interpretation. The authors therefore emphasized the potential role of computational EEG analysis in improving the objectivity and reproducibility of EEG biomarkers [69]. These findings support the need for more standardized and clinically interpretable quantitative EEG approaches capable of improving reproducibility and supporting clinical interpretation.

Rationale behind the Thesis

The identification of reliable electroencephalographic biomarkers capable of characterizing epileptic brain activity during sleep remains an important objective in pediatric epilepsy research. Sleep, particularly NREM sleep, is known to influence epileptiform activity and represents a physiological condition in which pathological oscillations become more prominent. This makes sleep EEG recordings a valuable source of information for investigating biomarkers associated with epileptic brain activity.

Among the electrophysiological phenomena observed during sleep, HFOs are particularly relevant because pathological HFOs have been associated with epileptogenic brain activity and investigated as markers of epileptogenic tissue, disease activity, and clinical outcome. However, HFO occurrence represents only one aspect of the electrophysiological activity recorded during sleep. Quantitative EEG analysis may provide complementary information on the organization and dynamics of brain activity associated with these events. In particular, measures of EEG complexity can characterize variations in signal regularity and temporal organization, providing a broader quantitative description of the EEG activity accompanying HFO occurrence.

Within this context, the present thesis combines a systematic review with an experimental analysis. The systematic review was conducted to examine the EEG biomarkers investigated in pediatric epilepsy during sleep and the methodological approaches adopted in previous studies. The reviewed literature highlighted growing interest in quantitative EEG features, including HFOs, entropy-based measures, and other indices related to signal complexity and temporal dynamics, while also revealing considerable methodological heterogeneity and a tendency to investigate individual biomarkers separately. These findings motivated the investigation of EEG complexity as a complementary approach to characterize the electrophysiological changes associated with HFO activity in pediatric patients with epilepsy.

Building on this rationale, the experimental study investigates whether different dimensions of EEG complexity are associated with HFO occurrence during N3 sleep. A further objective is to examine their temporal relationship, determining whether complexity changes are primarily associated with the HFO event itself or whether distinct alterations are also detectable immediately before or after its occurrence. Finally, the study assesses whether complexity-related information is sufficiently consistent across patients to discriminate EEG activity associated with HFOs from activity temporally distant from these events and, in particular, whether a distinctive complexity pattern can be identified immediately before HFO occurrence.

By integrating HFO information with quantitative measures of EEG complexity, this thesis aims to provide a more comprehensive characterization of the EEG dynamics associated with HFO activity during sleep. This integrated approach is particularly relevant in pediatric epilepsy, where sleep strongly modulates epileptiform activity and HFO occurrence. Ultimately, the study seeks to clarify whether complexity-based features can provide complementary information to HFOs in the quantitative characterization of epileptic brain activity.

2. Materials and Methods

2.1 Dataset description

The dataset used in this study comprises scalp EEG recordings enriched with high-frequency oscillation (HFO) annotations from 30 paediatric patients with epilepsy recruited at the University Children's Hospital Zurich [70]. All participants were under 18 years of age, with ages ranging from 0.7 to 17.4 years, thus covering a broad developmental period from infancy to adolescence. The cohort included patients with focal or generalized epilepsy and different underlying aetiologies, including structural, genetic, and unknown causes. The recordings were acquired during whole-night video-EEG monitoring performed for different clinical purposes, including differential diagnosis of epileptic and non-epileptic events, seizure and epilepsy syndrome classification, and pre-surgical evaluation. For each patient, one recording was selected according to two inclusion criteria: a high sampling frequency (>1000 Hz) and the presence of at least 10 min of N3 sleep.

Whole-night scalp EEG recordings were acquired using 21 electrodes positioned according to the international 10–20 system, with high sampling frequencies (≥1024 Hz) suitable for the analysis of high-frequency activity. Electrode impedances were typically maintained at or below 1 kΩ. Continuous video monitoring accompanied EEG acquisition throughout the night. Sleep staging was performed offline by experienced neurophysiologists according to the American Academy of Sleep Medicine (AASM) criteria. For the original study, N3 sleep intervals were selected from the first 3 h of sleep, since HFOs are less affected by muscle artefacts and occur at higher rates during N3 sleep than during other sleep stages. EEG intervals containing visible artefacts and channels affected by continuous interference were excluded, and the selected N3 data were divided into 5-min intervals for subsequent processing.

The dataset is organized according to the Brain Imaging Data Structure (BIDS) specification and includes both the original EEG recordings and derivative data. Raw EEG recordings are stored in EDF format, together with metadata containing channel and recording information. The derivatives directory contains processed EEG data corresponding to the selected N3 intervals. In these derivative data, the original EEG signals had been re-referenced by the dataset authors to 52 bipolar derivations constructed between neighbouring electrodes for HFO analysis. Each processed run represents a continuous 5-min segment of N3 sleep selected from the original whole-night EEG recording and provided in the derivatives directory after bipolar re-referencing. Multiple 5-min runs could therefore be available for the same patient, depending on the amount of N3 sleep identified within the first 3 h of sleep.

High-frequency oscillations were automatically detected in the bipolar signals using a clinically validated detector. Only events in the ripple frequency range (80–250 Hz) were considered. The detector identifies candidate oscillatory events and subsequently applies time-frequency and scalp-specific rejection criteria to distinguish HFOs from background activity and artefacts. The resulting HFO annotations are provided for each processed N3 interval. Additional metadata are provided to link the processed N3 intervals and the corresponding HFO annotations to the original whole-night EEG recordings. These metadata specify the temporal location of each processed interval within the original recording and provide the information required to align the HFO annotations with the corresponding EEG data.

2.2 Electroencephalography Preprocessing and Artifact Rejection

EEG preprocessing was performed in MATLAB R2026a (The MathWorks, Inc., Natick, MA, USA) using the EEGLAB toolbox [71]. Raw EEG recordings were imported in EDF format, while HFO annotations were processed separately and subsequently aligned with the preprocessed EEG recordings.

Prior to signal processing, non-EEG channels, including electrocardiographic (ECG/EKG), electrooculographic (EOG), electromyographic (EMG), respiratory, pulse, trigger, marker, and annotation channels, were excluded when present. Only EEG channels were retained for subsequent analyses.

The EEG signals were high-pass filtered at 1 Hz and low-pass filtered at 250 Hz. The 250 Hz cutoff was selected because the analysis focused on high-frequency EEG activity, particularly HFOs in the ripple range (80–250 Hz). A 49–51 Hz notch filter was additionally applied to attenuate power-line interference. The native sampling frequency of each recording was retained. Following filtering, the continuous EEG was divided into consecutive, non-overlapping 4-s windows until the end of the recording was reached.

Preliminary inspection showed relatively high-amplitude EEG activity, including slow waves and sharp transients that could reflect physiological sleep activity or epileptiform discharges rather than artifacts. Therefore, particular attention was given to the selection of an artifact-detection method that would limit the removal of potentially meaningful EEG activity.

As an initial approach, an amplitude-based criterion relying on the standard deviation (STD) was evaluated. For each EEG channel, the STD was calculated across the signal samples within each 4-s window, and channel-windows satisfying $4 \times \mathrm{STD} > 400\ \mu\mathrm{V}$ were classified as artifact-contaminated.

Joint Probability was subsequently evaluated as an alternative distribution-based artifact-detection method. This method identifies statistically atypical EEG activity by evaluating probability distributions both within individual channels and across the set of EEG channels. Its use was supported by Lopez et al. [72], who compared automated segment-rejection approaches with manual artifact classification within the HAPPILEE framework. Among the tested settings, Joint Probability at 2 standard deviations showed the highest overall classification accuracy (91.2%). Here, the 2-STD threshold refers to deviations of the probability measure from its distribution across EEG segments, rather than to the amplitude variability of the EEG signal within an individual 4-s window.

Based on this evidence, Joint Probability at 2 STD was selected as the final artifact-detection method and applied using both local and global probability criteria. The local criterion evaluated each EEG channel separately, identifying channel-windows with atypical probability relative to the distribution observed for that channel. The global criterion considered probability information across EEG channels to identify atypical overall activity. The STD-based criterion was retained only as a preliminary comparison.

Artifact rejection was performed at the channel-window level. Therefore, a channel-window classified as artifact-contaminated was excluded from subsequent analysis without excluding clean channels within the same 4-s interval. Joint Probability classifications were summarized for each subject by reporting the number of 4-s channel-windows classified as clean or artifact-contaminated. The resulting artifact classifications were then used in the subsequent EEG biomarker and HFO-related analyses.

2.3 Electroencephalographic Biomarkers Extraction

Following preprocessing and segmentation, a set of 14 quantitative EEG measures was extracted from the artifact-free 4-s windows of each EEG channel. The selected measures comprised Approximate Entropy (ApEn), Sample Entropy (SampEn), Spectral Entropy, Permutation Entropy (PE), Shannon Entropy, Rényi Entropy, Tsallis Entropy, Higuchi Fractal Dimension (HFD), Katz Fractal Dimension (KFD), Petrosian Fractal Dimension (PFD), Detrended Fluctuation Analysis (DFA) exponent, Hurst exponent, Lempel–Ziv Complexity (LZC), and Hjorth Complexity. These measures provide complementary descriptions of EEG irregularity, complexity, spectral organization, waveform geometry, and temporal scaling. In this study, they were evaluated in relation to HFO occurrence, given the established association between pathological HFOs and epileptogenic brain activity.

All measures were computed independently for each EEG channel and each artifact-free 4-s window using customized MATLAB functions, with the same parameter settings applied across all subjects (Table 2). Channel-windows classified as artifact-contaminated by the Joint Probability procedure described in Section 2.2 were excluded from the computation. Invalid or numerically degenerate values were also excluded from subsequent analyses.

Entropy-based measures

Entropy-based measures were used to characterize different aspects of EEG irregularity, predictability, and distributional complexity.

- **Approximate Entropy (ApEn).** ApEn quantifies the regularity and predictability of a time series by evaluating the recurrence of similar signal patterns [73]. In the present analysis, an embedding dimension $m = 2$, a time delay $\tau = 1$ sample, and a tolerance $r = 0.20\ \sigma$, where σ is the standard deviation of the corresponding EEG window, were used. Similarity between embedded vectors was evaluated using the Chebyshev distance, with self-matches included. ApEn was calculated according to Eq. (1):

$$ApEn = \phi(m) - \phi(m+1) \qquad (1)$$

where $m$is the embedding dimension and $\phi(m)$ represents the average logarithmic probability that embedded vectors of dimension $m$are similar within the tolerance r. Lower ApEn values indicate more regular and predictable signal patterns, whereas higher values indicate greater irregularity and unpredictability.

- **Sample Entropy (SampEn).** SampEn also quantifies temporal regularity but, unlike ApEn, excludes self-matches [74]. The same parameters used for ApEn were adopted ($m = 2, \tau = 1$ sample, and $r = 0.20\ \sigma$). SampEn was calculated according to Eq. (2):

$$SampEn = -\ln\left(\frac{A}{B}\right) \qquad (2)$$

where $B$is the number of matching pairs of embedded vectors of dimension m, and A is the number of pairs that remain matched when the dimension is increased to $m + 1$. Lower values indicate more regular and predictable activity, whereas higher values indicate greater irregularity.

- **Permutation Entropy (PE).** PE quantifies signal complexity from the distribution of ordinal patterns within the time series [75]. Embedded vectors were constructed using an embedding

dimension $m = 3$ and a time delay $\tau = 1$sample and converted into ordinal patterns according to the relative ordering of their values. PE was normalized by its theoretical maximum and therefore ranged from 0 to 1, with values approaching 0 indicating highly regular and predictable ordinal dynamics and values approaching 1 indicating an approximately uniform distribution of ordinal patterns.

- **Shannon, Rényi, and Tsallis Entropies.** These measures were estimated from the empirical amplitude distribution of each EEG window using 64 equally spaced bins, with histogram limits adapted to the amplitude range of each window. Shannon Entropy [76], Rényi Entropy [77], and Tsallis Entropy [78] characterize the distribution of signal amplitudes using different entropy formulations. Rényi and Tsallis entropies were computed with orders $\alpha = 2$ and $q = 2$, respectively. All three measures were normalized to their theoretical maxima, yielding values between 0 and 1. Values approaching 0 indicate that signal amplitudes are concentrated in a limited number of bins, whereas values approaching 1 indicate a more uniform amplitude distribution.

- **Spectral Entropy.** Spectral Entropy quantifies the distribution of EEG power across frequencies. The mean was removed from each window and the power spectral density was estimated using Welch's method with a Hamming window, 50% overlap, and a segment length of up to 1024 samples [79]. The PSD was normalized to obtain a probability distribution, and Spectral Entropy was calculated as its normalized Shannon entropy. Values approaching 0 indicate spectral power concentrated in a limited number of frequencies, whereas values approaching 1 indicate a more uniform distribution of spectral power.

Fractal-dimension measures

Fractal-dimension measures were used to characterize the geometric complexity and irregularity of the EEG waveform through three complementary algorithms.

- Higuchi Fractal Dimension (HFD)**.** HFD quantifies the fractal complexity of a time series by evaluating how its estimated curve length changes across different temporal scales [80]. In the present analysis, curve lengths were calculated for scales $k = 1, \dots, k_{max}$, with $k_{max} = 10$, and averaged across the possible initial points for each scale. HFD was estimated according to Eq. (3) as the slope of the linear regression between the logarithm of the mean curve length $L(k)$ and the logarithm of the inverse scale:

$$HFD = slope[log\, L\,(k)\ vs.\ log(1/k)] \qquad (3)$$

where $k$is the temporal scale and $L(k)$ is the mean curve length estimated at that scale. Higher HFD values indicate a more irregular and geometrically complex waveform, whereas lower values indicate a smoother and less complex temporal structure. No amplitude normalization was applied.

- Katz Fractal Dimension (KFD). KFD characterizes waveform complexity from the geometric trajectory of the EEG signal, taking into account its total curve length and its maximum distance from the first point [81]. KFD was calculated according to Eq. (4):

$$KFD = \frac{log_{10}(N)}{log_{10}(d/L) + log_{10}(N)} \qquad (4)$$

where $N$is the number of samples in the EEG window, $L$is the total geometric length of the signal trajectory, and $d$is the maximum geometric distance from the first point of the trajectory. Higher KFD values indicate a more geometrically complex and irregular waveform, whereas lower values indicate a simpler trajectory. No amplitude normalization was applied.

- Petrosian Fractal Dimension (PFD)**.** PFD provides a computationally efficient estimate of waveform complexity based on changes in the direction of the signal [82]. It was derived from the number of sign changes in the first discrete derivative and calculated according to Eq. (5):

$$PFD = \frac{log_{10}(N)}{log_{10}(N) + log_{10}\left(\frac{N}{N + 0.4N_{\Delta}}\right)} \qquad (5)$$

where N is the number of samples in the EEG window and N_{Δ} is the number of sign changes in its first discrete derivative. Zero-valued differences were excluded before counting sign changes. Higher PFD values indicate greater waveform irregularity and more frequent changes in signal direction, whereas lower values indicate a smoother and more regular waveform. No amplitude normalization was applied.

Temporal scaling measures

Temporal scaling measures were used to characterize the temporal organization and long-range dependence of the EEG signal through Detrended Fluctuation Analysis (DFA) and the Hurst exponent.

- Detrended Fluctuation Analysis (DFA). First-order DFA (DFA-1) was implemented according to Peng et al. [83] to quantify scale-dependent temporal correlations in the EEG signal. After removal of the signal mean, the cumulative profile was constructed and divided into segments at multiple temporal scales. Twenty approximately logarithmically spaced scales were defined between 16 samples and $N/4$, where Nis the number of samples in the 4-s EEG window. Segmentation was performed from both the beginning and the end of the signal to reduce boundary effects due to unused samples. Within each segment, a first-order polynomial trend was removed and the root-mean-square fluctuation $F(n)$ was calculated. The DFA exponent $\alpha$was then estimated according to Eq. (6) as the slope of the log-log relationship:

$$\log_{10}F(n) = \alpha\log_{10}(n) + c \qquad (6)$$

where nis the temporal scale, $F(n)$ is the corresponding fluctuation function, $\alpha$is the DFA scaling exponent, and cis the regression intercept. Higher αvalues indicate stronger temporal persistence, whereas lower values indicate weaker temporal correlations. The coefficient of determination (R^2) of the log-log regression was additionally retained as an indicator of fit quality.

- Hurst exponent. The Hurst exponent (H) was estimated using classical rescaled-range (R/S) analysis [84] to characterize long-range temporal dependence. At each temporal scale, the EEG signal was divided into segments from both the beginning and the end. Within each segment, the local mean was removed, the cumulative deviation series was calculated, and its range Rwas normalized by the corresponding standard deviation S. The resulting R/S values were averaged across valid segments at each scale. The same 20 approximately logarithmically spaced scales used for DFA, ranging from 16 samples to $N/4$, were adopted. The Hurst exponent was estimated according to Eq. (7) as the slope of the log-log relationship:

$$\log_{10}(R/S) = H\log_{10}(n) + c \qquad (7)$$

where nis the temporal scale, R/S is the mean rescaled range at that scale, H is the Hurst exponent, and c is the regression intercept. Values of $H > 0.5$ indicate persistent temporal behavior, $H \approx 0.5$ indicates approximately uncorrelated behavior, and $H < 0.5$ indicates antipersistent behavior. The R^2 of the log-log regression was also retained as an indicator of fit quality.

Lempel–Ziv Complexity

- Lempel–Ziv Complexity (LZC). LZC was used to quantify the diversity of temporal patterns in the EEG signal according to the sequence-complexity framework introduced by Lempel and Ziv [85]. Each EEG window was converted into a binary sequence using its median amplitude as the threshold, with samples above the median assigned a value of 1 and all remaining samples assigned a value of 0. The resulting binary sequence was processed using the LZ76 exhaustive parsing algorithm to determine the number of distinct subsequences encountered during sequential parsing. Normalized LZC was calculated according to Eq. (8):

$$LZC = C_{\mathrm{raw}} \frac{\log_2(N)}{N} \qquad (8)$$

where C_{raw} is the number of subsequences identified by the LZ76 parsing algorithm and $N$is the length of the binary sequence. Higher normalized LZC values indicate greater diversity and novelty of temporal patterns, whereas lower values indicate a more repetitive and regular sequence. No z-score or additional amplitude normalization was applied before binarization.

Hjorth Complexity

- Hjorth Complexity**.** Hjorth Complexity was calculated according to the time-domain descriptors introduced by Hjorth [86] and characterizes changes in the temporal dynamics of the signal relative to its first derivative. It was calculated according to Eq. (9):

$$HC = \frac{\sqrt{\mathrm{Var}(\Delta^2 x)/\mathrm{Var}(\Delta x)}}{\sqrt{\mathrm{Var}(\Delta x)/\mathrm{Var}(x)}} \qquad (9)$$

where x is the EEG signal, Δx is its first discrete derivative, $\Delta^2 x$ is its second discrete derivative, and $\mathrm{Var}(\cdot)$ denotes the population variance. Values approaching 1 indicate temporal dynamics closer to those of a pure sinusoidal signal, whereas larger values indicate greater deviation from sinusoidal behavior and greater waveform complexity. No z-score or amplitude normalization was applied.

For each subject, the resulting complexity measures were organized as channel × window matrices. Channel-windows classified as artifact-contaminated were represented as NaN and excluded from subsequent analyses. The complexity measures were then combined with the temporally mapped HFO annotations for the HFO-related statistical and classification analyses.

Table 2. Summary of the quantitative EEG biomarkers extracted from each artifact-free 4-s EEG window, including the main computational parameters and methodological references.

Biomarker	Category	Main parameters / implementation	Reference
Approximate Entropy	Entropy	$m = 2, \tau = 1, r = 0.2SD$; Chebyshev distance; self-matches included	[73]
Sample Entropy	Entropy	$m = 2, \tau = 1, r = 0.2SD$; self-matches excluded	[74]
Permutation Entropy	Entropy	$m = 3, \tau = 1$; normalized by $\ln(m!)$	[75]
Shannon Entropy	Entropy	64-bin amplitude distribution; normalized	[76]
Rényi Entropy	Entropy	64 bins; $\alpha = 2$; normalized	[77]
Tsallis Entropy	Entropy	64 bins; $q = 2$; normalized	[78]
Spectral Entropy	Spectral	Welch PSD; Hamming; 50% overlap; normalized Shannon entropy	[76][79]
Higuchi FD	Fractal	$k_{\max} = 10$	[80]
Katz FD	Fractal	Curve length and maximum distance	[81]
Petrosian FD	Fractal	Sign changes of first derivative	[82]
DFA exponent	Scaling	DFA-1; scales 16–$N/4$; log-log regression	[83]
Hurst exponent	Scaling	Classical R/S; scales 16–$N/4$	[84]
Lempel–Ziv Complexity	Complexity	Median binarization; LZ76; normalized	[85]
Hjorth Complexity	Time-domain	Mobility of signal and first derivative	[86]

2.4 High Frequency Oscillation Analysis

HFO Mapping and Alignment with EEG Windows

High-frequency oscillation (HFO) annotations provided with the dataset were temporally mapped onto the continuous EEG recordings to investigate their relationship with the quantitative EEG measures described above. The annotations corresponded to ripple events in the 80–250 Hz frequency range detected in bipolar EEG derivations during selected N3 sleep intervals. The dataset also provided an indicator specifying whether each detected HFO had passed the rejection criteria applied

by the dataset authors. In the present analysis, only events classified as accepted were considered [87].

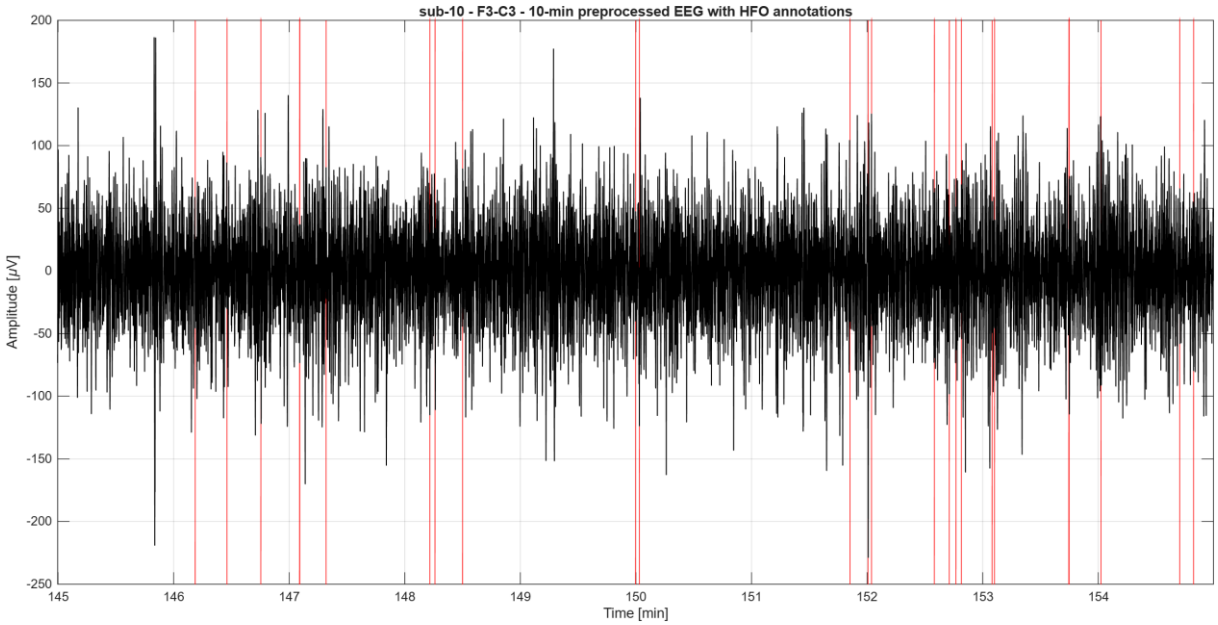
For each subject, the temporal information provided with the dataset was used to align the HFO annotations with the corresponding continuous EEG recording. Since the HFO annotations referred to derivative recordings sampled at 2000 Hz, their start and end positions were converted to the time base of the continuous EEG using the subject-specific native sampling frequency. In this way, each accepted HFO event was assigned its corresponding start and end time in the continuous EEG recording.

The mapped HFO events were then aligned with the consecutive non-overlapping 4-s windows previously used for EEG complexity analysis. A window was classified as HFO-containing when its temporal interval overlapped with at least one accepted HFO event; otherwise, it was classified as HFO-free. This procedure allowed the complexity measures extracted from each 4-s window to be related to HFO occurrence.

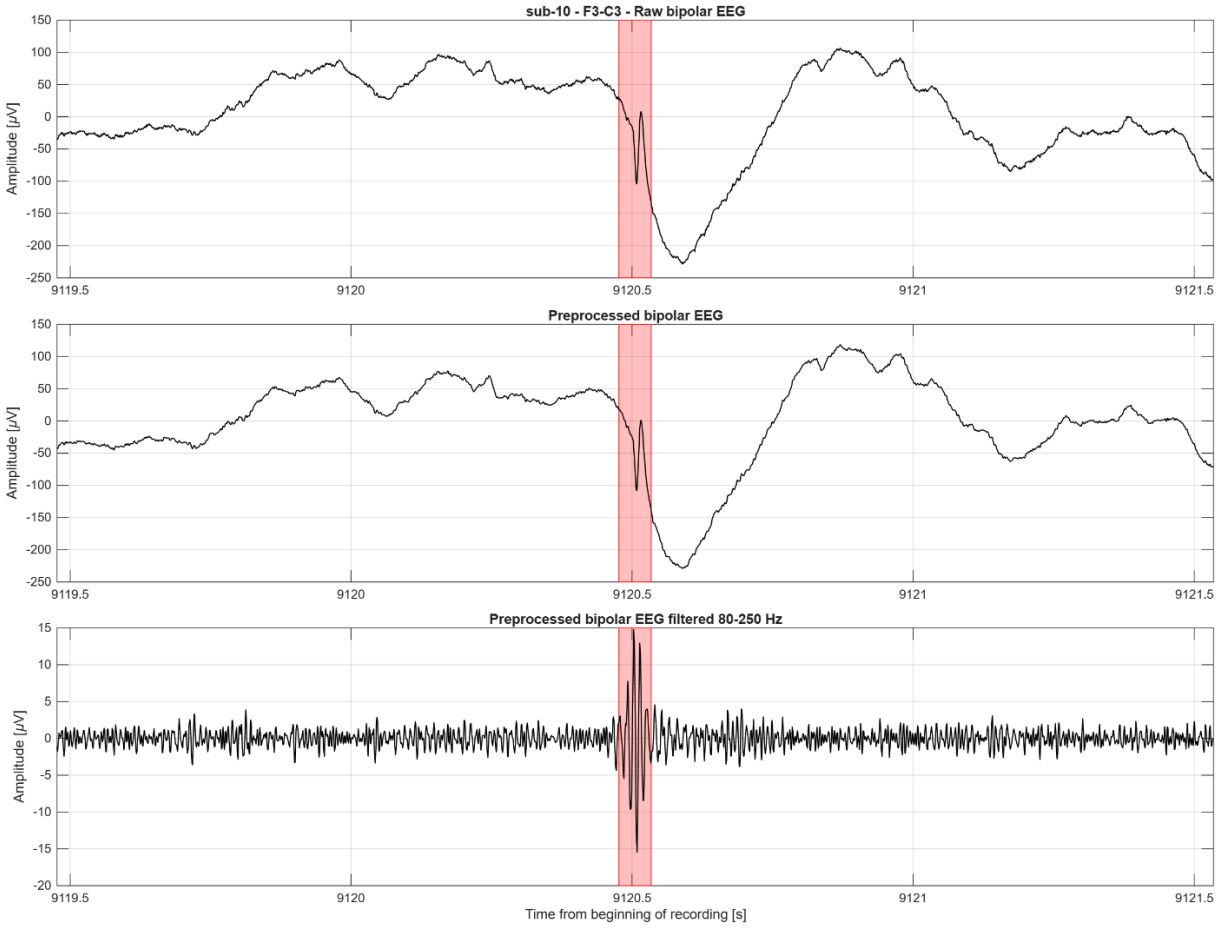
Visual Verification of HFO Alignment

As a procedural quality-control step, representative visualizations were generated to verify the temporal alignment between the provided HFO annotations and the continuous EEG. Subject 10 was selected as an illustrative example because it provided a clear visualization of the HFO mapping procedure and was used consistently across the subsequent representative visualizations to facilitate comparison between the different steps of the analysis. Within this subject, the bipolar derivation containing the largest number of accepted HFO events (F3–C3) was selected, providing a sufficient number of annotated events for visual inspection. Since HFO annotations were provided for bipolar derivations, the corresponding bipolar EEG signal was reconstructed from the two constituent monopolar channels.

First, a representative 10-min segment of the preprocessed broadband EEG was displayed, with time on the x-axis and EEG amplitude (μV) on the y-axis. The mapped HFO intervals were superimposed on the EEG trace and indicated in red (Fig. 22A). Individual HFO events were then inspected in greater detail within 2-s intervals. As shown in Fig. 22B, each event was visualized in the raw bipolar EEG (top), the preprocessed bipolar EEG (middle), and the preprocessed signal additionally filtered in the 80–250 Hz ripple band (bottom). The annotated HFO interval was highlighted in red in all three representations. The 80–250 Hz filtering was applied exclusively for visualization and was not used for biomarker computation.



(A)



(B)

Figure 22. *Visual verification of HFO annotation alignment with the continuous EEG. (A) Representative 10-min segment of preprocessed broadband bipolar EEG, with accepted HFO annotations indicated in red. (B) Detailed visualization of a representative annotated HFO event (red shaded interval) in the raw bipolar EEG (top), preprocessed bipolar EEG (middle), and preprocessed EEG filtered in the 80–250 Hz ripple band (bottom). Time is reported on the x-axis and EEG amplitude in μV on the y-axis. The 80–250 Hz filtering was applied exclusively for visualization.*

Regional Complexity Analysis

To investigate the spatial distribution of EEG complexity in relation to HFO occurrence, the 14 complexity measures previously extracted from artifact-free 4-s EEG windows were summarized across five anatomical regions: frontal (Fp1, Fp2, F7, F3, Fz, F4, F8), central (C3, Cz, C4), temporal (T1, T2, T3, T4, T5, T6), parietal (P3, Pz, P4), and occipital (O1, O2). For each biomarker and 4-s window, the regional value was calculated as the mean of the available values from the monopolar channels belonging to that region. Channel-window values previously classified as artifact-contaminated by Joint Probability were excluded from the regional average.

Regional biomarker trajectories were represented over the entire available recording to visualize the temporal evolution of EEG complexity across the five anatomical regions. In Fig. 23A, time from the beginning of the recording is reported on the x-axis, while the corresponding regional biomarker value is reported on the y-axis; separate traces represent the frontal, central, temporal, parietal, and occipital regions. To facilitate visualization of the temporal trends, a three-window moving average, corresponding to a 12-s temporal span, was applied. Smoothing was used exclusively for visualization, while all numerical analyses were performed on the original unsmoothed data.

To visualize regional complexity changes more clearly around HFO activity, representative HFO-centred portions of the temporal trajectories were also examined. Consecutive HFO-positive 4-s windows were grouped into HFO blocks, with the first HFO-positive window defining the beginning of each block. Up to three HFO blocks distributed across the recording were selected for each subject. For each selected block, a 2-min interval extending approximately 1 min before and 1 min after its beginning was displayed, with HFO-positive windows highlighted on the regional complexity trajectories (Fig. 23B). The same three-window moving average described above was applied for visualization.



Figure 23. Representative regional temporal evolution of Katz Fractal Dimension in subject 10. (A) Full-recording regional trajectories. Time from the beginning of the EEG recording (h) is shown on the x-axis and the regional mean Katz Fractal Dimension on the y-axis. Separate traces represent the frontal, central, temporal, parietal, and occipital regions. A three-window moving average, corresponding to 12 s, was applied exclusively to facilitate visualization of the temporal trends. (B) Representative raw 2-min HFO-centred zoom. Time relative to the beginning of the selected HFO block (min) is shown on the x-axis and the regional mean Katz Fractal Dimension on the y-axis. The dashed vertical line at 0 indicates the beginning of the HFO block, defined by its first HFO-positive 4-s window, while the markers along the bottom indicate HFO-positive 4-s windows within the displayed interval.

HFO-Centred Temporal Analysis

The same HFO blocks defined above were subsequently used to examine the temporal evolution of regional complexity around HFO occurrence. The first HFO-positive 4-s window of each block was defined as the common reference point (t = 0). For each block, regional complexity values were extracted from the five windows preceding and the five windows following this reference point,

corresponding to a −20 to +20 s interval with a temporal resolution of 4 s. Only blocks for which the complete peri-HFO interval was contained within an annotated N3 sleep interval were included, ensuring that complexity changes around HFO occurrence were evaluated within the same sleep stage.

To align HFO blocks occurring at different times during the recording, each block was expressed relative to this common reference point. The same relative time points (−20, −16, −12, −8, −4, 0, +4, +8, +12, +16, and +20 s) could therefore be compared across HFO blocks. For each subject, biomarker, and brain region, the median complexity value across all eligible HFO blocks was calculated separately at each relative time point, resulting in a subject-specific HFO-centred trajectory.

Population-level trajectories were then obtained by calculating, at each relative time point and for each region, the median of the subject-specific values. The 25th and 75th percentiles were used to represent the interquartile range across subjects. This two-level aggregation ensured that each subject contributed equally to the population trajectory, independently of the number of HFO blocks available.

Definition of Temporal Conditions

In addition to the HFO-centred trajectories described above, the temporal relationship between EEG complexity and HFO activity was examined by grouping N3 windows into four discrete conditions: Distant Baseline, Pre-HFO, HFO, and Post-HFO. This complementary analysis was used to compare complexity values during HFO activity with those immediately preceding and following HFO blocks and with activity temporally distant from HFOs.

The HFO condition included all HFO-positive N3 windows. The Pre-HFO condition corresponded to the single 4-s N3 window immediately preceding the beginning of each HFO block, whereas the Post-HFO condition corresponded to the single 4-s N3 window immediately following its end. Windows simultaneously satisfying the Pre-HFO and Post-HFO definitions, which could occur between closely spaced HFO blocks, were excluded from both conditions.

Distant Baseline was defined as N3 activity temporally separated from HFO occurrence. Specifically, the five 4-s windows preceding and following each HFO-positive window, corresponding to a ±20-s interval, were excluded from the baseline condition. Thus, Distant Baseline included only N3 windows located outside these peri-HFO intervals.

For each subject, biomarker, brain region, and temporal condition, the median regional complexity value across the available windows was calculated. These subject-level values were used to generate descriptive regional boxplots comparing Distant Baseline, Pre-HFO, HFO, and Post-HFO across subjects. Inferential comparisons among the four conditions were performed separately, as described in the Statistical Analysis section.

2.5 Statistical Analysis and Classification

Statistical analyses were performed to identify EEG complexity biomarkers associated with HFO occurrence and to characterize their temporal evolution before, during, and after HFO activity. To account for the presence of multiple bipolar derivations and EEG windows from the same individual, the analyses described below were based on subject-level values.

First, complexity values obtained during HFO-containing windows were compared with those obtained during No-HFO windows within annotated N3 sleep. HFO occurrence was defined separately for each bipolar derivation. For each derivation, the corresponding two monopolar EEG channels were identified, and a derivation-level complexity value was obtained for each 4-s window as the median across the available artifact-free constituent electrodes. Since channel-windows rejected by the Joint Probability procedure had already been stored as NaN, the median was calculated using the available finite values; when neither constituent electrode provided a valid value, the observation remained unavailable. HFO windows were defined as annotated N3 windows overlapping at least one accepted HFO event on the considered bipolar derivation, whereas No-HFO windows comprised the remaining annotated N3 windows without HFO activity on that derivation. For each biomarker, a derivation was retained only when at least three valid HFO and three valid No-HFO windows remained after exclusion of artifact-contaminated or numerically invalid observations.

For each retained derivation and biomarker, the median complexity value was calculated separately for the two conditions, and their difference was defined as HFO minus No-HFO. These derivation-level differences were subsequently aggregated within each subject using the median, yielding one subject-level value per biomarker. The distribution of subject-level differences was tested against zero using a two-sided Wilcoxon signed-rank test, a non-parametric test for paired observations that does not require normally distributed differences [88]. This analysis therefore assessed whether each biomarker showed a systematic HFO-related change across subjects. Since all 14 complexity biomarkers were independently tested, the resulting *p*-values were corrected for multiple comparisons

using the Benjamini–Hochberg false discovery rate (FDR) procedure [89]. Statistical significance was defined as an FDR-adjusted $p < 0.05$.

Biomarkers showing a significant HFO-versus-No-HFO difference after FDR correction were subsequently investigated across the four HFO-related temporal conditions defined in the previous section (Distant Baseline, Pre-HFO, HFO, and Post-HFO). As above, conditions were defined separately for each bipolar derivation. For this statistical analysis, conditions were defined separately for each bipolar derivation.

The same derivation-level representation described above was applied, using the median complexity value across the two corresponding monopolar electrodes and the available artifact-free observations. For each biomarker and derivation, at least three valid HFO windows, three valid distant-baseline windows, one valid Pre-HFO window, and one valid Post-HFO window were required. Median complexity values were then calculated separately for the four conditions. For each subject and biomarker, condition-specific values were obtained as the median across those bipolar derivations for which all four conditions were available, yielding one repeated-measures observation per subject and condition.

Differences among the four conditions were first assessed using the Friedman test, a non-parametric test for repeated measures that does not require normally distributed observations [90]. Since the test was independently performed for the selected biomarkers, the resulting p-values were corrected using the Benjamini–Hochberg FDR procedure. Paired post-hoc comparisons were subsequently performed using two-sided Wilcoxon signed-rank tests for the six possible condition pairs: Pre-HFO versus Baseline, HFO versus Baseline, Post-HFO versus Baseline, HFO versus Pre-HFO, Post-HFO versus HFO, and Post-HFO versus Pre-HFO. The p-values from all post-hoc comparisons were jointly corrected using the Benjamini–Hochberg FDR procedure. In both analyses, an FDR-adjusted $p < 0.05$ was considered statistically significant.

Subject-level values were also used to generate boxplots illustrating the distributions of statistically significant markers across the four temporal conditions, with the principal FDR-significant paired comparisons indicated graphically.

In addition to the univariate statistical analyses, a supervised machine-learning analysis was performed to investigate whether EEG complexity biomarkers jointly contained sufficient information to discriminate HFO-related activity from distant baseline activity. To avoid feature-selection leakage, all 14 predefined complexity biomarkers were included as predictors, independently of their statistical significance in the preceding univariate analyses.

A classification dataset was generated from the subject-specific complexity results obtained after Joint Probability artifact rejection. Only annotated N3 windows classified as either HFO-containing or distant baseline were retained. In contrast to the derivation-specific statistical analyses, HFO occurrence was defined globally at the window level for classification: an N3 window was assigned to the HFO class when it contained at least one temporally mapped HFO event, irrespective of the bipolar derivation on which the event occurred. Distant baseline windows were defined as annotated N3 windows located outside a ±20-s interval around any HFO-containing window. The number of 4-s windows corresponding to this exclusion interval was derived from the actual window duration for each recording.

For each selected window and biomarker, a single predictor value was obtained as the median across the available artifact-free EEG channels. Observations containing at least one non-finite value among the 14 predictors were excluded, thereby retaining only complete predictor vectors. Subjects were included only when at least three valid HFO and three valid distant-baseline windows remained.

As a preliminary model-selection step, different supervised classifiers were compared using the MATLAB Classification Learner App with five-fold cross-validation. To retain models representing different classification approaches, the classifier achieving the highest balanced accuracy within each of three model families was selected. This procedure resulted in the selection of a Medium Gaussian Support Vector Machine (SVM), a Bagged Trees ensemble, and a Narrow Neural Network for subsequent subject-independent validation. The Medium Gaussian SVM used a Gaussian kernel with a kernel scale equal to the square root of the number of predictors and standardized predictors. The Bagged Trees classifier consisted of an ensemble of 100 classification trees generated through bootstrap aggregation. The Narrow Neural Network consisted of a single hidden layer with 10 units and standardized predictors.

Final performance assessment was performed programmatically using a leave-one-subject-out (LOSO) cross-validation strategy. In each fold, all EEG windows belonging to one subject were held out as the test set, while data from all remaining subjects were used for model training. This procedure was repeated until each eligible subject had served once as the independent test subject. Thus, EEG windows from the same individual could not be simultaneously represented in the training and test sets, preventing subject-related information leakage and providing a more stringent assessment of classifier generalization to previously unseen subjects.

Because the numbers of HFO and distant-baseline windows were unequal, class balancing was applied exclusively to the training data. Within each LOSO fold, the majority class was randomly

undersampled to match the number of observations in the minority class, while the complete test set was retained with its natural class distribution. To reduce dependence on a particular random undersampling, the complete LOSO procedure was repeated 20 times using different reproducible random seeds.

Classification performance was evaluated using accuracy, sensitivity, specificity, balanced accuracy, and the area under the receiver operating characteristic curve (ROC-AUC). For the primary HFO-versus-distant-baseline classification task, HFO windows were considered the positive class and distant-baseline windows the negative class. Accordingly, true positives (TP) and true negatives (TN) represented correctly classified HFO and distant-baseline windows, respectively, whereas false positives (FP) corresponded to distant-baseline windows incorrectly classified as HFO and false negatives (FN) to HFO windows incorrectly classified as distant baseline. The metrics were defined according to the following Eq. (1), (2), (3):

$$\text{Accuracy} = \frac{TP + TN}{TP + TN + FP + FN} \quad (1)$$

$$\text{Sensitivity} = \frac{TP}{TP + FN} \quad (2)$$

$$\text{Specificity} = \frac{TN}{TN + FP} \quad (3)$$

Thus, in the primary HFO-versus-distant-baseline task, HFO sensitivity represented the proportion of HFO windows correctly identified as HFO, whereas distant-baseline specificity represented the proportion of baseline windows correctly identified as baseline.

Balanced accuracy was calculated according to Eq (4):

$$\text{Balanced Accuracy} = \frac{\text{Sensitivity} + \text{Specificity}}{2} \quad (4)$$

and was considered the primary metric for model comparison because it assigns equal importance to the correct classification of the two classes, independently of their relative frequencies in the test set. ROC-AUC quantified the classifier's ability to discriminate between the two classes across classification thresholds, with a value of 0.5 corresponding to chance-level discrimination and a value of 1 indicating perfect discrimination.

Performance metrics were first calculated separately for each held-out subject. Within each repetition of the LOSO procedure, these subject-specific metrics were averaged across subjects, so that each subject contributed equally regardless of the number of available EEG windows. This yielded one performance value for each metric and classifier per repetition. Since the LOSO procedure was repeated 20 times with different training-set undersampling, the resulting 20 performance values were then summarized by their mean and standard deviation.

A second classification analysis investigated whether the same 14 complexity biomarkers could discriminate EEG activity immediately preceding an HFO from distant baseline activity. Pre-HFO observations corresponded to the valid 4-s N3 window immediately preceding the beginning of an HFO block, whereas distant baseline windows were located outside the ±20-s interval surrounding HFO activity. Predictor values were obtained using the same channel-wise median approach described for the primary classification task. Observations containing at least one non-finite predictor were excluded, and subjects were retained only when at least three valid Pre-HFO and three valid distant-baseline windows were available.

The classifier showing the highest balanced accuracy in the primary HFO-versus-distant-baseline LOSO comparison was retained for this secondary task. Accordingly, the Pre-HFO analysis was performed using the Medium Gaussian SVM, while maintaining the same subject-wise LOSO validation strategy, training-set balancing procedure, and 20 repeated undersampling runs. This sequential approach avoided a new model-selection procedure specifically on the Pre-HFO comparison and allowed the previously selected classifier to be evaluated on the more challenging distinction between Pre-HFO and distant baseline activity.

Performance was quantified using accuracy, Pre-HFO sensitivity, distant-baseline specificity, balanced accuracy, and ROC-AUC. In the secondary Pre-HFO-versus-distant-baseline task, Pre-HFO windows were considered the positive class and distant-baseline windows the negative class. Accordingly, Pre-HFO sensitivity represented the proportion of Pre-HFO windows correctly identified as Pre-HFO, whereas distant-baseline specificity represented the proportion of baseline windows correctly identified as baseline. As in the primary classification analysis, metrics were calculated separately for each held-out subject and subsequently macro-averaged across subjects within each repetition.

3. Results

EEG Preprocessing and Artifact Rejection

EEG preprocessing was successfully completed for all 30 subjects. Following channel selection, 23 EEG channels were retained for most subjects, while 24 channels were retained for three subjects (sub-04, sub-15, and sub-18). Continuous recordings were segmented into non-overlapping 4-s windows, resulting in 2700 windows per channel for all subjects except sub-19, whose shorter EEG recording resulted in 1805 windows per channel.

Overall, 1,850,515 channel-windows were evaluated using the Joint Probability artifact-rejection procedure. Of these, 1,773,787 (95.85%) were retained as valid, whereas 76,728 (4.15%) were identified as artifact-contaminated. The percentage of artifact-contaminated channel-windows varied across subjects, from 1.33% in sub-05 to 6.70% in sub-08, with a median of 3.84%. Thus, more than 95% of the available EEG data were retained for subsequent complexity analysis.

The 14 EEG complexity biomarkers were subsequently computed for the valid 4-s channel-windows and combined with the HFO annotations for the following statistical analyses.

EEG Complexity Biomarkers and HFO Occurrence

The association between EEG complexity and HFO occurrence was evaluated in 29 of the 30 subjects by comparing HFO-containing and No-HFO windows within annotated N3 sleep. One subject (sub-30) was excluded from this analysis because none of its bipolar derivations met the predefined minimum requirement of at least three valid HFO and three valid No-HFO windows. Although 28 HFO events were identified in this subject, they were distributed across 23 bipolar derivations, with each derivation containing only one or two HFO-positive N3 windows.

Among the 14 investigated biomarkers, seven showed significant differences between HFO and No-HFO conditions after FDR correction, indicating that HFO occurrence was associated with changes in multiple measures of EEG complexity. Katz Fractal Dimension showed the strongest statistical evidence of an HFO-related difference and was the only significant biomarker with higher values during HFO activity. Its median HFO–No-HFO difference was +0.00440 ($p = 2.56 \times 10^{-6}$, FDR-adjusted $p = 3.59 \times 10^{-5}$), with the same direction of change observed in all 29 subjects. In contrast, the other six significant biomarkers showed lower values during HFO activity. Petrosian Fractal Dimension decreased by a median of −0.000163 ($p = 1.76 \times 10^{-4}$, FDR-adjusted $p = 9.73 \times 10^{-4}$), with a negative difference in 25 over 29 subjects. Permutation Entropy similarly decreased by −0.00403 ($p = 2.09 \times 10^{-4}$, FDR-adjusted $p = 9.73 \times 10^{-4}$), also showing a negative difference in 25

of 29 subjects. Significant reductions were additionally observed for Hjorth Complexity (median difference = −0.766, FDR-adjusted p = 0.00463), Shannon Entropy (−0.00270, FDR-adjusted p = 0.00556), Tsallis Entropy (−0.000260, FDR-adjusted p = 0.00556), and Rényi Entropy (−0.00293, FDR-adjusted p = 0.00893) (Table 3).

The remaining seven biomarkers, Higuchi Fractal Dimension, DFA exponent, Sample Entropy, Spectral Entropy, Approximate Entropy, Hurst exponent, and Lempel–Ziv Complexity, did not show statistically significant differences after FDR correction (FDR-adjusted $p > 0.05$). Therefore, the HFO-related differences were specific to a subset of the investigated complexity measures rather than being observed across all 14 biomarkers.

Table 3. EEG complexity biomarkers showing significant differences between HFO-containing and No-HFO N3 windows. N indicates the number of subjects included in the group-level analysis. Δ represents the subject-level median difference between HFO-containing and No-HFO windows. Positive values indicate higher complexity during HFO activity, whereas negative values indicate lower values during HFO activity. FDR-adjusted p-values were obtained using the Benjamini–Hochberg procedure.

Biomarker	**N**	**Median Δ (HFO − No-HFO)**	***p*-value**	**FDR-adjusted *p***
Katz Fractal Dimension	29	+0.004397	2.56×10^{-6}	3.59×10^{-5}
Petrosian Fractal Dimension	29	−0.000163	1.76×10^{-4}	9.73×10^{-4}
Permutation Entropy	29	−0.004035	2.09×10^{-4}	9.73×10^{-4}
Hjorth Complexity	29	−0.765705	0.00132	0.00463
Shannon Entropy	29	−0.002703	0.00238	0.00556
Tsallis Entropy	29	−0.000260	0.00238	0.00556
Rényi Entropy	29	−0.002934	0.00446	0.00893

The seven biomarkers showing significant HFO-versus-No-HFO differences were carried forward to the subsequent temporal analysis.

Temporal Complexity Changes around HFOs

After identifying the seven complexity measures that showed significant differences between HFO and No-HFO activity, their temporal behavior around HFO occurrence was further investigated. HFO-centered regional trajectories were first examined descriptively to visualize how these measures evolved before, during, and after HFO-block onset across the five predefined brain regions. This descriptive analysis was then complemented by statistical comparisons among the predefined Distant Baseline, Pre-HFO, HFO, and Post-HFO conditions.

Population-level profiles were obtained from subject-level trajectories over the −20 to +20 s interval relative to HFO-block onset. Figure 24 summarizes the regional temporal profiles of the seven significant complexity measures. Overall, the trajectories showed relatively limited temporal fluctuations, with the magnitude and temporal pattern of the changes varying across complexity measures and brain regions.

The seven biomarkers showing statistically significant HFO-versus-No-HFO differences after FDR correction were subsequently evaluated across Distant Baseline, Pre-HFO, HFO, and Post-HFO conditions in the 29 subjects retained for the derivation-specific analysis. A significant overall effect of HFO-related condition was found for all seven biomarkers after FDR correction.

The strongest statistical evidence was observed for Katz Fractal Dimension (FDR-adjusted $p = 3.08 \times 10^{-8}$). Significant effects were also found for Hjorth Complexity (FDR-adjusted $p = 7.36 \times 10^{-4}$), Permutation Entropy (FDR-adjusted $p = 0.0115$), Rényi Entropy (FDR-adjusted $p = 0.0115$), Tsallis Entropy (FDR-adjusted $p = 0.0115$), Petrosian Fractal Dimension (FDR-adjusted $p = 0.0163$), and Shannon Entropy (FDR-adjusted $p = 0.0163$). Pairwise comparisons showed that statistically significant differences mainly involved comparisons between the HFO condition and the other temporal conditions. All seven biomarkers differed significantly between HFO and Distant Baseline. Six of the seven also differed significantly between HFO and Pre-HFO; Permutation Entropy was the only biomarker for which the HFO versus Pre-HFO comparison did not remain significant after FDR correction (FDR-adjusted $p = 0.0633$). In contrast, none of the seven biomarkers differed significantly between Pre-HFO and Distant Baseline. A similar pattern was observed after HFO activity. Post-HFO values differed significantly from HFO values for all seven biomarkers, whereas none differed significantly from Distant Baseline. Post-HFO and Pre-HFO values were also not significantly different for six of the seven biomarkers, with Hjorth Complexity representing the only significant comparison (FDR-adjusted $p = 0.0257$). Overall, these results indicate that significant complexity differences were predominantly associated with the HFO condition, whereas no consistent differences from Distant Baseline were detected immediately before or after HFO activity (Fig. 25).

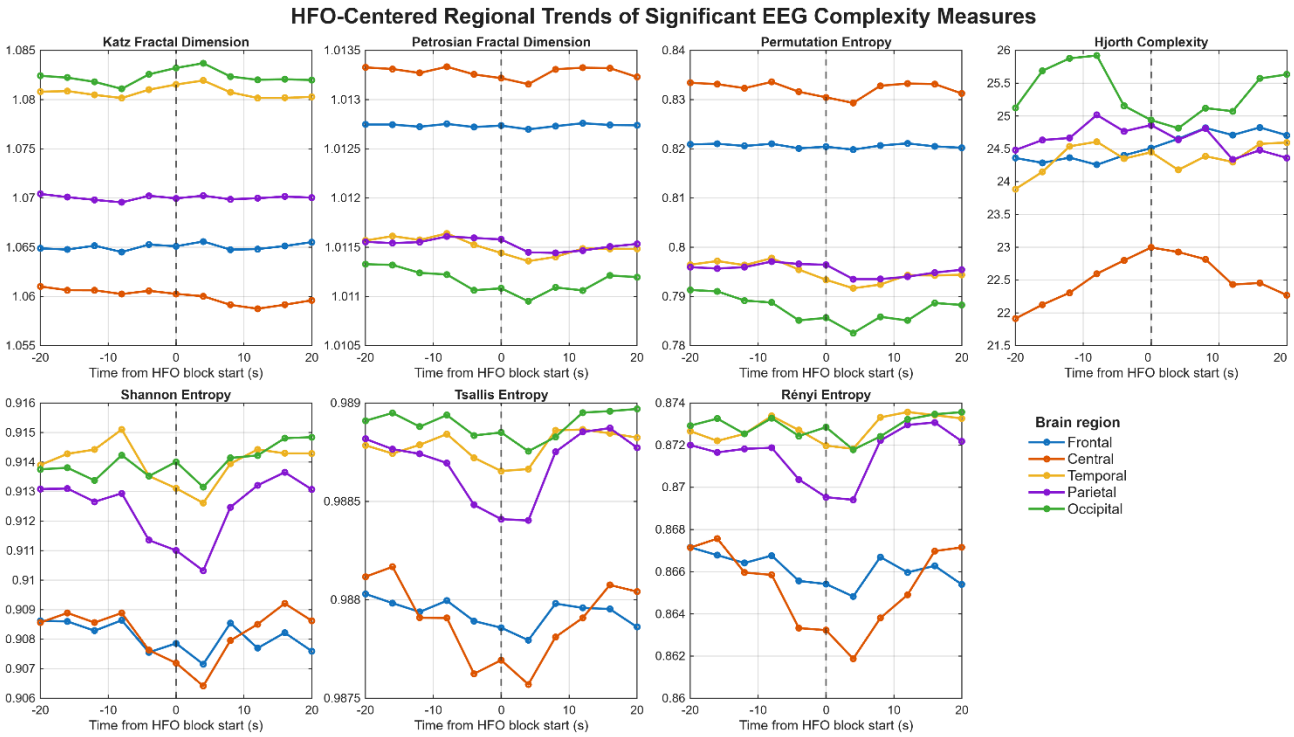


Figure 24. Population HFO-centered regional trajectories of the seven EEG complexity measures showing significant HFO–No-HFO differences after FDR correction. Curves represent the population-level temporal profiles across the five predefined brain regions over the −20 to +20 s interval relative to HFO-block onset. A three-window moving mean was applied for visualization only. The dashed vertical line at 0 s indicates the start of the HFO block.

A similar pattern was observed after HFO activity. Post-HFO values differed significantly from HFO values for all seven biomarkers, whereas none differed significantly from distant Baseline. Post-HFO and Pre-HFO values were also not significantly different for six of the seven biomarkers, with Hjorth Complexity representing the only significant comparison (FDR-adjusted $p = 0.0257$). Overall, these results show that the largest complexity differences occurred during HFO activity, whereas no consistent difference from distant baseline was detected immediately before or after HFO activity (Fig.25).

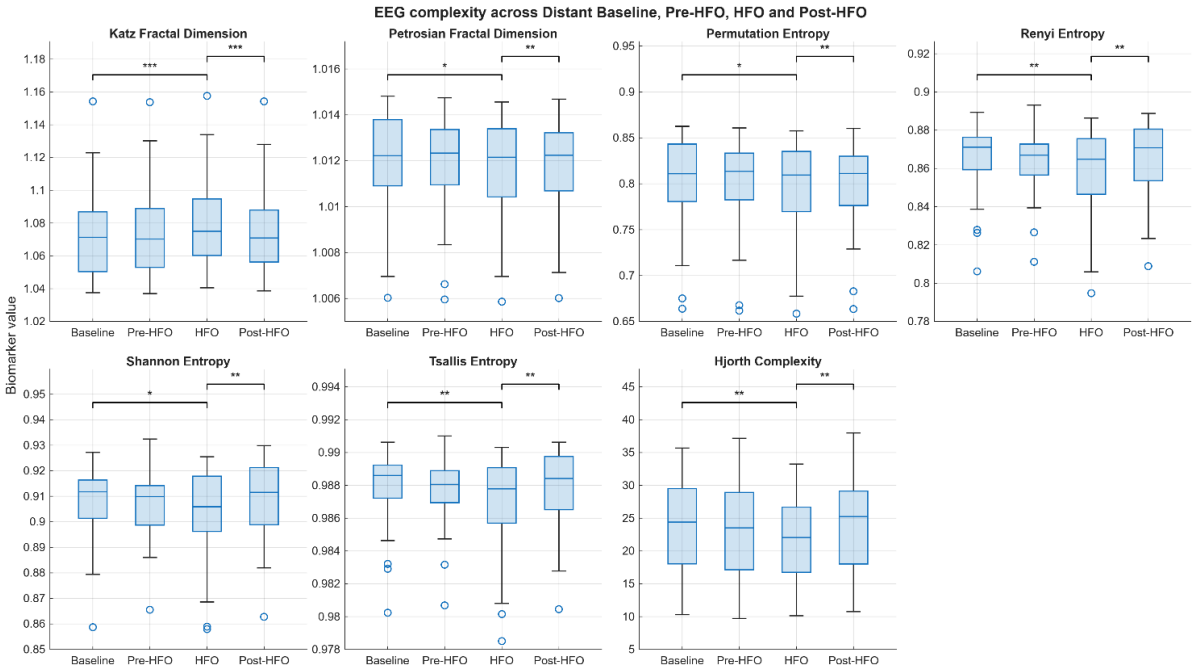


*Figure 25. EEG complexity across distant Baseline, Pre-HFO, HFO, and Post-HFO conditions. Boxplots show the subject-level distributions of the seven complexity biomarkers that exhibited significant HFO-versus-No-HFO differences after FDR correction. Boxes represent the interquartile range, central lines indicate the median, whiskers show the non-outlier range, and circles indicate outliers. Brackets indicate the principal pairwise comparisons that remained significant after Benjamini–Hochberg FDR correction ($q < 0.05$). *$q < 0.05$, **$q < 0.01$, ***$q < 0.001$.*

Classification Results

The combined discriminative ability of the 14 EEG complexity biomarkers was evaluated for distinguishing HFO-related EEG activity from distant baseline activity. Classification performance was modest for all three classifiers selected during the preliminary model-selection step and evaluated using subject-independent LOSO cross-validation. The Medium Gaussian SVM achieved the highest balanced accuracy (53.73 ± 0.27%) and ROC-AUC (0.577 ± 0.003). Its overall accuracy was 61.36 ± 0.22%, with an HFO sensitivity of 57.54 ± 0.38% and a distant-baseline specificity of 49.93 ± 0.49%. The Narrow Neural Network showed a comparable balanced accuracy of 53.72 ± 0.88% and an ROC-AUC of 0.575 ± 0.014, whereas Bagged Trees achieved a balanced accuracy of 53.30 ± 0.51% and an ROC-AUC of 0.545 ± 0.007. Although Bagged Trees showed the highest overall accuracy (63.16 ± 0.77%) and HFO sensitivity (65.31 ± 0.95%), its distant-baseline specificity was lower (41.30 ± 1.42%). Overall, balanced accuracy remained only slightly above the 50% chance level for all three classifiers (Table 4).

Table 4. Repeated LOSO classification performance for HFO versus distant baseline. Values are reported as mean ± standard deviation across 20 repetitions.

Model	Accuracy (%)	HFO Sensitivity (%)	Baseline Specificity (%)	Balanced Accuracy (%)	ROC-AUC
Medium Gaussian SVM	61.36 ± 0.22	57.54 ± 0.38	49.93 ± 0.49	53.73 ± 0.27	0.577 ± 0.003
Narrow Neural Network	62.49 ± 1.69	60.91 ± 2.16	46.54 ± 2.85	53.72 ± 0.88	0.575 ± 0.014
Bagged Trees	63.16 ± 0.77	65.31 ± 0.95	41.30 ± 1.42	53.30 ± 0.51	0.545 ± 0.007

Since Medium Gaussian SVM achieved the highest balanced accuracy in the HFO-versus-distant-baseline task, it was retained for the subsequent discrimination of Pre-HFO from distant baseline activity. The Pre-HFO classification dataset comprised 4,234 windows from 23 subjects, including 1,911 Pre-HFO and 2,323 distant-baseline observations. In this second classification task, performance decreased to approximately chance level. The Medium Gaussian SVM achieved a balanced accuracy of 49.28 ± 0.38% and an ROC-AUC of 0.497 ± 0.004. Overall accuracy was 54.94 ± 0.28%, with a Pre-HFO sensitivity of 63.64 ± 0.73% and a distant-baseline specificity of 34.92 ± 0.84%. Thus, the 14 complexity biomarkers did not provide meaningful subject-independent discrimination between Pre-HFO and distant-baseline activity. Figure 26 summarizes the balanced accuracy obtained for the HFO-versus-distant-baseline and Pre-HFO-versus-distant-baseline classification tasks.

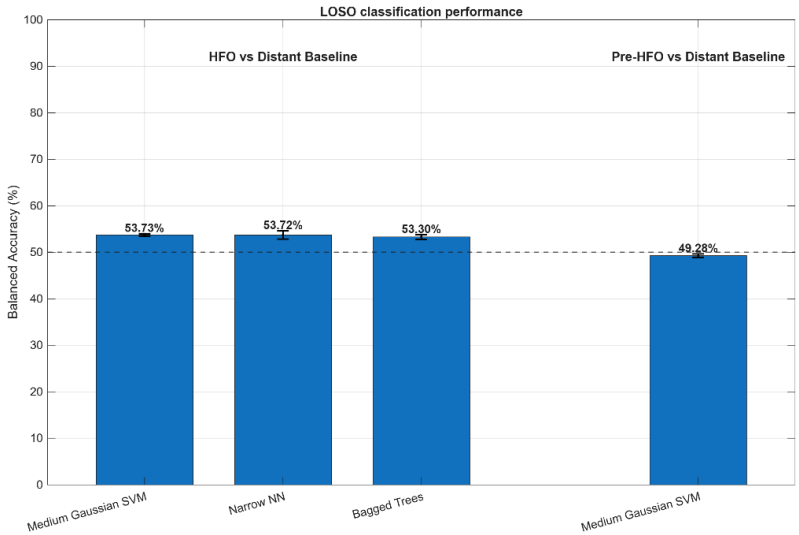


Figure 26. LOSO classification performance for HFO-versus-distant-baseline and Pre-HFO-versus-distant-baseline discrimination. Bars represent the mean subject-macro-averaged balanced accuracy across 20 repeated LOSO runs, and error bars indicate the corresponding standard deviation. For the HFO-versus-distant-baseline task, Medium Gaussian SVM, Narrow Neural Network, and Bagged Trees were compared. Medium Gaussian SVM, which achieved the highest balanced accuracy in the primary task, was subsequently retained for Pre-HFO-versus-distant-baseline classification. The dashed horizontal line indicates the 50% chance level.

4. Discussion

The present study investigated the relationship between HFO occurrence and EEG complexity during N3 sleep in pediatric patients with epilepsy. The analysis included EEG preprocessing and artifact rejection, the comparison of complexity measures between HFO and No-HFO activity, the evaluation of their temporal changes around HFO occurrence, and subject-independent classification.

The EEG recordings were filtered between 1 and 250 Hz, with an additional 49–51 Hz notch filter. The upper cutoff of 250 Hz preserved the frequency range of the ripple HFOs considered in this study (80–250 Hz). The continuous EEG was divided into consecutive non-overlapping 4-s windows, providing sufficient samples for complexity analysis while maintaining a relatively short observation interval. However, this temporal resolution may have limited the identification of brief changes immediately preceding HFO occurrence.

Particular attention was given to artifact detection, since high-amplitude activity during pediatric sleep does not necessarily represent artifact and may include physiological or epileptiform activity. An initial threshold of 150 μV resulted in excessive rejection of EEG observations. A higher threshold of 400 μV was therefore evaluated after inspecting signal amplitude distributions and representative EEG segments, although this remained a dataset-dependent choice rather than a standardized criterion. Joint Probability at 2 STD was ultimately selected for the final analysis because it provided a distribution-based approach without relying on a fixed amplitude threshold. Using this method, 4.15% of the evaluated channel-windows were classified as artifact-contaminated.

Fourteen complexity measures were investigated, seven of which showed statistically significant differences between HFO and No-HFO activity after correction for multiple comparisons. Katz Fractal Dimension increased during HFO activity, whereas Petrosian Fractal Dimension, Permutation Entropy, Hjorth Complexity, Shannon Entropy, Tsallis Entropy, and Rényi Entropy decreased.

From a physiological perspective, these findings suggest that HFO occurrence is associated with changes in different properties of EEG dynamics rather than with a uniform increase or decrease in signal complexity. The reduction in Shannon, Rényi, and Tsallis Entropy may indicate a more concentrated distribution of signal amplitudes, whereas lower Permutation Entropy suggests reduced diversity of local temporal patterns. Previous research has shown that entropy measures can characterize alterations in epileptic EEG activity, including during sleep [57], [91]. Nevertheless, changes in entropy cannot be directly interpreted as evidence of increased neuronal synchronization, since different measures describe distinct properties of the signal [92].

The opposite behavior of Katz and Petrosian Fractal Dimensions may reflect their different mathematical definitions. Katz Fractal Dimension depends on the geometric trajectory of the signal, whereas Petrosian Fractal Dimension is based on changes in signal direction [81], [82]. These differences highlight the importance of considering multiple complexity measures when characterizing EEG dynamics [91], [92].

From a clinical perspective, previous research has shown that nonlinear EEG features, including Petrosian Fractal Dimension, can contribute to distinguishing physiological from pathological HFOs in intracranial recordings [93]. Although this supports the potential clinical relevance of combining HFO and complexity analyses, the present findings cannot establish whether the observed changes are specifically associated with pathological HFOs. Future investigations should therefore examine their relationship with clinical variables such as seizure burden, treatment response, and epileptogenic-zone localization.

The analysis focused specifically on N3 sleep because HFO occurrence is influenced by sleep stage and has been reported to be particularly prominent during N3 in pediatric epilepsy [55]. Previous studies have also investigated scalp HFOs during sleep as quantitative biomarkers in different pediatric epilepsy contexts [56], [61]. Restricting the analysis to a single sleep stage reduced the potential influence of differences between vigilance states on the relationship between HFOs and EEG complexity.

The temporal analysis showed that the most consistent complexity changes occurred during HFO activity. All seven selected measures differed significantly between HFO and distant Baseline, whereas no significant differences were detected between Pre-HFO and distant Baseline or between Post-HFO and distant Baseline. In addition, all seven measures differed significantly between HFO and Post-HFO. These findings suggest that the observed changes were primarily associated with HFO-containing windows rather than with consistent alterations in the immediately preceding or following periods. However, the absence of statistically significant differences does not establish equivalence with baseline, but only indicates that no consistent changes were detected using the measures and temporal definitions adopted in this study.

The final analysis investigated whether the fourteen complexity measures could automatically discriminate between EEG conditions. Three classifiers selected during preliminary model selection were evaluated using subject-independent leave-one-subject-out (LOSO) cross-validation. Despite the statistically significant differences observed for several complexity measures, classification performance remained modest. The Medium Gaussian SVM achieved the highest balanced accuracy

for HFO versus distant Baseline (approximately 53.7%), whereas Pre-HFO versus distant Baseline classification remained close to chance level, with a balanced accuracy of 49.3% and an ROC-AUC of approximately 0.50. These results indicate that the complexity differences observed at the group level were not sufficiently consistent across subjects to provide reliable discrimination in unseen patients. The poor Pre-HFO classification performance is also consistent with the temporal analysis, which did not identify significant differences between Pre-HFO and distant Baseline.

Several limitations should be considered. The study population included patients of different ages and with different epilepsy types and etiologies, potentially contributing to inter-subject variability. Furthermore, the fourteen complexity measures represent only part of the information contained in EEG signals. Other quantitative approaches, including functional connectivity, time-frequency analysis, and combinations of linear and nonlinear measures, have also been investigated in pediatric epilepsy [64], [65], [67]. Their integration with complexity analysis could provide a more comprehensive characterization of HFO-related EEG activity.

An additional limitation concerns the temporal definition of Pre-HFO activity, which was restricted to the single 4-s window immediately preceding an HFO block. Changes occurring at different temporal scales may therefore have been missed. Moreover, the analysis was limited to N3 sleep and to the ripple HFO annotations provided with the original dataset, preventing direct generalization to other sleep stages or types of high-frequency activity. Future studies could investigate different Pre-HFO intervals and larger pediatric populations to assess the robustness of the observed patterns.

Overall, the findings indicate that HFO occurrence during N3 sleep is associated with measurable changes in specific EEG complexity properties, although these changes showed limited generalizability across subjects and no robust Pre-HFO pattern was identified. The clinical validity of scalp HFOs remains debated because of methodological variability and difficulties in distinguishing physiological from pathological activity [94]. In this context, the observed complexity differences may provide complementary quantitative evidence for characterizing HFO-containing EEG activity. However, they do not independently confirm the physiological origin or clinical significance of the annotated HFOs, since residual artifacts and surrounding EEG activity may also influence complexity estimates. Further studies combining HFO detection with additional EEG features and clinical information are therefore needed to determine whether these measures can improve the characterization and clinical interpretation of HFO-related activity.

Conclusion

The aim of this thesis was to investigate the role of high-frequency electroencephalographic oscillations during sleep in pediatric patients with epilepsy, with particular attention to their relationship with quantitative changes in EEG complexity. The study combined a systematic review of the available literature with an experimental analysis of pediatric sleep EEG recordings, focusing on N3 sleep and on the temporal relationship between HFO occurrence and different measures of signal complexity.

The results showed that HFO occurrence was associated with significant changes in seven complexity measures, mainly concentrated during HFO-containing windows. These findings suggest that complexity analysis can provide complementary quantitative information about EEG activity associated with HFOs. However, no consistent changes were identified in the immediately preceding period, indicating that the investigated measures and temporal resolution did not reveal a reliable Pre-HFO pattern.

The subject-independent classification analysis further showed that the differences observed at the group level were not sufficiently consistent across patients to achieve reliable discrimination in previously unseen subjects. These results highlight the importance of inter-subject variability and the limitations of using complexity measures alone to characterize HFO-related EEG activity.

Overall, this work supports the potential value of integrating HFO analysis with quantitative EEG complexity measures. In the context of the ongoing debate regarding the clinical validity of scalp HFOs, the observed complexity differences provide additional information about HFO-containing EEG activity, although they do not independently establish the physiological origin or clinical relevance of these events. Future studies should investigate larger pediatric populations, different temporal intervals around HFOs, and the integration of complexity measures with other EEG features and clinical information to assess their potential contribution to HFO characterization and clinical interpretation.

Bibliography

[1] Purves D, Augustine GJ, Fitzpatrick D, et al. *Neuroscience*. Oxford University Press. 2018. 6th ed.

[2] Kandel ER, Koester JD, Mack SH, Siegelbaum SA. *Principles of Neural Science*. McGraw-Hill. 2021. 6th ed.

[3] Herculano-Houzel S. *The human brain in numbers: a linearly scaled-up primate brain*. Front Hum Neurosci (2009 Nov 9). 3:31.doi: 10.3389/neuro.09.031.2009.

[4] Yeo BT, Krienen FM, Sepulcre J, Sabuncu MR, Lashkari D, Hollinshead M, Roffman JL, Smoller JW, Zöllei L, Polimeni JR, Fischl B, Liu H, Buckner RL. *The organization of the human cerebral cortex estimated by intrinsic functional connectivity*. J Neurophysiol (2011 Sep). 106(3):1125-65. doi: 10.1152/jn.00338.2011.

[5] https://my.clevelandclinic.org/health/body/21202-nervous-system. May 22.

[6] Buzsáki G, Draguhn A. *Neuronal oscillations in cortical networks*. Science (2004 Jun 25). 304(5679):1926-9. doi: 10.1126/science.1099745.

[7] Buzsáki, György. *Rhythms of the Brain*. Oxford Academic (1 May 2009), https://doi.org/10.1093/acprof:oso/9780195301069.001.0001.

[8] Başar E, Başar-Eroğlu C, Karakaş S, Schürmann M. *Brain oscillations in perception and memory*. Int J Psychophysiol (2000 Mar). 35(2-3):95-124. doi: 10.1016/s0167-8760(99)00047-1.

[9] Galván A. *Cognitive Neuroscience Methods to Study the Adolescent Brain*. Cambridge University Press (2017). In: *The Neuroscience of Adolescence*: 50-84.

[10] Fries P. *A mechanism for cognitive dynamics: neuronal communication through neuronal coherence*. Trends Cogn Sci (2005 Oct). 9(10):474-80. doi: 10.1016/j.tics.2005.08.011.

[11] Buzsáki G, Wang XJ. *Mechanisms of gamma oscillations*. Annu Rev Neurosci (2012). 35:203-25. doi: 10.1146/annurev-neuro-062111-150444.

[12] Fisher RS, Acevedo C, Arzimanoglou A, Bogacz A, Cross JH, Elger CE, Engel J Jr, Forsgren L, French JA, Glynn M, Hesdorffer DC, Lee BI, Mathern GW, Moshé SL, Perucca E, Scheffer IE, Tomson T, Watanabe M, Wiebe S. *ILAE official report: a practical clinical definition of epilepsy*. Epilepsia (2014 Apr). 55(4):475-82. doi: 10.1111/epi.12550.

[13] Fiest KM, Sauro KM, Wiebe S, Patten SB, Kwon CS, Dykeman J, Pringsheim T, Lorenzetti DL, Jetté N. *Prevalence and incidence of epilepsy: A systematic review and meta-analysis of international studies*. Neurology (2017 Jan 17). 88(3):296-303. doi: 10.1212/WNL.000000000000 3509.

[14] Thurman DJ, Beghi E, Begley CE, Berg AT, Buchhalter JR, Ding D, Hesdorffer DC, Hauser WA, Kazis L, Kobau R, Kroner B, Labiner D, Liow K, Logroscino G, Medina MT, Newton CR, Parko K, Paschal A, Preux PM, Sander JW, Selassie A, Theodore W, Tomson T, Wiebe S. *ILAE Commission on Epidemiology. Standards for epidemiologic studies and surveillance of epilepsy*. Epilepsia (2011 Sep). 52 Suppl 7:2-26. doi: 10.1111/j.1528-1167.2011.03121. x.

[15] Devinsky O, Vezzani A, O'Brien TJ, Jette N, Scheffer IE, de Curtis M, Perucca P. *Epilepsy*. Nat Rev Dis Primers (2018 May 3). 4:18024. doi: 10.1038/nrdp.2018.24. PMID: 29722352.

[16] Thurman DJ, Logroscino G, Beghi E, Hauser WA, Hesdorffer DC, Newton CR, Scorza FA, Sander JW, Tomson T. *The burden of premature mortality of epilepsy in high-income countries: A systematic review from the Mortality Task Force of the International League Against Epilepsy*. Epilepsia (2017 Jan). 58(1):17-26. doi: 10.1111/epi.13604.

[17] GBD 2016 Epilepsy Collaborators. *Global, regional, and national burden of epilepsy, 1990-2016: a systematic analysis for the Global Burden of Disease Study 2016*. Lancet Neurol (2019 Apr). 18(4):357-375. doi: 10.1016/S1474-4422(18)30454-X.

[18] Noebels JL, Avoli M, Rogawski MA, Olsen RW, Delgado-Escueta AV, editors. *Jasper's Basic Mechanisms of the Epilepsies*. Bethesda (MD): National Center for Biotechnology Information (US) (2012). 4th ed.

[19] Bromfield EB, Cavazos JE, Sirven JI, editors. *An Introduction to Epilepsy*. West Hartford (CT): American Epilepsy Society (2006). Chapter 1, Basic Mechanisms Underlying Seizures and Epilepsy.

[20] Blumenfeld H. *Cellular and network mechanisms of spike-wave seizures*. Epilepsia (2005). 46 Suppl 9:21-33. doi: 10.1111/j.1528-1167.2005.00311.x.

[21] Jiruska P, de Curtis M, Jefferys JG, Schevon CA, Schiff SJ, Schindler K. *Synchronization and desynchronization in epilepsy: controversies and hypotheses*. J Physiol (2013 Feb 15). 591(4):787-97. doi: 10.1113/jphysiol.2012.239590.

[22] Kramer MA, Cash SS. *Epilepsy as a disorder of cortical network organization*. Neuroscientist (2012 Aug). 18(4):360-72. doi: 10.1177/1073858411422754.

[23] El Achkar CM, Olson HE, Poduri A, Pearl PL. *The genetics of the epilepsies*. Curr Neurol Neurosci Rep (2015 Jul). 15(7):39. doi: 10.1007/s11910-015-0559-8.

[24] Scheffer IE, Berkovic S, Capovilla G, Connolly MB, French J, Guilhoto L, Hirsch E, Jain S, Mathern GW, Moshé SL, Nordli DR, Perucca E, Tomson T, Wiebe S, Zhang YH, Zuberi SM. *ILAE classification of the epilepsies: Position paper of the ILAE Commission for Classification and Terminology*. Epilepsia (2017 Apr).58(4):512-521. doi: 10.1111/epi.13709.

[25] Fisher RS, Cross JH, French JA, Higurashi N, Hirsch E, Jansen FE, Lagae L, Moshé SL, Peltola J, Roulet Perez E, Scheffer IE, Zuberi SM. *Operational classification of seizure types by the International League Against Epilepsy: Position Paper of the ILAE Commission for Classification and Terminology*. Epilepsia (2017 Apr). 58(4):522-530. doi: 10.1111/epi.13670.

[26] Seeck M, Koessler L, Bast T, Leijten F, Michel C, Baumgartner C, He B, Beniczky S. *The standardized EEG electrode array of the IFCN*. Clin Neurophysiol (2017 Oct). 128(10):2070-2077. doi: 10.1016/j.clinph.2017.06.254.

[27] Beniczky S, Schomer DL. *Electroencephalography: basic biophysical and technological aspects important for clinical applications*. Epileptic Disord (2020 Dec 1). 22(6):697-715. doi: 10.1684/epd.2020.1217.

[28] Nalwaya, Aditya & Das, Kritiprasanna & Pachori, Ram. *Emotion identification from TQWT-based EEG rhythms*. IGI Global (2022 May). doi: 10.4018/978-1-6684-3947-0.ch011.

[29] Peltola ME, Leitinger M, Halford JJ, Vinayan KP, Kobayashi K, Pressler RM, Mindruta I, Mayor LC, Lauronen L, Beniczky S. *Routine and sleep EEG: Minimum recording standards of the International Federation of Clinical Neurophysiology and the International League Against Epilepsy*. Epilepsia (2023 Mar). 64(3):602-618. doi: 10.1111/epi.17448.

[30] Benbadis SR. *What type of EEG (or EEG-video) does your patient need?*. Expert Rev Neurother. (2015 May). 15(5):461-4. doi: 10.1586/14737175.2015.1029918.

[31] Kural MA, Duez L, Sejer Hansen V, Larsson PG, Rampp S, Schulz R, Tankisi H, Wennberg R, Bibby BM, Scherg M, Beniczky S. *Criteria for defining interictal epileptiform discharges in EEG: A clinical validation study*. Neurology (2020 May 19). 94(20):e2139-e2147. doi: 10.1212/WNL.0000000000009439.

[32] Kane N, Acharya J, Benickzy S, Caboclo L, Finnigan S, Kaplan PW, Shibasaki H, Pressler R, van Putten MJAM. *A revised glossary of terms most commonly used by clinical*

electroencephalographers and updated proposal for the report format of the EEG findings. Clin Neurophysiol Pract (2017 Aug 4). 2:170-185. doi: 10.1016/j.cnp.2017.07.002.

[33] W.O. Tatum, G. Rubboli, P.W. Kaplan, S.M. Mirsatari, K. Radhakrishnan, D. Gloss, L.O. Caboclo, F.W. Drislane, M. Koutroumanidis, D.L. Schomer, D. Kasteleijn-Nolst Trenite, Mark Cook, S. Beniczky. *Clinical utility of EEG in diagnosing and monitoring epilepsy in adults*. Clinical Neurophysiology (2018). Volume 129, Issue 5, Pages 1056-1082. https://doi.org/10.1016/j.clinph.2018.01.019.

[34] W. O. Tatum, B. A. Dworetzky, and D. L. Schomer. *Artifact and Recording Concepts in EEG*. Journal of Clinical Neurophysiology (Jun. 2011). vol. 28 no. 3 pp. 252–263. doi: 10.1097/WNP.0b013e31821c3c93.

[35] Chen G, Zhang Z, Wang M, Geng Y, Jin B, Aung T. *Update on the Neuroimaging and Electroencephalographic Biomarkers of Epileptogenesis: A Literature Review*. Front Neurol. (2021 Aug 27). doi: 10.3389/fneur.2021.738658.

[36] Engel J Jr, Pitkänen A, Loeb JA, Dudek FE, Bertram EH 3rd, Cole AJ, Moshé SL, Wiebe S, Jensen FE, Mody I, Nehlig A, Vezzani A. *Epilepsy biomarkers*. Epilepsia (2013 Aug). 54 Suppl 4(04):61-9. doi: 10.1111/epi.12299.

[37] Gallotto S, Seeck M. *EEG biomarker candidates for the identification of epilepsy*. Clin Neurophysiol Pract. (2022 Dec 14). 8:32-41. doi: 10.1016/j.cnp.2022.11.004.

[38] Frauscher B, Bartolomei F, Kobayashi K, et al. *High-frequency oscillations: The state of clinical research*. Epilepsia. 2017;58(8):1316–1329. doi: 10.1111/epi.13829.

[39] Luján, M. Á., Jimeno, M. V., Mateo Sotos, J., Ricarte, J. J., & Borja, A. L. *A Survey on EEG Signal Processing Techniques and Machine Learning: Applications to the Neurofeedback of Autobiographical Memory Deficits in Schizophrenia*. Electronics (2021). *10*(23), 3037. https://doi.org/10.3390/electronics10233037

[40] Acharya, U. & Subbhuraam, Vinitha Sree & Goutham, Swapna & Martis, Roshan & Suri, Jasjit. *Automated EEG analysis of epilepsy: A review*. Knowledge-Based Systems (2013). doi:147-165. 10.1016/j.knosys.2013.02.014.

[41] Subasi, Abdulhamit. *EEG signal classification using wavelet feature extraction and a mixture of expert model*. Expert Systems with Applications (2007). 32 1084-1093. Doi: 10.1016/j.eswa.2006.02.005.

[42] Adeli H, Zhou Z, Dadmehr N. *Analysis of EEG records in an epileptic patient using wavelet transform*. J Neurosci Methods (2003 Feb 15). 123(1):69-87. doi: 10.1016/s0165-0270(02)00340-0.

[43] Al-Fahoum AS, Al-Fraihat AA. *Methods of EEG signal features extraction using linear analysis in frequency and time-frequency domains*. ISRN Neurosci. (2014 Feb 13). doi: 10.1155/2014/730218.

[44] Faust O, Acharya UR, Adeli H, Adeli A. *Wavelet-based EEG processing for computer-aided seizure detection and epilepsy diagnosis*. Seizure (2015 Mar). 26:56-64. doi: 10.1016 /j.seizure.2015.01.012.

[45] Rajalakshmi, A. & Sridhar, Dr.S.S. *A Study of Time Domain Features of EEG Signal Analysis*. International Conference on Recent Trends in Data Science and its Applications (2023 January). 874-878. doi:10.13052/rp-9788770040723.171.

[46] Poomipat Boonyakitanont, Apiwat Lek-uthai, Krisnachai Chomtho, Jitkomut Songsiri. *A review of feature extraction and performance evaluation in epileptic seizure detection using EEG*. Biomedical Signal Processing and Control (2020). Volume 57. https://doi.org/10.1016/ j.bspc.2019.101702.

[47] Wang, Deng & Miao, Duoqian & Xmm, Cmm. *Best basis-based wavelet packet entropy feature extraction and hierarchical EEG classification for epileptic detection*. Expert Syst. Appl (2011). 38. 14314-14320. doi:10.1016/j.eswa.2011.05.096.

[48] Qin Y, Zhang Y, Zhang Y, Liu S, Guo X. *Application and Development of EEG Acquisition and Feedback Technology: A Review*. Biosensors (Basel) (2023 Oct 17).13(10):930. doi: 10.3390/bios13100930.

[49] Ren, Qirui & Sun, Xiaofan & Fu, Xiangqu & Zhang, Shuaidi & Yuan, Yiyang & Wu, Hao & Li, Xiaoran & Wang, Xinghua & Zhang, Feng. *A review of automatic detection of epilepsy based on EEG signals*. Journal of Semiconductors (2023). 44. 121401. doi:10.1088/1674-4926/44/12/121401.

[50] Shoeb, Ali & Guttag, John. *Application of Machine Learning To Epileptic Seizure Detection*. ICML 2010 - Proceedings, 27th International Conference on Machine Learning (2010). 975-982.

[51] Roliz AH, Kothare S. *The Interaction Between Sleep and Epilepsy*. Curr Neurol Neurosci Rep. (2022 Sep). 22(9):551-563. doi: 10.1007/s11910-022-01219-1.

[52] Ng M, Pavlova M. *Why are seizures rare in rapid eye movement sleep? Review of the frequency of seizures in different sleep stages*. Epilepsy Res Treat. (2013). doi: 10.1155/ 2013/932790.

[53] Halász, Peter. *How Sleep Activates Epileptic Networks?*. Epilepsy Research and Treatment (2013). 19 pages. https://doi.org/10.1155/2013/425697.

[54] Kothare SV, Kaleyias J. *Sleep and epilepsy in children and adolescents*. Sleep Med. (2010 Aug). 11(7):674-85. doi: 10.1016/j.sleep.2010.01.012.

[55] Cserpan D, Rosch R, Lo Biundo SP, Sarnthein J, Ramantani G. *Variation of scalp EEG high frequency oscillation rate with sleep stage and time spent in sleep in patients with pediatric epilepsy*. Clin Neurophysiol. (2022 Mar). 135:117-125. doi: 10.1016/j.clinph.2021.12.013.

[56] Cao D, Chen Y, Liao J, Nariai H, Li L, Zhu Y, Zhao X, Hu Y, Wen F, Zhai Q. *Scalp EEG high frequency oscillations as a biomarker of treatment response in epileptic encephalopathy with continuous spike-and-wave during sleep (CSWS)*. Seizure (2019 Oct). 71:151-157. doi: 10.1016/ j.seizure.2019.05.023.

[57] Sathyanarayana A, El Atrache R, Jackson M, Alter AS, Mandl KD, Loddenkemper T, Bosl WJ. *Measuring the effects of sleep on epileptogenicity with multifrequency entropy*. Clin Neurophysiol. (2021 Sep). 132(9):2012-2018. doi: 10.1016/j.clinph.2021.06.001.

[58] Zhang W, Xin M, Song G, Liang J. *Childhood absence epilepsy patients with cognitive impairment have decreased sleep spindle density*. Sleep Med. (2023 Mar). 103:89-97. doi: 10.1016/j.sleep.2023.01.012.

[59] Scheffer IE, Berkovic S, Capovilla G, Connolly MB, French J, Guilhoto L, Hirsch E, Jain S, Mathern GW, Moshé SL, Nordli DR, Perucca E, Tomson T, Wiebe S, Zhang YH, Zuberi SM. *ILAE classification of the epilepsies: Position paper of the ILAE Commission for Classification and Terminology*. Epilepsia (2017 Apr). 58(4):512-521. doi: 10.1111/epi.13709.

[60] Zuberi SM, Wirrell E, Yozawitz E, Wilmshurst JM, Specchio N, Riney K, et al. *ILAE classification and definition of epilepsy syndromes with onset in neonates and infants: Position statement by the ILAE Task Force on Nosology and Definitions*. Epilepsia (2022). 63:1349–1397. https://doi.org/10.1111/epi.17239

[61] Kart PO, Özdemir C, Kayikcioglu T, Cansu A. *High-Frequency Oscillations in Self-Limited Epilepsy With Centrotemporal Spikes: Potential Predictors of Attention Deficit Hyperactivity Disorder?*. Int J Dev Neurosci. (2025 May). 85(3): e70020. doi: 10.1002/jdn.70020.

[62] Nariai H, Hussain SA, Bernardo D, Motoi H, Sonoda M, Kuroda N, Asano E, Nguyen JC, Elashoff D, Sankar R, Bragin A, Staba RJ, Wu JY. *Scalp EEG interictal high frequency oscillations*

as an objective biomarker of infantile spasms. Clin Neurophysiol. (2020 Nov). 131(11):2527-2536. doi: 10.1016/j.clinph.2020.08.013.

[63] Azeem A, Kirton A, Appendino JP, Kozlik S, Mineyko A. *Automated quantification of spike-wave activity may be used to predict the development of electrical status epilepticus in sleep (ESES) in children with perinatal stroke*. Clin Neurophysiol. (2021 Jan). 132(1):146-153. doi: 10.1016/ j.clinph.2020.11.003.

[64] Hu DK, Pinto-Orellana MA, Rana M, Do L, Adams DJ, Hussain SA, et al. *Discovering EEG biomarkers of Lennox–Gastaut syndrome through unsupervised time–frequency analysis*. Epilepsia (2025). 66:541–553. https://doi.org/10.1111/epi.18211.

[65] Davis PE, Kapur K, Filip-Dhima R, Trowbridge SK, Little E, Wilson A, Leuchter A, Bebin EM, Krueger D, Northrup H, Wu JY, Sahin M, Peters JM. *Tuberous Sclerosis Autism Centers of Excellence Research Network. Increased electroencephalography connectivity precedes epileptic spasm onset in infants with tuberous sclerosis complex*. Epilepsia (2019 Aug). 60(8):1721-1732. doi: 10.1111/epi.16284.

[66] Stam CJ. *Nonlinear dynamical analysis of EEG and MEG: review of an emerging field*. Clin Neurophysiol. (2005 Oct). 116(10):2266-301. doi: 10.1016/j.clinph.2005.06.011.

[67] Mercier M, Pepi C, Carfi-Pavia G, De Benedictis A, Espagnet MCR, Pirani G, Vigevano F, Marras CE, Specchio N, De Palma L. *The value of linear and non-linear quantitative EEG analysis in paediatric epilepsy surgery: a machine learning approach*. Sci Rep. (2024 May 13). 14(1):10887. doi: 10.1038/s41598-024-60622-5.

[68] Qing Cai, Jianpeng An, Mengying Wang, Zhongke Gao, Matjaž Perc, Huicong Kang. *Entropy-based complexity of EEG microstates differentiates ADHD comorbidity in children with SeLECTS*. Chaos, Solitons & Fractals (2026). Volume 208, Part 2. https://doi.org/10.1016/j.chaos.2026 .118210.

[69] Hu DK, Rana M, Adams DJ, Do L, Shrey DW, Hussain SA, Lopour BA. *Interrater reliability of interictal EEG waveforms in Lennox-Gastaut Syndrome*. Epilepsia Open. (2024 Feb). 9(1):176-186. doi: 10.1002/epi4.12858.

[70] https://openneuro.org/datasets/ds003555/versions/1.0.1

[71] Delorme A, Makeig S. *EEGLAB: an open source toolbox for analysis of single-trial EEG dynamics including independent component analysis.* Journal of Neuroscience Methods (2004), 134(1), 9–21.

[72] Lopez KL, Monachino AD, Morales S, Leach SC, Bowers ME, Gabard-Durnam LJ. , *HAPPILEE: HAPPE In Low Electrode Electroencephalography, a standardized pre-processing software for lower density recordings*, NeuroImage. 2022; 260:119390. doi: 10.1016/j.neuroimage.2022.119390.

[73] Pincus SM. *Approximate entropy as a measure of system complexity*. Proc Natl Acad Sci U S A. 1991 Mar 15;88(6):2297-301. doi: 10.1073/pnas.88.6.2297. PMID: 11607165; PMCID: PMC51218.

[74] Richman JS, Moorman JR. Physiological time-series analysis using approximate entropy and sample entropy. Am J Physiol Heart Circ Physiol. 2000 Jun;278(6):H2039-49. doi: 10.1152/ajpheart.2000.278.6.H2039. PMID: 10843903.

[75] Bandt & Pompe, *Permutation Entropy: A Natural Complexity Measure for Time Series,* Phys. Rev. Lett. 88, 174102, 11 April 2002, DOI: https://doi.org/10.1103/PhysRevLett.88.174102.

[76] Shannon, C. E. *A Mathematical Theory of Communication*. Bell System Technical Journal 1948, 27, 379–423, 623–656.

[77] Rényi, A. *On Measures of Entropy and Information.* In Proceedings of the Fourth Berkeley Symposium on Mathematical Statistics and Probability 1961, Vol. 1, pp. 547–561. University of California Press.

[78] Tsallis, C. *Possible generalization of Boltzmann-Gibbs statistics*. Journal of Statistical Physics 1988, 52(1–2), 479–487.

[79] Welch, P. D. *The use of fast Fourier transform for the estimation of power spectra: A method based on time averaging over short, modified periodograms.* IEEE Transactions on Audio and Electroacoustics 1967, 15(2), 70–73. doi: 10.1109/TAU.1967.1161901

[80] T. Higuchi. *Approach to an irregular time series on the basis of the fractal theory*. Physica D: Nonlinear Phenomena 1988. Volume 31. Issue 2. Pages 277-283. ISSN 0167-2789. https://doi.org/10.1016/0167-2789(88)90081-4.

[81] Katz MJ. *Fractals and the analysis of waveforms*. Comput Biol Med. 1988;18(3):145-56. doi: 10.1016/0010-4825(88)90041-8. Erratum in: Comput Biol Med 1989;19(4):291. PMID: 3396335.

[82] Petrosian, A. *Kolmogorov complexity of finite sequences and recognition of different preictal EEG patterns*. Proceedings of the Eighth IEEE Symposium on Computer-Based Medical Systems 1995, pp. 212–217.

[83] Peng CK, Buldyrev SV, Havlin S, Simons M, Stanley HE, Goldberger AL. *Mosaic organization of DNA nucleotides*. Phys Rev E Stat Phys Plasmas Fluids Relat Interdiscip Topics. 1994 Feb; 49(2):1685-9. doi: 10.1103/physreve.49.1685. PMID: 9961383.

[84] Hurst, H. E. *Long-Term Storage Capacity of Reservoirs*. Transactions of the American Society of Civil Engineers 1951. 116(1), 770–799.

[85] A. Lempel and J. Ziv. *On the Complexity of Finite Sequences*, in IEEE Transactions on Information Theory. vol. 22, no. 1, pp. 75-81, January 1976, doi: 10.1109/TIT.1976.1055501.

[86] Hjorth B. *EEG analysis based on time domain properties*. Electroencephalogr Clin Neurophysiol. 1970 Sep; 29(3):306-10. doi: 10.1016/0013-4694(70)90143-4.

[87] Cserpan D, Boran E, Lo Biundo SP, Rosch R, Sarnthein J, Ramantani G. *Scalp high-frequency oscillation rates are higher in younger children*. Brain Commun. 2021 Mar 23;3(2):fcab052. doi: 10.1093/braincomms/fcab052.

[88] Wilcoxon. *Individual comparisons by ranking methods*. Biometrics Bulletin (1945). 1(6), 80–83.

[89] Benjamini, Y., & Hochberg, *Controlling the false discovery rate: A practical and powerful approach to multiple testing*. Journal of the Royal Statistical Society: Series B (Methodological) (1995), 57(1), 289–300.

[90] Friedman. *The use of ranks to avoid the assumption of normality implicit in the analysis of variance*. Journal of the American Statistical Association (1937). 32(200), 675–701.

[91] Mei Z, Zhao X, Chen H, Chen W. *Bio-Signal Complexity Analysis in Epileptic Seizure Monitoring: A Topic Review*. Sensors. 2018;18(6):1720. doi: 10.3390/s18061720.

[92] Lau ZJ, Pham T, Chen SHA, Makowski D. *Brain entropy, fractal dimensions and predictability: A review of complexity measures for EEG in healthy and neuropsychiatric populations*. European Journal of Neuroscience. 2022; 56(7):5047–5069. doi: 10.1111/ejn.15800.

[93] Li Z, Zhao B, Hu W. *Machine learning-based classification of physiological and pathological high-frequency oscillations recorded by stereoelectroencephalography.* Seizure - European Journal of Epilepsy, 2023; 113, 58-65.

[94] Noorlag et al. *High-frequency oscillations in scalp EEG: A systematic review of methodological choices and clinical findings*. Clinical Neurophysiology (2022), 137, 46–58. doi: 10.1016/j.clinph.2021.12.017.

APPENDIX I

1 Systematic Review

1.1 Literature search strategy and design

The systematic review was conducted in accordance with the PRISMA (Preferred Reporting Items for Systematic Reviews and Meta-Analyses) 2020 guidelines. The literature search was performed in the period between January and February 2026 using two major electronic bibliographic databases: PubMed and Scopus. The aim of the search strategy was to identify scientific studies related to EEG sleep monitoring and the identification of biomarkers in pediatric epilepsy. Based on this objective, the search query was defined as follows: *"EEG AND sleep AND pediatric AND epilepsy AND biomarker"*. The selected keywords represent the main components of the research topic. In particular, the term "EEG" was used to identify studies involving electroencephalographic recordings; "sleep" was included to focus on sleep-related brain activity; "pediatric" and "epilepsy" were used to restrict the search to studies involving epileptic conditions in children; and "biomarker" was included to target studies investigating quantitative or clinically relevant EEG features. These keywords were combined using the Boolean operator "AND" in order to retrieve studies that simultaneously addressed all aspects of interest. The search was further refined by applying a set of automatic filters in order to improve the relevance of the retrieved results. Specifically, only articles published in the last 10 years were included, and the search was restricted to studies involving human subjects. In addition, an age filter was applied to include only pediatric populations (birth–18 years). Furthermore, only articles written in English were considered. The same search strategy and filters were consistently applied to both PubMed and Scopus databases in order to ensure comparability and reproducibility of the results.

1.2 Study Selection Process

All documents resulting from the application of the search query in PubMed and Scopus were collected and screened for eligibility. Duplicate records identified across the two databases were removed prior to further analysis. The remaining studies were then screened manually through a multi-step selection process based on predefined inclusion and exclusion criteria. The screening was conducted sequentially, starting from titles, followed by abstracts, and finally full-text evaluation.

Studies were included if they met the following criteria:

• involved pediatric subjects (age 0–18 years);

• focused on epilepsy or epileptic conditions;

• included sleep-related EEG analysis or long-term recordings that encompass sleep;
• investigated EEG features or biomarkers (e.g., high-frequency oscillations, entropy, connectivity, or quantitative EEG measures).

Studies were excluded if they met one or more of the following criteria:
• involved adult populations only;
• did not focus on epilepsy;
• did not include EEG data;
• did not address sleep-related EEG or biomarker analysis;
• were not relevant to the objectives of the study (e.g., unrelated neurological conditions);
• were review articles, conference abstracts, or non-research papers.

The exclusion process followed an "OR" logic, meaning that studies meeting at least one exclusion criterion were discarded. Title screening was first performed to remove clearly irrelevant studies. Subsequently, abstract screening was conducted to further refine the selection. In cases where the abstract did not provide sufficient information, full-text evaluation was performed. After the full selection process, a final set of relevant studies was obtained and included in the qualitative analysis.

1.3 Results of the Literature Search

The application of the search query resulted in a total of 53 documents, including 40 from PubMed and 13 from Scopus. After the removal of 3 duplicate records, 50 documents remained for the screening process. Based on title evaluation, 19 documents were excluded as they were not relevant to the research topic. Subsequently, abstract screening led to the exclusion of an additional 10 documents that did not meet the inclusion criteria. The remaining 21 articles were assessed through full-text evaluation. During this phase, 9 documents were excluded due to absence of EEG-based analysis, insufficient relevance to sleep-related processes, and limited investigation of EEG biomarkers. In addition, some studies were excluded because they focused on different neurological conditions or did not align with the specific objectives of this review. At the end of the selection process, a total of 12 studies were included in the qualitative analysis as compliant with the inclusion criteria. The overall study selection process is summarized in the PRISMA flow diagram in figure 27. Table 5 provides a summary of the main characteristics of the included studies, including sample size, type of epilepsy, EEG modality, the aim and analysis methods and the results of the study.

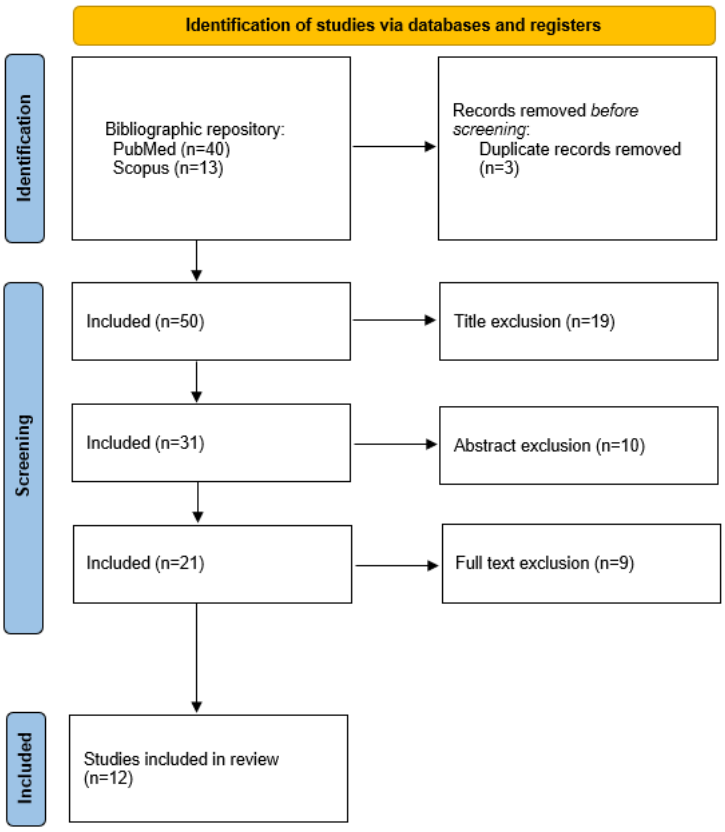


Figure 27: Process of literature search and study selection.

Table 5. Overview of the studies of the included documents.

Reference	N (patients)	Age	Epilepsy Type	EEG type	Aim/ Method	Key Findings
[55]	16	Pediatric	Focal epilepsy	Scalp EEG (sleep)	HFO detection across sleep stages	HFOs highest in N3; optimal detection in early sleep
[56]	22	Pediatric	CSWS/ESES	Scalp EEG	HFO as treatment biomarker	HFOs predict cognitive and seizure outcome
[57]	31	Pediatric	BECTS	EEG (sleep vs wake)	Entropy analysis	Reduced entropy linked to epileptogenicity
[58]	29 CAE + 30 controls	Pediatric	Childhood absence epilepsy (CAE)	Overnight scalp EEG (N2 sleep)	Sleep spindle analysis during N2 sleep	Reduced sleep spindle associated with cognitive impairment.

[61]	40	Pediatric	SeLECTS (± ADHD)	Scalp EEG (NREM sleep)	Automatic ripple (HFO) detection to predict cognitive comorbidities	Higher ripple rates in SeLECTS+ADHD group
[62]	30	Infants	Infantile spasms	Overnight scalp EEG	HFO + coupling analysis	HFOs outperform hypsarrhythmia as biomarkers
[63]	43	Pediatric	ESES	Sleep EEG	Spike frequency + PSD analysis	Increased network synchrony in epilepsy
[64]	dataset-based	Pediatric	Lennox–Gastaut syndrome	Scalp EEG (sleep/NREM)	Time–frequency + unsupervised learning	Identification of beta/gamma biomarkers; reduced sleep spindles;
[66]	44	Infants	TSC-related epilepsy	Scalp EEG (sleep)	Functional connectivity analysis	Increased connectivity precedes epileptic spasms
[68]	123	Mean ~7.3 yrs	Drug-resistant epilepsy	Long-term video-EEG	qEEG + machine learning for outcome prediction	EEG features predict surgical outcome (~65%)
[69]	58	Mean ~11 yrs	SeLECTS	Long-term EEG (sleep+wake)	Microstates + entropy	HFOs remain reliable biomarkers vs spikes
[70]	20 LGS + 20 controls	Pediatric	Lennox–Gastaut syndrome (LGS)	Scalp EEG (NREM sleep)	Automated EEG waveform detection and interrater reliability analysis	Computational biomarkers may improve EEG classification.

1.4 Discussion of results

This systematic review explored the current literature on EEG sleep monitoring and the identification of biomarkers in pediatric epilepsy. The main objective was to analyze how sleep-related EEG features and advanced signal processing techniques are used to characterize epileptic activity and support diagnosis and prognosis in pediatric patients. A total of 12 studies were included in the final analysis, all of which were primary research articles focusing on EEG-based investigations.

The analysis of the selected studies highlights a growing interest in the use of sleep EEG for the detection of epileptiform activity and the identification of reliable biomarkers. In particular, several studies focused on high-frequency oscillations (HFOs), which have been increasingly recognized as more specific indicators of epileptogenicity compared to traditional interictal spikes. The results consistently show that HFOs are strongly influenced by sleep, with higher occurrence during deep NREM stages, confirming the importance of including sleep in EEG analysis. In addition to HFOs, other quantitative EEG features such as entropy-based measures, functional connectivity, and spectral characteristics have been investigated. These approaches provide a more detailed and objective representation of brain dynamics, allowing the identification of subtle abnormalities that may not be detectable through conventional visual EEG analysis. In particular, reduced signal complexity and altered connectivity patterns were associated with epileptogenic regions and disease progression, suggesting that advanced EEG analysis can offer valuable insights into the underlying mechanisms of epilepsy. Another relevant finding concerns the application of machine learning techniques to EEG data. Several studies employed data-driven approaches to extract features and build predictive models for seizure outcome or disease progression. Although these methods showed promising results, their performance varied depending on the dataset and the selected features, highlighting the need for standardized methodologies.

From a clinical perspective, the reviewed studies suggest that sleep EEG and advanced biomarkers may improve both diagnostic accuracy and prognostic evaluation in pediatric epilepsy. For example, sleep-related EEG features have been associated with cognitive impairment, treatment response, and early identification of severe epilepsy syndromes. However, despite these promising findings, the clinical application of these techniques remains limited, and further validation is required before their routine use.